DISSECTION AND FUNCTIONAL CHARACTERIZATION OF WHEAT QTL-FHB5 BASED ON FORWARD AND REVERSE GENETICS APPROACH

Shivappa Hukkeri

Department of Plant Science

McGill University, Montreal, Canada

December 2016

A thesis submitted to the McGill University in partial fulfillment of the requirements of the degree of Doctor of Philosophy

DEDICATED TO MY BELOVED PARENTS, BROTHERS, SISTER, FRIENDS

AND ALL MY TEACHERS

TABLE OF CONTENTS

LIST OF TABLES

LIST OF FIGURES

Figure 3.6: Comparative mapping of wheat QTL-Fhb5 genetic and physical maps encompassing *TaMYBFhb5* gene. The markers in red and green color were consistently associated with the QTL-Fhb5. The *TaMYBFhb5* gene lying between green color flanking markers (0.3cM) was found within the deletion bin 5AS-1(http://wheat.pw.usda.gov/cgi-bin/westsql/bin_candidates.cgi?bin=5AS1-0.40-0.75). Left side for deletion map are bin numbers; Left side for genetic map=linkage distance (cM); Left side for gene predicted= NCBI IDs. The predicted genes have synteny with Brachypodium, rice, sorghum, barley, Arabidopsis and wheat.

Figure 3.7: Schematic representation of resistance related metabolites mapped onto KEGG pathway and major phenylpropanoid and flavonoid gene regulation through *TaMYBFhb5* gene.

Figure 3.8: Virus induced gene silencing of phytoene desaturase (PDS) gene in resistant near isogenic line (R-NIL) spikelets carrying *TaMYBFhb5* gene at 6 days post inoculation (dpi). Where, BSMV:PDS = BSMV carrying fragment of PDS gene (Scofield et al., 2005); BSMV:00 = BSMV without PDS fragment.

Figure 3.9: Differential expression analysis of structural genes, *PAL*, *ACT* and *CHS* at 72 hpi of *Fusarium graminearum*. Where, RP=resistant near isogenic line (NILs) inoculated with pathogen, SP= susceptible NIL inoculated with pathogen.

Figure 3.10: Differential expression of *TaMYBFhb5* between R-NIL and S-NIL 72 hpi of *Fusarium graminearum*. Where, RP=resistant near isogenic line (NILs) inoculated with pathogen, SP= susceptible NIL inoculated with pathogen, R-NIL_silenced= *TaMYBFhb5* transcription factor silenced in resistant near isogenic line (NILs) inoculated with pathogen.

Figure 3.11: Differential expression analysis of host structural genes after silencing the *TaMYBFhb5* gene in wheat R-NIL. Where, *PAL*=phenylalanine ammonia lyase, *ACT*=agmatine coumaroyl transferase and *CHS*=chalcone synthase genes.

Figure 3.12: The *TaMYBFhb5* interaction with promoter regions of downstream genes; A) chalcone synthase (*CHS*) 8% PAGE, B) agmatine coumaroyl transferase (*ACT*) 4% Agarose gel, C) phenylalanine ammonia lyase (*PAL*), 4% Agarose gel.

Figure 3.13: Post-docking interactions between the active site residues of the *TaMYBFhb5* (3ZQC) with ligands, *PAL*, *CHS* and *ACT* DNA sequences. The 3ZQC is depicted in surface view and ligands as a stick in the binding pocket.

Figure 4.1: Virus induced gene silencing of phytoene desaturase (*PDS*) gene in Sumai3 spikelets at 6 days post inoculation (dpi). Where, BSMV: PDS = BSMV carrying fragment of PDS gene (Scofield et al., 2005); BSMV:00 = BSMV without PDS fragment.

Figure 4.2: *TaMYBFhb5* gene differential expression between silenced and non-silenced Sumai3 spikelets and rachis. The relative transcript abundance of *TaMYBFhb5* gene was calculated using wheat actin as housekeeping gene at 72 hpi.

Figure 4.3: Disease symptoms of *TaMYBFhb5* transcription factor gene silenced sumai3 spikelets inoculated with *Fusarium graminearum* after 72 hpi. The red arrow mark indicates the spread of disease seen only in rachis of the silenced spikes and not in nonsilenced spikes.

Figure 4.4: *Fusarium graminearum* fungal biomass quantified in Sumai3 silenced and non-silenced spikelets, two pairs of inoculated along with two uninoculated pairs, and rachis in the region of inoculation at 72hpi. 4A) the relative gene copy number of *GaO* in spikelets. 4B) the relative gene copy number of *Tri6_10* in rachis.

Figure 4.7: Schematic representation of RR metabolites induced upon *Fusarium graminearum* infection in Sumai3 *TaMYBFhb5* gene non-silenced and silenced were mapped on to KEGG pathways. The phenylpropanoids and flavonoids were derived from the shikimate pathway and terpenoids were derived from mevalonate pathway.

Figure 4.6: Metabolic pathway genes relative transcript abundances in Sumai3 *TaMYBFhb5* gene silenced and non-silenced spikelets and rachis. 6A) Differential expression of a structural gene, *PAL* at 72 hpi of *Fusarium graminearum* in spikelets. 6B) Differential expression of structural gene *CHS* at 72 hpi of *Fusarium graminearum* in rachis.

Figure 4.5: Accumulation of *Fusarium graminearum* resistance indicator (RI) metabolite, deoxynivalenol (DON) within Sumai3 *TaMYBFhb5* gene silenced and non-silenced spikelets at 72 hpi.

Figure 5.1: Disease severity in Sumai3 and Roblin genotypes, based on visual observations, following spray inoculation with *Fusarium graminearum,* trichothecene producing isolate (*FgT*) and fungal biomass quantification based on real-time qPCR in resistant (Sumai3) and susceptible (Roblin) spikelets, at 72 hpi; A) Proportion of spikelets diseased (PSD); B) Area under disease progress curve (AUDPC), calculated based on every 3 d observations until 21 dpi; C) *Fusarium graminearum* fungal biomass quantification. Where, RP_*FgT*= resistant genotype, Sumai3 point inoculated with trichothecene producing isolate of pathogen isolate (*FgT*); SP_*FgT*= susceptible genotype, Roblin inoculated with pathogen, *FgT*); RP_*Fgt*= Sumai3 inoculated with trichothecene non-producing mutant isolate of pathogen (*Fgt*); SP_*Fgt*= susceptible Roblin inoculated with trichothecene non-producing mutant isolate of pathogen (*Fgt*).

Figure 5.2: The chemical groups of resistant related induced (RRI) metabolites detected in resistant (Sumai3) and susceptible genotypes (Roblin). RRI metabolites accumulated only in Sumai3 upon inoculation of trichothecene producing isolate (*FgT*) and non-producing isolate (*Fgt*) of *F. graminearum* are called as RR_{FgTq} and RR_{Fgtq} respectively. A) RRI metabolites accumulated upon inoculation of trichothecene producing isolate of *F. graminearum* (*FgT*), (B) RRI metabolites accumulated upon inoculation of trichothecene non-producing isolate of *Fg* (*Fgt*), C) A ven diagram showing the classification of identified resistance related induced (RRI), qualitative (not detected in susceptible Roblin) (RR_{FgTq} and RR_{Fgtq}) and RR constitutive (RRC) metabolites following inoculation of *FgT* and *Fgt* isolate.

Figure 5.3: Resistant related metabolites mapped to phenylpropanoid, flavonoid, fatty acids and lipids schematic pathways. Where, 1=phenylalanine ammonia lyase, 2= cinnamate 4-hydroxylase, 3= 4-coumarate:CoA ligase, a = resistant related induced metabolites upon isolate *FgT* inoculation, a*= resistant related induced metabolites only in *FgT* isolate inoculated spikelets but not in mock, b= resistant related induced metabolites upon isolate *Fgt* inoculation, b* = resistant related induced metabolites only in *Fgt* isolate inoculated spikelets but not in mock and e = resistant related constitutive metabolites.

Figure 5.4: Differential expression of host resistance related genes based on semi-quantitative reverse-transcriptase polymerase chain reaction (qRT-PCR) and quantitative real-time PCR (qPCR), in Sumai3 and Roblin spikelets following *F. graminearum FgT* and *Fgt* isolates, at 72 hpi. A) Quantification of host gene expression levels at different cycles of PCR based on band

intensities; B) relative quantification of host genes transcript accumulation based qRT-PCR. Samples inoculated with sterile water are considered as mock control. Wheat Actin gene used as a control for amplicons optimization of the test genes like *TaPR1* (*T. aestivum* Pathogenesis-related 1), *TabHLH* (*T. aestivum* basic helix-loop-helix), *TaSTPK* (*T. aestivum* serine-threonine protein kinase), *TaTLP* (*T. aestivum* thaumatin-like protein) and *TaAGPAT* (*T. aestivum* acyl-glycerol-3phosphate acyl transferase). Where, RP= resistant genotype (Sumai3) inoculated with *FgT*, SP= susceptible genotype (Roblin) inoculated with *FgT*.

Figure 5.5: *T. aestivum* acyl-glycerol-3phosphate acyl transferase (*TaAGPAT*), the orthologous gene *(LPAT2*) from *Arabidopsis thaliana* showing interaction with other host genes and metabolites like glycerophospholipid transferases, phosphatidate, and glycerophospholipid RR metabolites. The highest score for interacting partner of *TaAGPAT* is alpha-glycero-phosphate and phosphatidate cytidyltransferase. Protein-protein interactions are shown in blue, chemical compounds-protein interactions in green and interactions between chemical compounds in red.

LIST OF APPENDICES

RM; resistant genotype (Sumai3) inoculated with mock (sterile water), RP; resistant genotype (Sumai3) inoculated with trichothecene producing pathogen (*FgT*), SM; susceptible genotype (Roblin) inoculated with mock (sterile water), SP; susceptible genotype (Roblin) inoculated with trichothecene non-producing pathogen (*Fgt*).

LIST OF ABREVATIONS

AME	Accurate mass error
AUDPC	Area under the disease progress curve
BAC	Bacterial artificial chromosome
bHLH	Basic helix loop helix
BLAST	Basic local alignment search tool
BSMV	Barley stripe mosaic virus
cDNA	Complimentary deoxyribonucleic acid
CFIA	Canadian food inspection agency
D3G	DON-3-O-glucoside
Da	Daltons
DNA	Deoxyribonucleic acid
DON	Deoxynivalenol
Dpi	Days post inoculation
FC	Fold change
Fg	*Fusarium graminearum*
FHB	Fusarium head blight
GCMS	Gas chromatography and mass spectrometry
GO	Gene ontology
HCAA	Hydroxycinnamic acid amide
Hpi	Hours post inoculation

HPLC	High performance liquid chromatography
ACT	Agmatine coumaroyl transferase
CHS	Chalcone synthase
JA	Jasmonic acid
KEGG	Kyoto encyclopedia of genes and genomes
LCMS	Liquid chromatography and mass spectrometry
LC-HRMS	Liquid chromatography and high resolution mass spectrometry
MAVEN	Metabolomics analysis and visualization engine
MYB	Myeloblastosis
MYC	Myelocytomatosis
NAC	Nascent Polypeptide-Associated Complex
NIL	Near isogenic line
NIV	Nivalenol
NLS	Nuclear localization signal
PAL	Phenylalanine ammonia lyase
PCR	Polymerase chain reaction
PDA	Potato dextrose agar
PDB	Protein database bank
PDS	Phytoene desaturase
Ppm	Parts per million

PR	Pathogenesis related
PSD	Proportion of spikelet diseased
PTGS	Post transcriptional gene silencing
qRT-PCR	Quantitative reverse transcriptase polymerase chain reaction
qPCR	Quantitative polymerase chain reaction
QTL	Quantitative trait loci
RAPD	Random amplified polymorphic DNA
RCBD	Randomized complete block design
RFLP	Restricted fragment length polymorphism
RIL	Recombinant inbred line
RR	Resistance related
RR_{FgTq}	RR Qualitative metabolites upon *Fg* wild isolate inoculation
SNP	Single nucleotide polymorphism
TF	Transcription factor
VIGS	Virus induced gene silencing
ZEN	Zearalenone

ABSTRACT

Fusarium head blight (FHB) is a devastating and dreadful disease of wheat (*Triticum aestivum* L), which not only reduces the yield but also, affects the grain quality by contaminating with health hazardous mycotoxins. Resistance to FHB in wheat is quantitative in nature, and has led to the identification of several quantitative trait loci (QTL), indicating the additive effects of several genes in governing the resistance. Though, more than hundred QTL conferring FHB resistance have been identified in wheat, genetic controls underlying them are still unknown. The QTL-Fhb5 is one of the major FHB resistant QTL conferring high spikelet resistance and has been consistently mapped using different mapping populations in various environments. However, the gene(s) underlying QTL-Fhb5 conferring resistance and the resistance mechanisms are not elucidated. In our study, we made an attempt to dissect the QTL-Fhb5 and functionally characterize it using integrated a metabolo-genomics approach to identify the putative candidate gene(s) and the plausible mechanisms of resistance. To further explore the candidate genes from QTL-Fhb5 the wheat near-isogenic lines (NILs) carrying resistant (R-NIL) and susceptible (S-NIL) alleles of QTL-Fhb5 derived from Sumai3 genetic background were subjected to semi-comprehensive metabolomic profiling. The metabolomic profiling of NILs identified several resistance related (RR) metabolites belonging to phenylpropanoid pathway in R-NIL as compared to S-NIL. Mapping of RR metabolites in metabolic pathways identified phenylalanine ammonia lyase (*PAL*), chalcone synthase (*CHS*) and agmatine p-coumaroyl transferase (*ACT*) as key metabolic pathway enzymes encoding genes. Further, upon dissection of QTL-Fhb5 using flanking markers, we identified an MYB transcription factor, designated here as *TaMYBFhb5*, GenBank ID: AHZ33834.1, is localized within the QTL locus. The transcriptional regulation of RR metabolite biosynthetic genes by *TaMYBFhb5* TF was confirmed through electrophoretic mobility shift assay (EMSA). The functional characterization of *TaMYBFhb5* gene through virus induced gene silencing (VIGS), not only reduced the RR metabolite abundances through downregulation of metabolic pathway genes expressions, but also increased the fungal biomass accumulation and disease severity in silenced R-NIL as compared to non-silenced R-NIL. Further, the resistance functions of *TaMYBFhb5* gene was also validated by silencing in Sumai-3 (resistance source of QTL-Fhb5) based on VIGS. To identify the spikelet resistance genes and metabolites induced during *F. graminearum* (*Fg*) invasion, we inoculated two wheat genotypes Sumai-3 (resistant) and Roblin (susceptible) with trichothecene producing wild-isolate (*FgT*) and

non-producing mutant-isolate (*Fgt*) of *Fusarium graminearum* and subjected them to metabolome profiling and disease severity analysis. Interestingly, both the genotypes showed spikelet infection symptoms within 48 hours post inoculation (hpi) with *FgT* and *Fgt*, indicating both the isolates can cause infection. This clearly suggested that the trichothecenes are not essential to infect spikelets. However, the disease severity was higher in the susceptible than in the resistant genotype, especially following *FgT* infection. In addition, we observed a higher accumulation of phenylpropanoids, lipids, fatty acids and flavonoids in spikelets of the resistant genotype than in susceptible genotype. A semi-quantitative and real-time quantitative PCR revealed the differential accumulation of transcripts for selected biotic stress resistance *R* genes, in Sumai3 and Roblin spikelets infected with *FgT* and *Fgt*. The fungal biomass and deoxynivalenol (DON) trichothecene accumulation in spikelets of Sumai3 were significantly lower than in Roblin. This is the first report on decoding the genetic controls underlying QTL-Fhb5 in wheat for FHB spikelet resistance. The *TaMYBFhb5* gene can be used for replacement in commercial elite wheat genotypes, based on genome editing to improve resistance against FHB.

RÉSUMÉ

La fusariose de l'épi du blé (FEB) est une pathologie dévastatrice du blé (*Triticum aestivum* L), qui en plus de réduire le rendement des récoltes, affecte la qualité des grains alors que l'agent pathogène les contamine en produisant des mycotoxines dangereuses pour la consommation humaine. La résistance à la FEB chez le blé est de nature quantitative comme en témoigne la découverte de plusieurs locus à caractère quantitatif (abrégé par QTL pour *quantitative trait loci*). D'ailleurs, la découverte de ces derniers suggère que le contrôle de la résistance à la FEB est orchestré par l'intervention de plusieurs gènes. Bien que plus d'une centaine de QTLs associés à la résistance à la FEB aient été identifiés chez le blé, les facteurs génétiques qui contrôlent cette résistance restent jusqu'à ce jours inconnus. Conférant une résistance accrut des épillets face à la FEB, le QTL-Fhb5 est reconnu comme étant l'un des principaux QTL de résistance à la FEB pour avoir été mappé de façon cohérente en utilisant différentes populations provenant d'environnements variés. Malgré tout, le ou les gène(s) associé(s) au QTL-Fhb5 qui contribue à la résistance ainsi que le mécanisme contrôlant cette résistance n'ont toujours été élucidés. Dans cette étude, nous avons tenté de disséquer et caractériser la fonction du QTL-Fhb5 en utilisant une approche métabolo-génomique intégrée pour identifier le ou les gène(s) candidat(s) putatif(s) et un mécanisme plausible de résistance. Dans le but d'approfondir nos recherches pour des genes candidats de QTL-Fhb5, des lignées de blé quasi-isogéniques (abrégé par NILs pour *near-isogenic lines*) dérivé du bagage génétique du genotype Sumai3, et possédant des allèles résistants (R-NIL) et susceptibles (S-NIL) du QTL-Fhb5 ont été sujets à un profilage métabolique semi-compréhensif. Ce profilage a permis d'identifier plusieurs métabolites reliés aux résistances (RR) provenant du cycle de production des phénylpropanoïdes chez R-NIL lorsque comparé au S-NIL. Un mappage des métabolites RR au niveau des voies métaboliques a permis d'identifier les enzymes phénylalanine ammonia-lyase (*PAL*), chalcone synthase (*CHS*) et agmatine p-coumaroyl transferase (*ACT*) comme étant cruciales à l'encodage de gènes *R*. De plus, la dissection du QTL-Fhb5 par l'utilisation de marqueurs flanquants nous a permis d'identifier un facteur de transcription de type MYB, désigné *TaMYBFhb5*, GenBank ID: AHZ33834.1, localizé dans le locus du QTL. La régulation transcriptionnelle des gènes necessaire à la biosynthèse des métabolites RR par *TaMYBFhb5* fut confirmer par la conduite d'une analyse de mobilité électrophorétique (abrégé par EMSA pour *electrophoretic mobility shift assay*). Par ailleurs, une charactérization fonctionelle du gène *TaMYBFhb5* par silençage

génique viral (abrégé par VIGS pour *virus induced gene silencing*) a réduit l'abondance des métabolites RR via la régulation négative de l'expression des gènes associé aux voies métaboliques en plus d'augmenter la biomasse fongique et la sévérité pathologique pour la lignée silencée R-NIL lorsque comparée à la lignée R-NIL non-silençée. De plus, la fonction de résistance pour le gène *TaMYBFhb5* a aussi été validé en le silençant par VIGS dans le genotype Sumai3 (source de la résistance du QTL-Fhb5). Dans le but d'identifier les gènes de résistance des épillets et les métabolites produits lors d'une invasion par *F. graminearum* (*Fg*), nous avons inoculé deux genotype s de blé, Sumai-3 (résistant) et Roblin (susceptible) avec un isolat sauvage du pathogène produisant des trichothecenes (*FgT*) et un isolat mutant déficient en trichothecenes pour finalement conduire des analyses de sévérité pathologique et produire un profilage métabolique. Fait intéressant, les deux genotype s ont démontré des symptômes d'infection 48 heures après l'inoculation (hpi) avec *FgT* and *Fgt,* indiquant que les deux isolats peuvent générer une infection. Ceci suggère fortement que les trichlothecenes ne sont pas essentiels à l'infection des épillets. Cependant, lorsque comparé aux plantes résistantes, la sévérité pathologique fu plus élevé chez les plantes susceptibles surtout lorsque infectées avec *FgT*. Additionnellement, nous avons observé une accumulation plus importante de phenylpropanoïdes, lipides, acides gras et flavonoïdes dans les épillets des plantes résistantes plutôt que dans ceux des plantes du genotype susceptible. Des techniques de PCR semi-quantitative ainsi que quantitative en temps réel nous ont permis d'observer une différence dans l'accumulation des transcrits de genes de résistance aux stress biotiques *R* sélectionnés entre les épillets infectés par *FgT* et *Fgt* des genotype s Sumai3 et Roblin. La biomasse fongique et l'accumulation de deoxynivalenol (DON) dans les trichothecenes pour les épillets du genotype Sumai3 sont significativement plus bas que dans les épillets du genotype Roblin. Cette publication est la première à rapporter le décodage du contrôle génétique du QTL-Fhb5 chez le éblé pour la résistance des épillets à la FEB. Ainsi, le gène *TaMYBFhb5* pourrait être remplac par éditage génomique dans les genotype s commerciaux élites dans le but d'améliorer leur résistance à la FEB.

ACKNOWLEDGEMENT

My memories about the initial days at the Plant Science Department and MacDonald campus are unforgettable. This piece of work would not have been a reality had it not been for one man in the Plant Science Department i.e., **Dr. Ajjamada C. Kushalappa**, Associate Professor, McGill University. It is my immense pleasure to have such a wonderful supervisor with a constant bundle of inspiration during my Ph.D. program. He was always encouraging and very open to the fresh thoughts and new ideas to fulfill my Ph.D. research objectives. I take this opportunity to express my whole hearted gratitude for his constant support during ups and downs of my Ph.D. research. Thank you very much sir, for your valuable guidance and timely comments that gave me immense pleasure to work with you and because of which my stay at the Plant Science Department was a memorable one. My sincere thanks to **Dr. Jean-Benoit Charron** and **Dr. Jaswinder Singh,** the members of my Advisory Committee for their critical evaluation and valuable suggestions during my research work.

I am also grateful and wish to express my whole hearted thanks to Dr. Martina Stromvik for serving as chair for my Ph.D. comprehensive exam and her constant guidance in bioinformatics work. Special thanks to Professor. Timothy Geary from Institute of Parasitology, Dr. Raj Duggavathi from Animal Science Department and Dr. Joan Whalen from Department of Natural Resource Sciences for their valuable suggestions and serving as committee members for my Ph.D. comprehensive exams. Most importantly, my humble thanks to Dr. C. McCartney from Agriculture and Agri-Food Canada, Winnipeg, Canada for valuable suggestions and genetic materials (wheat seeds) used in my Ph.D. research.

I am equally grateful to my lab mates, Dr. Raghavandra Gunnaiah, Dr. Shailesh Karre, Dhananjay Dhokane, Dr. Uday Kumar, Liyao Ji, Kobir Sarkar, Pushpa, Nancy Soni and Sripad Joshi, Russiachand, Niranjan Hegde, Fatemeh Kalantari, Xue Huali, Dr. Arun Kumar, Dr. Yogendra Kalenahalli, Dr. Kareem Mosa and Dr. Kundan Kumar for their constant support and healthy discussion about the recent articles on science and troubleshooting the research problems. Without them my research work would not have been successful. Their critical comments and suggestions helped me to bring out this thesis in the best way possible.

It would be hypocrisy if I forget to mention the help, criticism, timely suggestions and

care that Dr. Alinne Ambrosio. Reshmi Raman, Meena, Dr. Shashidhar Parsi, Dr. Impa SM, Dr. Nadaradjan S, Dr. Mohan Kumar, Dr. Shalini R, Sujitha AS, Ms. Pratyusha Chennupati, Dr. Asma Tufail, Dr. Selvakumari Arunachelam, Dr. Asim Biswas and Dr. Sheshshayee MS bestowed on me during ups and downs of my stay at McGill University.

I also express my deep sense of gratitude to Carolyn, Lynn Bachand and other staff members of Plant Science Department for their help during my stay at Plant Science Department. I also thank Mr. Guy Rimmer and Mr. David Wees and Mr. Ian Ritchie for their help in smooth conduct of lab work as well as greenhouse work.

I would like to thank my undergrad friends Mr. Mahantesh. T (PSI)., J. Prakash Reddy, Kallanagouda Patil (Inspector), Satish HS (PSI), Prashant Kulkarni (Bank Manager), Shivasharana and Bhima Shankar Teggelli (Asst Commissioner) and my brothers, Mr. Gangadhar Hukkeri and Mr. Madiwal Hukkeri for their constant support and encouragement during my studies.

On a Personal note I would like to thank my parents, brothers and sister without their moral support I would not have ventured out seeking to undertake my higher studies.

PREFACE AND CONTRIBUTION OF THE AUTHORS

Preface

This thesis is written in a manuscript format according to the McGill University guidelines. The overall thesis work is presented in three chapters (III to V) representing three separate manuscripts, all of which are either submitted for publication or in submission process. Each chapter involves both metabolomics and genomics to understand the plant-pathogen interaction and to identify the resistance related metabolites and host resistance gene(s) against *Fusarium graminearum* infection in wheat. Functional characterization of identified genes were carried out to understand their role in Fusarium head blight (FHB) disease resistance based on metabolomics, differential expression analysis and virus induced gene silencing (VIGS) in wheat genotypes and near isogenic lines (NILs). The major outcomes of each study may help in combatting against FHB and improve the food security and detailed description of the author's contributions scientific knowledge is mentioned below.

- The MYB transcription factor *TaMYBFhb5* gene identified from wheat QTL-Fhb5 is regulating both phenylpropanoid and flavonoid pathway enzymes encoding genes necessary for controlling Fusarium infection.
- The RR metabolites identified in this study were submitted in McGill metabolome database and genes sequences and the QTL-Fhb5 flanking markers and *TaMYBFhb5* gene were submitted to NCBI database.
- The identified MYB transcription factor *TaMYBFhb5* gene in the current study can be employed in developing the FHB resistant genotype s based on genome editing in susceptible wheat and barley genotype s.
- The methodology developed in this study to dissect the QTL and functionally characterize the fine mapped QTLs can be employed to several other major effect QTLs conferring FHB resistance in wheat and barley.
- The host resistance gene(s) identified in this study can be used to introgress into susceptible genotypes based on marker assisted breeding upon functional characterization and marker validation.

Authors contribution

This thesis contains three studies as chapter III, IV and V presented in manuscripts formats. All the three studies were designed by me with my supervisor Dr. Ajjamada C. Kushalappa. I have conducted the both greenhouse and growth chamber experiments, standardized the wheat QTL sequencing methodology, analyzed the metabolic data and genomic sequences. The data presented in manuscripts and with the help of my supervisor Dr. Ajjamada C. Kushalappa. He has provided research funds, guided in conducting the experiments, facilitated for molecular research, and writing the manuscripts.

The first manuscript (chapter III) was co-authored by Karre S., Kushalappa AC, Charron JB and Raj Duggavathi. Dr. Karre helped in greenhouse and laboratory experiments. Dr. Kushalappa helped in designing the experiments and guided in writing and thoroughly edited the manuscript. Dr. Raj Duggavathi supervised qRT-PCR experiment and edited the manuscript. The second manuscript (chapter IV) was co-authored by Udaykumar Kage, Kushalappa and Dion Y. Dr. Dion Y developed wheat genotypes used in the study and helped in correcting the manuscript. Dr. Udaykumar helped in conducting the greenhouse experiments and metabolites analysis. Dr. Kushalappa helped in designing the experiment and thoroughly edited the manuscript. Third manuscript (chapter V), co-authored by Ji L. and Kushalappa A.C. Dr. Kushalappa guided in conducting the experiments and correcting the manuscript. Ms. Ji L contributed in MSMS fragments matching from the existing metabolome databases.

CHAPTER I: GENERAL INTRODUCTION

Cereals are the most important food crops providing more than 50% of the food energy on earth (Stoskopf, 1985). Among the top three cereals representing about 90% of cereals production globally, Wheat (*Triticum aestivum* L.) is one of the major contributors (http://faostat.fao.org//). Globally wheat is grown in more than 70 countries and is a major food supplier in the world (Dixon et al., 2009). Global forecast of wheat production for the year 2015/16 was 733.0 million tons covering one-third of the world's total grain production (FAO 2016: http://www.fao.org/worldfoodsituation/csdb/en/). Canada has jumped its position to sixth among leading projected wheat producing countries for 2015/16 (USDA), due to significant improvement in genetic potential of elite cultivars and agronomic practices. On the other hand, ever-increasing global population, innumerable biotic and abiotic stresses, reducing cultivable land and uncertainty of climate changes are constantly enforcing the need for improvement in wheat productivity (Chakrabarti et al., 2011). It is inevitable to have a large gap between global food demand and actual wheat production in the near future. This is one of many ways to meet global food demand by increasing the wheat yield potential through overcoming biotic and abiotic stresses (Hawkesford et al., 2013).

Among the biotic stresses of wheat, Fusarium head blight (FHB), caused by *Fusarium graminearum* Schwabe (Teleomorph: *Gibberella zeae* (Schwein) Petch), is one of the major destructive and dreadful diseases of common wheat (*T. aestivum* L.), as it has drastic impacts not only on the economy, but also on human and animal health (Bai et al., 2002; Gilbert and Tekauz, 2000; McMullen et al., 2003). The drastic reduction in grain yield and mycotoxins contamination is inevitable upon *Fusarium graminearum* infection in wheat (Goswami and Kistler, 2004). The mycotoxins contaminated food grains from the field continue its degradation during their improper storage, making unsuitable for consumption (Schmidt et al., 2016). The Food and Agriculture Organization (FAO) survey indicates that, annually 25% of the agriculture crops were contaminated with mycotoxins worldwide, with waste accounting for nearly 1 billion metric tons of foods and food products. Particularly, mycotoxin contaminated loss in the United States and Canada is estimated to be $5 billion per year (Matny, 2015). These mycotoxins belonging to the group trichothecenes, of which deoxynivalenol (DON) and nivalenol (NIV) possess serious health concerns (Desjardins and Hohn, 1997). The estimated losses due to DON

contamination alone accounts up to $655 million/year in United States (Matny, 2015). The Canadian Food Inspection Agency (CFIA) rejects grains with more than 1ppm DON for human consumption (McMullen et al., 1997). These mycotoxins affect the proteins biosynthesis, ribosomal activities and DNA synthesis at the cellular level in animals (Yoshio et al., 1973). Hence, there is an urgent need to control the FHB disease and its impact on economy.

The integrated approaches are essential to tackle the FHB menace in cereal crops. The components of an integrated pest management (IPM) system should be employed to manage the disease (Razdan and Sabitha, 2009). To manage FHB, mainly three strategies have been used to manage FHB: a) cultural management practices, b) fungicide application and c) development of resistant varieties. Cultural practices include crop rotation, weed management and tillage practice, which can reduce fungal survival on crop residue, and staggered planting of small grain crops (Stack, 2000). FHB severity can be reduced by 50 to 60 % through application of fungicides, but it is environmentally undesirable and also the results are variable, depending on the environmental conditions (Stack, 2000). Growing genotypes that have host resistance against *F. graminearum* infection and toxin production is the best way to manage mycotoxins. However, the resistance in wheat to FHB is complex and inherited quantitatively, involving cumulative resistance effects of several genes. Also, the interactions among pathogen, trichothecenes, environments and genotypes makes it a more arduous task to understand the resistance mechanism. Apart from that, the development of resistant cultivars has been very challenging because of limited genetic understanding of resistance and lack of cost-effective means of phenotyping (Bai and Shaner, 1994; McMullen et al., 1997). Based on conventional breeding approaches, several resistant varieties have been identified in wheat against FHB and DON accumulation (Bartos et al., 2002; Mesterhazy, 1997). However, the conventional breeding approaches for selecting a variety with suitable levels of resistance to biotic stress or abiotic stress will take six to seven generations. To overcome this, molecular breeders have identified several QTL which can provide hints for genomic regions encompassing FHB resistance-associated genes.

Resistance in wheat to FHB has been mainly quantified as spikelet resistance to initial infection (Type I), based on disease incidence, and resistance to spread of the disease within the spike (Type II), based on disease severity, (Schroeder and Christensen, 1963), and resistance to

accumulation of DON (Type III) (Miller and Sampson, 1985). The Type I resistance is considered to be mainly due to morphological characters, which is also considered as avoidance. However, the Type I resistance to spikelet infection was assessed as percentage or proportion of spikelets diseased in a spike (Buerstmayr et al., 2003). For the discovery of resistance related (RR) metabolites, the true resistance in wheat and barley against FHB was defined as: i) Proportion of spikelets diseased (PSD): based on proportion of spikelets diseased in an average spike, following spray inoculation; ii) Resistance to spread within spikelet: based on amount of fungal biomass in individually inoculated spikelets; iii) Rachis resistance or resistance to spread within spike through rachis: based on single spikelet inocultion and assessment of PSD or the amount of fungal biomass in rachis (Bollina et al., 2010; Kumar et al., 2015; Kage et al., 2016). The molecular breeding approaches can reduce the duration of development of cultivar with suitable levels of resistance based on the molecular markers. More than one hundred FHB resistant QTL have been mapped, and a few of them have been validated and used in molecular breeding (Buerstmayr et al., 2009). Among these, the QTL mapped on the chromosomes 3BS, 2D, 5A and 6B are reported to be stable across different genetic backgrounds and environments (Anderson et al., 2001; Bai and Shaner, 2004; Yang et al., 2005a; Yang et al., 2005b). The resistance mechanisms governed by these QTL are yet to be understood, except for the QTL-Fhb1 with rachis resistance. Though earlier FHB resistance was claimed due to detoxification of DON within plant cells through glucosyltransferase (D3G) gene from *Fhb1,* no significant difference was observed for proportion of DON converted to D3G (PDC) in wheat NILs (Lemmens et al., 2005: Gunnaiah et., 2012). Recent study shows that the *Fhb1* resistance function is associated with the pore forming toxin-like (PFT) gene (Rawat et al., 2016). However, the same research team said that this is just a beginning as actual function of the gene is yet to be revealed. In the same study, QTL-Fhb5 has shown additive effect on conversion of DON to D3G in combination with the *Fhb1* locus but, not individually. Although, *Fhb5* has shown resistance to DON accumulation in combination with *Fhb1* locus, its individual effect and other resistance mechanisms associated to FHB resistance are yet to be understood. However, the Canadian spring wheat showed high rate of conversion of toxic DON to non-toxic D3G when challenged with DON and 15-ADON producing isolates (Amarasinghe et al., 2016). Also, the transcriptomic analysis of wheat FHB resistant genotype, Sumai3 upon 3ADON and 15-ADON chemotypes exposure revealed differential expression of host genes (Al-Taweel et al., 2014).

The transcriptomics analysis of the wheat lines carrying both QTL-Fhb1 and QTL-Fhb5 also revealed that the complimentary effect of uridine diphosphate (UDP)-glycosyltransferase gene during *Fusarium* pathogenesis (Schweiger et al., 2013). Recently, several FHB resistance QTLs identified by using a native Canadian spring wheat as one of the donor parent for RILs of the cross Kenyon/86ISMN 2137 (McCartney et al., 2016). Meta QTL analysis of FHB resistance related QTLs revealed QTL-Fhb5 as major effect QTL for FHB resistance in RILs derived from the cross HYZ and Wheaton (Cai, 2016). Four FHB spikelet resistance QTLs mapped on 1BL, 2BL and 3AS explainbetween 7.44 to 12.20% variance in wheat (Sun et al., 2016). The additive effect of both QTL-Fhb1 and QTL-Fhb5 in DH lines derived from Sumai3 genetic background, significantly reduced the FHB disease severity, *Fusarium spp.* damaged grains (FDG) and DON accumulation (Suzuki et al., 2012). The QTL *Fhb5* (*Qfhs.ifa-5A*) on the short arm of 5A chromosome has explained 60% of phenotypic variance in spikelet resistance (Xue et al., 2011). However, genes controlling the spikelet resistance are unknown. The QTL *Fhb5* has been consistently associated with spikelet resistance in different genetic backgrounds, such as CM-82036 (Buerstmayr et al., 2003), DH181 (Yang et al., 2005b), Wangshuibai (Lin et al., 2006; Xue et al., 2011), W14 (Chen et al., 2006; Somers et al., 2003). It has explained 34%, 36% and 60% of phenotypic variance for spikelet resistance, in three different studies (Chen et al., 2006; Lin et al., 2006; Xue et al., 2011). *Fhb5* has shown an additive effect when pyramided with other QTL such as *Fhb1* for enhanced FHB resistance (Somers et al., 2005), and increased DON detoxification (Lemmens et al., 2005). Therefore, targeted sequencing of the genomic hot spot regions is essential to unravel the underlying genes. The next generation sequencing technologies has enabled the fast release of the first survey of chromosome 5A DNA sequence (Vitulo et al., 2011).

The dissection of QTL to identify the co-localized genes and validate their function remains a challenge due to the highly repetitive sequences of the wheat genome. Several molecular approaches have also been used to identify the genes involved in FHB resistance, like map based positional cloning, *in-silico* analysis, mutational breeding, fine mapping and RNA sequencing. Positional cloning of QTL-Fhb1 has revealed seven putative genes underlying a 261kb region of BAC clones, and the transgenic wheat lines developed for four putative genes revealed no rachis resistance (Liu et al., 2008). A mutation induced recessive allele (*Mlo*) showing broad spectrum resistance to a fungal pathogen, *Erisiphe graminis* f.sp. *hordei* was

isolated using positional cloning approach in barley (Buschges et al., 1997). The *VRN1* gene controlling vernalization has been identified through positional cloning in *T. monococcum* (Yan et al., 2003). However, positional cloning has been limited to small genomes, and its application remains very difficult for large genome species like hexaploid wheat and diploid barley with high repetitive (>80%) genomes (Feuillet et al., 2003). Fine mapping of wheat QTL-Fhb1 based on expressed sequence tags (ESTs) STS markers revealed orthologous genes between rice and barley (Liu et al., 2006) Similarly, the dissection of QTL associated with agronomic traits based on molecular markers revealed the association of plant productivity gene(s) on chromosome 7AL (Quarrie et al., 2006). *In-silico* mining of eight FHB resistance QTLs led to the identification of plant defense related, immune regulation and cellular detoxification genes (Choura et al., 2016). The QTL-Fhb1 (*Qfhs.ndsu-3BS*) conferring rachis resistance was fine mapped to 1.27cM using mapping populations derived from the cross Sumai3*Thatcher and to 6.05cM in HC374/3*98B69-L47 cross. These tightly associated QTL-Fhb1 flanking markers were suggested for marker assisted breeding in wheat (Cuthbert et al., 2006). Further, fine mapping of QTL-Fhb1 based on BAC sequencing and RNA sequencing revealed nearly 28 genes. However, only Gly-Asp-Ser-(Leu) (GDSL) motif bearing lipid hydrolyzing enzyme (lipase) encoding gene was up-regulated during *F. graminearum* infection in wheat (Schweiger et al., 2016). The candidate genes from the resistance QTL controlling the *Phytophthora sojea* disease were identified by dissecting the QTL through long range PCR (LR-PCR) product sequencing and consequently SNPs (1025) were identified in soybean (Wang et al., 2012). The activation tagging also led to the identification of MYB transcription factor, which regulates phenylpropanoid biosynthesis in Arabidopsis (Borevitz et al., 2000).

In recent years, the advancement in high through-put technologies, such as metabolomics, proteomics and transcriptomics, simplify the complexity of *F. graminearum* and host interactions during pathogenesis. The metabolo-proteomic analysis of *Fhb1* in NILs, derived from Nyubai cultivar, showed the association of cell wall strengthening of the rachis with hydroxycinnamic acid amides (HCAAs), phenolic glucosides and flavonoids against FHB (Gunnaiah et al., 2012). The metabolomics technology is one of the cutting edge tools for the elucidation of plant resistance mechanisms against biotic stress (Bollina et al., 2010; Tohge and Fernie, 2010). Several resistance-related (RR) metabolites in barley spikelets against FHB have been identified and linked to their metabolic pathways (Bollina et al., 2010; Bollina et al., 2011;

Kumaraswamy et al., 2011a). Among these RR secondary metabolites, *p*-coumaric acid, Sinapic acid, Naringenin, Catechin and Kaempferol glucoside metabolites were selected as biomarker metabolites for potential application in plant breeding (Bollina et al., 2011; Kumaraswamy et al., 2011b). Similarly, the NMR analysis of *Fusarium spp.* infected spikelets in wheat varieties like FL62R1, Stettler, Muchmore and Sumai3 revealed the RR metabolic pathways activation against FHB resistance and these metabolites can be employed as biomarkers (Cuperlovic-Culf et al., 2016). The FHB resistance mechanism controlled by QTL-Fhb1 has been shown to be due to cell wall apposition, through hydroxycinnamic acids (HCAAs), flavonoids and phenolic glucosides (Gunnaiah et al., 2012). The metabolites act as phenotype for identifying the genes responsible for variations within genetic mapping population is called as forward genetics, whereas gene mutation or transgenic plants revealing the differences in metabolite accumulation is called reverse genetics (Tohge and Fernie, 2010). Therefore, metabolomics is a forward genetics approach, where metabolites are the end products of cellular processes and thus can be used as clear phenotypes for identifying the genes encompassed by FHB QTLs. Metabolome analysis of wheat NILs upon *F. graminearum* inoculations identified the hydroxycinnamoyl transferase (HCT) gene from phenylpropanoid pathway through semi-quantification of *Fusarium spp.* induced RR metabolites (Gunnaiah et al., 2012). Transcriptomics of wheat and barley, upon *Fusarium spp*. infection, revealed high fold transcripts accumulation for genes encoding mycotoxin detoxification, transport proteins, ubiquitination-related proteins, programmed cell death proteins and transcription factors (Boddu et al., 2006; Golkari et al., 2007).

Among the various proteins expressed during biotic and abiotic stresses, plant transcription factors (TF), such as MYB, AP2, NAC, MYC and WRKY were known to regulate the downstream genes involved in defense mechanisms (Bray, 1997; Mengiste et al., 2003). Particularly, the plant MYB TF encoding genes were well characterized against biotic and abiotic stresses in Arabidopsis (Ambawat et al., 2013). The presence of conserved MYB domains and divergent C- terminal regions are the key criteria to classify the MYB proteins. These conserved motifs were used to classify the MYB genes in Arabidopsis (Kranz et al., 1998; Stracke et al., 2001). The identification of avian myeloblastosis virus oncogene gene (*v-myb*) has led to the discovery of MYB genes and family MYB related genes (Lipsick and Wang, 1999). Functional genomic analysis, of MYB transcription factor overexpression in Arabidopsis, based on transcriptomics and metabolomics revealed the molecular network of glucosinolate

metabolism and a few novel genes involved in flavonoid biosynthesis (Tohge et al., 2005). The transcriptional regulations of metabolic pathways genes like ferulate-5-hydroxylase (*F5H*) and phenyl ammonia lyase (*PAL*) in arabidopsis and tobacco, respectively were regulated by MYB transcription factors (Braun et al., 2001). The FHB resistance mechanism involves ethylene and JA signaling along with upregulation of several transcription factors in wheat (Li et al., 2008b). Hence, it is imperative to study the co- regulation of host genes involved in FHB disease resistance mechanisms.

The functional characterization of novel genes identified is pivotal to apply for breeding programs. Among the tools employed to functional characterization, RNA interference (RNAi) induced gene silencing is more efficient, eco-friendly and easy to handle (Waterhouse and Helliwell, 2003; Younis et al., 2014). Similarly, the transient suppression of the target gene without carrying forward the mutation to the next generation is essential. Hence, RNAi-based virus induce gene silencing (VIGS) is a highly effective, easy to handle, and powerful tool for transient suppression of a target gene for crop improvement in different crops, such as wheat (Scofield and Brandt, 2012), rice (Kant et al., 2015), barley (Holzberg et al., 2002), tobacco (Ramegowda et al., 2013), tobacco (Liu et al., 2002), and tomato (Fantini et al., 2013). The attenuated barley stripe mosaic virus (BSMV) is more efficient and less damaging to host cells and hence, we can reduce the stress induced by the viral vectors (Buhrow et al., 2016). Other major functional genomics tools employed to understand the gene functions are, loss of function through mutagenesis in *Arabidopsis thaliana* (Ostergaard and Yanofsky, 2004), gain of functions (Kondou et al., 2010), over expression (Aukerman and Sakai, 2003) and activation tagging (Nakazawa et al., 2003). However, the afore-mentioned tools are associated with the permanent suppression, or gain of the gene function, meaning absent or over expression of the gene in progeny. This might cause the imbalance in genetic evolution in future. Hence, VIGS is an eco-friendly and efficient tool for functional elucidation of novel genes in plants. Recently a novel concept of resistance has been proposed. The resistance in plants against biotic stress is due to hierarchies of genes that eventually biosynthesize RR metabolites, which in turn suppress the pathogen, or contain the lesion to initial infection (Kushalappa et al., 2016a). The commercial cultivars are expected to have most of the hierarchies of *R* genes, except for a few which are polymorphic and disabling them to biosynthesize RR metabolites which suppress the pathogen progress in plant, thus the resistance (Kushalappa et al., 2016b).

In this direction, the current study was carried out by integrated genomics and metabolomics approach to identify the genes underlying QTL-Fhb5 and functional characterization of candidate genes based on transient suppression of their expression to understand the spikelet resistance against *F. graminearum* in wheat near isogenic lines (NILs). The novel gene (*TaMYBFhb5*) encoding the transcription factor (TF) identified through QTL-Fhb5 (*Qfhs.ifa-5A*) dissection, based on primer walking approach was functionally characterized based on metabolo-genomics approach and several host genes identified were assessed based on differential genes expression during *F. graminearum* infection. Further, the transient expression and metabolome analysis of *TaMYBFhb5* TF encoding gene in Sumai3 confirmed MYB TF is a key regulator of RR metabolic pathway enzymes encoding genes.

General Hypothesis

The wheat NILs with contrasting alleles for spikelet resistance to FHB at QTL-Fhb5 derived from Sumai3 also vary in their metabolites accumulation and associated genes expressions, especially following pathogen inoculation. Resistance in plant against biotic stress is due to hierarchies of genes that eventually biosynthesize resistance related metabolites. In susceptible genotypes, however, most of these genes in the hierarchy are functional except for one or a few which disables the genotype to produce RR metabolites and RR proteins (metabolic pathway enzymes), thus rendering it to susceptibility. Therefore, the candidate resistance genes are functional in resistant NIL and are mutated or nonfunctional in susceptible NIL, disabling it to produce a few specific metabolic pathway related RR metabolites.

General Objectives

1. To identify the candidate genes in the QTL-Fhb5 and to functionally characterize the most important genes associated with FHB resistance.

2. To validate the function of *TaMYBFhb5* TF in Sumai3 wheat genotype, harboring QTL-Fhb5, for spikelet resistance against FHB, based on virus induced gene silencing (VIGS).

3. To identify spikelet resistance related metabolites in FHB resistant and susceptible wheat genotype s Sumai3 and Roblin, respectively, based on trichothecene producing and non-producing *F. graminearum* infection and differential expression analysis of resistance gene(s).

CHAPTER II: REVIEW OF LITERATURE

2.1 Importance of wheat

The expected global population by the end of 2050 is speculated to increase from the current 7.3 billion to 9.7 billion according to the United Nations report (http://www.un.org/2015-report). As per International Development Research Centre (IDRC) wheat is one of the major staple food crops for more than 35 percent of the global population (http://www.idrc.ca/565). Improving wheat production to meet the ever increasing global food demand is an arduous task due to constant confrontation with extreme biotic and abiotic stresses. The major wheat breeding institutes like International Maize and Wheat Improvement Center (CIMMYT) and International Center for Agricultural Research Dry Areas (ICARDA) have developed around 4604 varieties. The Consultative Group on International Agricultural Research (CGIAR) has released 2893 varieties from 1994-2014 (Lantican et al., 2016). Wheat is one of the rich sources of food grain for proteins, starch, soluble sugars, cellulose, fats and micronutrients like iron (Fe) and Zn and vitamins like thiamine and riboflavin. Several wheat lines were identified in Mexico, India and Pakistan with high Fe and Zn concentrations (Velu et al., 2012). More than two billion people are facing serious health problems due to Fe and Zn deficiency, globally (Velu et al., 2014). Exploring the existing wheat germplasm for improved micronutrient content to develop the varieties is an attractive and more sustainable solution to overcome the micronutrient deficiency in human diet (Borrill et al., 2014).

With the Green revolution the productivity of wheat increased, however, overcoming the biotic stress has always been a bottleneck, resulting in drastic reduction in both quantity and quality of agriculture products. Among the biotic stress, Fusarium head blight (FHB) is considered to be the most devastating disease, reducing both yield and quality of wheat grains by contaminating with mycotoxins (Gilbert and Tekauz, 2000).

2.2 Fusarium head blight of wheat

Fusarium head blight (FHB) is a serious problem for small grain cereals in warm and humid weather conditions around the globe (Parry et al., 1995). There are more than 17 *Fusarium* species (*spp*) known to cause FHB in small grains, and some common ones are: *F. culmorum, F. avenaceum, F. sporotrichioides, F. poae* and *Microdochium nivale* (Mesterhazy et

al., 2005). Among these the *Fusarium graminearum* Schwabe [Teleomorph: *Gibberella zeae* (Schweinitz) Petch], is the most prevalent species in most parts of the world. FHB largely caused by *F. graminearum* in wheat, is a destructive disease (Schroeder and Christensen 1963). The warm and humid climatic conditions favor the perithecia (fruiting body) to develop and produce the ascospores (Doohan et al., 2003; Shaner and Buechley, 2003). The most favorable condition for infection and development is 25^{o} C and moisture for 36 to 72 hours (Rossi et al., 2001). The dark brown spots are the first symptoms observed after the infection, and later the entire spikelet becomes blighted. The spikelets are most susceptible at anthesis. Following this, the pathogen colonizes other spikelets through rachis (Jansen et al., 2005).The fungus can survive as a saprophyte in infected crop residue of wheat, rice or maize (Gilbert and Tekauz, 2000; Muthomi et al., 2002). The sexual and asexual spores, ascospores and macroconidia, respectively, are the major source of inoculum, and the dissemination is aerial (Osborne and Stein, 2007; Parry et al., 1995; Sutton, 1982). These spores are deposited on spikelets by wind or water splash, and they germinate and enter through cracks between the lemma and palea of wheat (Schmale and Bergstorm, 2003; Shaner and Buechley, 2003; Yoshida et al., 2005).

2.3 Fusarium mycotoxins as virulent factors during pathogenesis

Fusarium spp. produces a group of sesquiterpenoid compounds called trichothecenes. Mainly, four types of trichothecenes (A, B, C and D) have been identified from the trichothecene producing fungi. The major trichothecenes produced by the *Fusarium spp*. includes deoxinivalenol (DON) and their acetyl derivatives, such as, 3-*O*-acetyl 4-deoxynivalenol (3ADON) and 15-ADON, nivalenol and zearelonone belonging to Type B trichothecenes (Desjardins and Proctor, 2007; Foroud and Eudes, 2009). The investigation of mycotoxin accumulation and *F. graminearum* chemotype diversity on consecutive years in southwestern Ontario, showed a shift from 15-ADON to 3ADON chemotypes (Tamburic-Ilincic et al., 2015). Recently, a new species *Fusarium cerealis* was reported in Canada, which biosynthesizes NIV trichothecene, causing FHB in winter wheat (Amarasinghe et al., 2015). The NIV and DON producing isolate inoculations at post flowering stage in wheat indicated that the NIV chemotypes are less damaging as compared to DON chemotypes (Nicolli et al., 2015).

The DON contaminated grains in the feed has led to reduced feed intake, and the concentrations of more than 10 ppm are known to cause vomiting and feed refusal (De Wolf et

al., 2003). Trichothecenes inhibit peptidyl transferase activity of ribosomal 60s subunit in animals and disrupts protein biosynthesis in eukaryotes (Bae and Pestka, 2008; Poppenberger et al., 2003). It also disrupts nucleic acid synthesis, mitochondrial function, membrane integrity and cell division. Around the globe, regulations have passed on maximum allowed levels of DON and other trichothecenes in small grains for human safety. The European Union regulation allows a maximum level of 1.25 ppm of DON in unprocessed bread wheat, 0.5 ppm in bread and bakery and 0.2 ppm in baby foods. The Canadian Food Inspection Agency (CFIA) and Health Canada have set a maximum DON limit of 2 ppm for Canadian soft wheat for adults and 1 ppm in baby food (McMullen et al., 1997).

2.4 Fusarium head blight resistance screening and mechanisms

Resistance to *F. graminearum* in wheat is complex. The genotypes are screened for resistance mainly based on spikelet resistance to initial infection (Type-I), spread of infection within spike (Type-II) (Schroeder and Christensen, 1963) and resistance to DON accumulation in grains (Type III) (Miller and Sampson, 1985), even though up to five types have been described (Mesterhazy, 1995). Resistance to initial infection or spikelet resistance is generally assessed as number of spikeinfected or the number of seeds infected following spray inoculation is measured as disease incidence (Proportion of spikes infected) and the resistance to pathogen spread is assessed as number or proportion of spikelets infected in a spike, following single spikelet inoculation (Schroeder and Christensen, 1963). The various types of resistance have been employed for screening the genotypes both under greenhouse and field conditions. Mainly, the Type-I resistance was assessed based on spray inoculations by counting the number of infected florets and total florets per spike to calculate the percent infected forests and the disease incidence (Somers et al., 2003; Buerstmayr et al. 2003). Screening for resistance based on types of resistance, especially spikelet resistance, was generally inconsistent over years and locations, because of variable inoculum reaching the spikelets, variation in plant growth stage during inoculation, and variation in physical factors affecting infection. However, several cultivars with high levels of resistance have been developed by breeders, ignoring the physical barriers and problems. On the other hand the experimental error in rachis resistance was generally low, and thus, has been quite successful in identifying and breeding for FHB resistance. Also, the resistance to DON accumulation has been extensively used for screening of genotypes.

2.4.1 Morphological and physiological mechanisms of FHB resistance

The mechanisms of resistance in plants to pathogen attack are grouped into apparent and true. The apparent resistance is generally due to florets morphological characters, mainly the cleistogamous (closed), as opposed to chasmogamous (open), with awns or without awns, spikelet density, compactness of spikelets, spikes erectness and height of the plants (Bai and Shaner, 1994; Mesterhazy, 1989; Yoshida et al., 2005). The closed florets do not allow deposition and penetration into florets and the taller plants have less duration of wetness due to blowing wind and hence, reduce the infection efficiency. The moist period required for the successful pathogen infection ranges from 36 to 72 hours (Andersen, 1948). The true resistance is directly governed by host resistance genes, either producing phytoanticipins or phytoalexins (Dixon and Harrison, 1990). The true resistance can be structural or biochemical and both of these can be either constitutive or induced. The constitutive structural mechanisms of host resistance are the preformed wax layers, cutin, lignin, cellulose, and pectins (Kushalappa et al., 2016b). The morphological barriers like stomatal numbers, location and diameter of guard cell openings also play a major role in restricting *Fusarium spp.* infection (Keen, 1999). The biochemical resistance involves the secondary metabolites and proteins like phenolics, saponins, terpenoids and steroids (Bollina et al., 2010; Ferreira et al., 2007).

2.5 Genetic and molecular basis of resistance in wheat against Fusarium head blight

2.5.1 FHB resistance sources in wheat

The availability of the resistance source germplasms is essential to harness the resistance genes. It is an arduous task to develop resistance cultivars against FHB in wheat. Crop breeders have invested considerable effort in identifying the FHB resistance source germplasm around the globe (Bai et al., 2003; Gilbert and Tekauz, 2000; Tekauz et al., 2004). The widely known FHB resistant source genotypeSumai3 has been used to analyze the genetic diversity, across six countries, using DArT markers. The FHB resistance QTL derived from Sumai3 clearly indicated the genetic variations in spikelet resistance are only on 5AS and 2DS, but not on 3BS and 6B (Niwa et al., 2014). The rachis resistance was explored mainly in Ning7840, W14, Nanda 2419, Wangshuibai (Buerstmayr et al., 2009; Jia et al., 2005; Li et al., 2008a; Lin et al., 2006; Marza et al., 2006), Brazilian cultivar: Frontana on chromosome 3A (Mardi et al., 2006; Steiner et al.,

2004), Swiss cultivar: Arina (Draeger et al., 2007) and American cultivars: Ernie, Goldfield, Freedom and Truman (Griffey et al., 2012). Therefore, identifying the resistance source and molecular mapping of the associated genomic regions is essential to develop the FHB resistant breeding lines (Buerstmayr et al., 2009). Lately, several wheat genotypes and lines has been used in breeding programs to explore the FHB resistance genomic regions such as, Huapei 57-2 (chinese cultivar), Chens, HD1220, Vitron, Longdon, Harvest, CDC Teal, Glenn, CDC Kernen, AAC Elie, AAC Iceberg, Carberry, 5602HR and Waskada (Amarasinghe et al., 2016; Sun et al., 2016; Touati-Hattab et al., 2016; Zhu et al., 2016).

2.5.2 Wheat molecular breeding for FHB resistance

The progress in molecular breeding due to the advancement in the high throughput molecular marker technologies helped in identifying the genomic regions associated with FHB resistance. DNA based marker techniques can be divided into two groups: Polymerase Chain Reaction (PCR) and hybridization based techniques (Agarwal et al., 2008). The PCR based marker techniques are useful tools in identifying the genetic locations of the targeted genomic regions. PCR based marker techniques mainly include, amplified fragment length polymorphism (AFLP), single nucleotide polymorphism (SNP), random amplified polymorphic DNA (RAPD), simple sequence repeats (SSR), and sequence tagged sites (STS) (Kage et al., 2016). Molecular markers are great tools used in genetic diagnosis, gene tagging and QTL identification for various physiological and biochemical traits in wheat (Gupta et al., 1999). Quantitative trait locus (QTL) refers to a region of DNA in a chromosome explaining the genetic variation of a quantitative trait. These traits are usually controlled by many genes. Resistance in wheat to FHB is quantitative and controlled by several genes. An effective approach for studying the complex and polygenic form of disease resistance is possible through QTL mapping (Collard et al., 2005). Cultivated wheat is a hexaploid, and thus, the complexity of the genome is a major challenge for genetic manipulations. However, molecular markers and QTL mapping allows identification of genomic regions responsible for complex traits (Anderson, 2007; McCough and Doerge, 1995). The recombinant inbred lines (RILs) have been used for constructing QTL maps and to identify the major resistance effects of QTLs controlling spikelet and rachis resistance. More than one hundred QTLs have been reported from wheat (Buerstmayr et al., 2009). However, very few have been identified as consistent and validated in different genetic

backgrounds. The QTLs localized on chromosomes 3Bs (rachis), 5A (spikelet), 6Bs (rachis) and 2DL (both spikelet and rachis), with high levels of resistance, have been validated using different mapping populations, and these were found to be stable across locations (Anderson, 2007; Somers et al., 2003; Somers et al., 2005). Similarly, two QTLs were identified in wheat accession (PI277012) on chromosome 5AS and 5AL associated with FHB severity, explaining 20 and 32% variation (Chu et al., 2011). Also, the fine mapping of spikelet resistance on QTL-4AS (*QFhs.jic-4AS*) in *Triticum macha* led to the identification of tightly associated SNP markers to aid in marker assisted selection (Burt et al., 2015). The comparative mapping of small effect FHB QTLs, particularly QTL-4AL and QTL-6BL, along with QTL-5AS, have shown good resistance in RILs mapping population derived from an Arina (resistant) by Capo (moderately resistant) cross (Buerstmayr and Buerstmayr, 2015).

The QTL-Fhb5 (*Qfhs.ifa-5A* = *Qfhi.nau-5A*) has been frequently reported on the short arm of chromosome 5A, conferring high level of FHB resistance. The QTL-Fhb5 has been reported to have spikelet resistance and its presence has reduced the percentage of FHB infected spikes (PIS) by over 64.8-82.2% and the percentage of diseased spikelets (PDS) by 62.9-77.4% (Xue et al., 2010). The QTL-Fhb5 has been associated with spikelet, rachis and DON resistance, in diverse sources like, Sumai-3, DH181, CM-82036, and W14, Japanese landrace Nyubai, and Brazilian cultivars Fontana and Ernie (Buerstmayr et al., 2009; Chen et al., 2006; Chen et al., 2005; Yang et al., 2005a; Yang et al., 2005b). However, QTL-Fhb5 mainly contributed for spikelet resistance in various studies (Chen et al., 2006; Lemmens et al., 2005; Xue et al., 2011). The fine mapping of QTL on 5AS controlling spikelet resistance was carried out in the double haploid (DH) lines derived from the cross DH181 and AC Foremost, leading to 0.6cM of the QTL region (Yang et al., 2005b) and 0.4cM in the population derived from the cross Nanda2419 and Wangshuibai (Lin et al., 2006). Further, the fine mapping of QTL-Fhb5 using the Wangshuibai derived NILs confirmed the presence of QTL-Fhb5 locus in different genetic backgrounds and the QTL size has been precisely mapped to 0.3cM (Xue et al., 2011). Identification of candidate genes for quantitative traits is possible if there is consistent association of genomic regions, with trait of interest during fine mapping and comparative mapping analysis (Glazier et al., 2002). Also, the fine mapped QTL can be transferred to susceptible elite cultivars through back cross breeding (Naz et al., 2012). However, linkage drag

is always a hindrance to introgress breeding of major QTLs due to unfavorable alleles transfer along with FHB resistant alleles (Bai and Shaner, 2004).

2.6 Functional elucidation of resistance mechanisms in wheat against Fusarium head blight

2.6.1 Mechanism of FHB resistance based on functional genomics

Functional genomics is a general approach in understanding the functions of unknown genes and their interaction in an organism by making use of the information provided by structural genomics (Hieter and Boguski, 1997). Functional genomics is also a technological platform that allows the analysis of different constituents of cell, such as metabolites, proteins and transcripts to deduce gene functions (Barone et al., 2008).

2.6.1.1 Mechanism of FHB resistance based on metabolomics

Metabolomics is the exhaustive extraction, identification and quantitative analytical determination of plant metabolites (Fiehn, 2002). Plants produce more than 200,000 metabolites. According to the forward genetics approach, the first step is to establish the metabolic pathways of qualitative metabolites (phenotype) induced in during *F. graminearum* infection (Kushalappa and Gunnaiah 2013). Semi-comprehensive metabolomics approaches have detected thousands of resistance related (RR) metabolites in wheat-FHB interaction systems (Figure 2.1). Isoflavonoids such as naringenin and kaempferol were high in abundance in several resistant barley genotypes (Bollina et al., 2010; Kumaraswamy et al., 2011b). Phenylpropanoid groups, especially monomers of lignin and lignan were abundant in wheat genotypes (Gunnaiah et al., 2012; Siranidou et al., 2002).

A signal molecule jasmonic acid was abundantly induced following infection with a trichothecene producing isolate, but not by a mutant lacking its production (Kumaraswamy et al., 2011a). An analysis of QTL-3BS derived from Nyubai revealed that the rachis resistance was due to cell wall reinforcement through the deposition of hydroxycinnamic acid amides and flavonoids (Gunnaiah et al., 2012). However, rachis resistance at 3BS was claimed to be associated with DON detoxification through UDP-glucosyltransferase enzyme in Sumai3 derived lines (Lemmens et al., 2005). However, no difference was observed between total DON produced and converted to non-toxic D3G in wheat at 3 dpi (Gunnaiah et al., 2012).

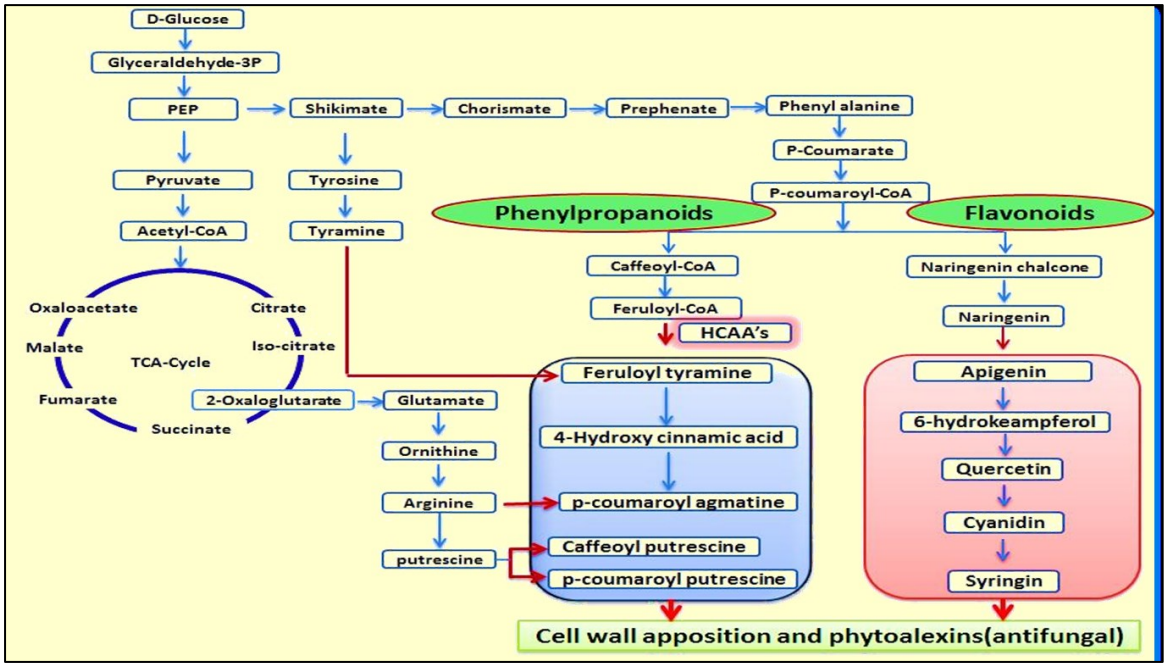

Figure 2.1: Shematic representation of phenylpropanoid and flavonoid pathways mapped with secondary metabolites identified in wheat and barley upon *Fusarium spp*. infection in different studies.

Not all metabolites can be extracted using one solvent and platform. However, the use of aqueous methanol has been successfully used to detect several thousand metabolites (Bollina et al., 2010). Similarly, no one analytical platform can detect all the metabolites. Nuclear magnetic resonance (NMR) is one of the best to detect and identify metabolites. However, it is not very sensitive and several plant resistance related metabolites are present in very small quantities, and thus are often not detected (Fernie and Schauer, 2009; Kitayama and Hatada, 2013). Gas Chromatography-Mass Spectrometry (GC-MS) has been used to detect thousands of metabolites (Fiehn et al., 2000; Hamzehzarghani et al., 2005; Lisec et al., 2006). However, GC-MS detects only volatile metabolites and several resistance related metabolites are non-volatile. The most commonly used platform now is the liquid chromatography and high resolution mass spectrometry (LC-HRMS). The mass spectral output from the LC-HRMS is complex. High resolution in LC-ESI-LTQ-Orbitrp, as compared to LC-Q-TOF, enables separation of metabolites in a complex mixture (De Vos et al., 2007; Moco et al., 2006; Rischer and Oksman-Caldentey, 2006; Tolstikov et al., 2003). This platform has been used to identify several RR

metabolites in barley and wheat against FHB (Bollina et al., 2010; Gunnaiah et al., 2012). Several bioinformatics tools are available to deconvolute peaks and to putatively identify metabolites. Most of these are equipment specific, and a few, such as (X) chromatography mass spectrometry (XCMS) and metabolomic analysis and visualization engine (MAVEN), can be used regardless of equipment (Clasquin et al., 2012; Tautenhahn et al., 2007). Similarly, high resolution spectra processing software called MZmine 2, has been in use to visualize the output files, which used random sample consensus (RANSAC) alignment algorithm and identifies the peaks based on online plant secondary metabolites databases (Pluskal et al., 2010). The use of XCMS for peak deconvolution and CAMERA for the filtration of isotopes and adducts has enabled processing of LC-HRMS data (Bollina et al., 2010). These metabolites mainly belong to secondary metabolic pathway(s), involved in plant defense mechanisms against *F. graminearum* pathogen. Several free fatty acids that reinforce the cuticle were identified using LC-HRMS in barley resistant genotype CI9831 following *F. graminearum* inoculation (Kumar et al., 2016). The LC-HRMS based metabolomics of wheat and barley genotypes with contrasting levels of FHB resistance led to the eventual identification of several candidate resistance genes (Dhokane et al., 2016; Gunnaiah et al., 2012; Kage et al., 2016). Several metabolites conferring resistance against *Phytophthora infestans* in potato were detected using LC-HRMS and their biosynthetic genes were identified and validated (Yogendra et al., 2015). Also, the integrated analysis of metabolomics and transcriptomics has shown the coordinated regulation of metabolites and genes in glucosinolate biosynthetic pathway of Arabidopsis (Hirai et al., 2005; Hirai et al., 2007).

2.6.1.2 Role of resistance related proteins in FHB resistance

The biotic stress in plants leads to large numbers of proteins expression and their post translational modifications. The classes of proteins induced during pathogen attack are called as pathogenesis-related (PR) proteins in plants (Linthorst and Van Loon, 1991). Among the PR proteins expressed during the defense mechanism against pathogen, glucanases and chitinases are considered as biochemical defense related PR proteins similar to cell wall strengthening plant lignin's (Ebrahim et al., 2011). Several defense related proteins induced during *Fusarium spp.* infection in wheat and barley act as antioxidants and antimicrobial (like beta-1,3 glucanase) and peroxidases (Geddes et al., 2008; Zhou et al., 2005). Therefore, plants defend against pathogen

by induced resistance through accumulating the defense proteins, phenolic compounds and phytoalexins (Oliveira et al., 2016). The comparison of differential proteins accumulation at different time point inoculations of *F. graminearum* in resistant wheat cultivar Wangshuibai indicated the two major categories of proteins, associated with carbon metabolism and photosynthesis (Wang et al., 2005). The PR proteins that are higher in abundance in resistant than in susceptible genotypes have been designated as resistance related (RR) proteins. The catalytic proteins thus are not RR proteins (Kushalappa and Gunnaiah 2013).

Although, there is no strong correlation between the abundance of mRNA and corresponding proteins, the quantitative analysis of transcripts and proteins turnover will provide the comprehensive understanding of signalling networks, for changes in transcripts and proteins abundance in Arabidopsis (Ding et al., 2011; Piques et al., 2009). The differential accumulation of JA and ET related proteins encoding transcripts was observed after *F. graminearum* infection in wheat resistant NIL pair carrying QTL-Fhb1 alleles (Jia et al., 2009). Steiner and associates (2009) have shown differential transcript accumulation of a UDP-glucosyltransferase, known for DON detoxification, and thaumatin-like protein-1, pathogenesis related (PR) protein, following *F. graminearum* infection, when both 3BS and 5A QTLs were together in wheat. However, DON detoxification was predicted to be associated only with QTL-Fhb1 but not with QTL-Fhb5 in a RIL population (Lemmens et al., 2005).

2.6.1.3 Host resistance genes and their functions against Fusarium head blight

The advancement in sequencing the genome has helped to unravel the hidden genes within the plant genome. The wheat genome is very complex due to its large size (17 Gb) and genome redundancy (Gill et al., 2004). Particularly, the bread wheat genome (AABBDD) has been derived from three ancestors, *T. urartu* (AA), *Aegeilops speltoides* (BB), and *A. tauschii* (DD) (Dubcovsky and Dvorak, 2007; Petersen et al., 2006). The next generation sequencing technology has enabled the fast release of first survey sequence of chromosome 5A and annotated nearly 392 genes on the short arm (5AS) and 1480 genes on the long arm (5AL) (Vitulo et al., 2011). Similarly, the fine mapping of QTL-Fhb1 in NILs mapping populations derived from CM-82036 and Remus backcross (BC5F2) using BAC sequencing and RNA sequencing revealed nearly 28 genes, where a susceptible sister line carrying *Qhfs.ifa-5A* was used as control. However, only Gly-Asp-Ser-(Leu) (GDSL) motif bearing the lipid hydrolyzing

enzyme (lipase) encoding gene was up-regulated among several genes identified during *F. graminearum* infection in wheat (Schweiger et al., 2016). *In-silico* mining of eight FHB resistance QTLs led to identification of 18 genomic scaffolds located on chromosome 2AL, 2DL, 3B and 4BS harboring plant defense related, immune regulation and cellular detoxification genes (Choura et al., 2016). QTL dissection using long range PCR (LR-PCR) product sequencing and expression analysis revealed SNPs (1025) and genes (153) against *Phytophthara sojea* disease in soybean (Wang et al., 2012). The MYB transcription factor was identified using activation tagging approach in Arabidopsis, which regulates phenylpropanoid biosynthesis (Borevitz et al., 2000). Similarly, the transcriptomic analysis of wheat upon fungus *Rhizoctonia cerealis* infection led to MYB TF encoding gene (*TaRIM1*) expression, which in-turn regulates the defense genes (Shan et al., 2016).

2.7 MYB Transcription factors controlling Fusarium head blight

All biological processes are generally associated with genes expression, which in turn are regulated through proteins (mainly transcription factors) by interacting with gene promoter DNA sequences called as *cis*-elements. The MYB proteins are the most abundant TFs in plant system, involved in abiotic and biotic stress resistance mechanisms. The identification of avian myeloblastosis virus oncogene gene (*v-my*) has led to the discovery of MYB genes and family *MYB*-related genes (Lipsick and Wang, 1999). The plant *MYB* genes originated from an ancestral gene, which codes for MYB proteins containing three repeat units or domains in animals (*c-MYB*) and in plants *pc-MYB* family genes (Braun and Grotewold, 1999; Lipsick, 1996). The TF with high amino acid conservation at 3rd helices of the R2 and R3 repeats forms helix-turn-helix (HTH) structure (Frampton et al., 1991). The basic helix-loop-helix (bHLH) domain transcription factor identified in animals shares the similar domain in plants (Heim et al., 2003). The MYB/bHLH complex regulates the specific cellular process by responding to plant developmental and environmental cues (Pireyre and Burow, 2015). The R2R3 MYB (GmMYB) in soya bean was significantly induced following pathogen infection and regulated the lignin synthesis in resistant genotypes (Aoyagi et al., 2014). The genome-wide analysis in *Jatropha curcas* identified 128 R2R3vMYB genes against abiotic stress (Peng et al., 2016). The R2R3-MYB TF EsAN2 regulates the structural genes, chalcone synthase (*CHS*), chalcone isomerase

(*CHI*) and anthocyanidin synthase during anthocyanin biosynthesis in *Epimedium sagittatum* plants (Huang et al., 2016).

2.8 Gene resistance function elucidation based on virus induced gene silencing (VIGS)

The gene functions were assessed using several functional genomic tools, such as downregulation, though mutation, gene silencing, up-regulation through over expression of genes (Aukerman and Sakai, 2003; Kondou et al., 2010; Ramegowda et al., 2013; Scofield and Brandt, 2012). Virus induced gene silencing (VIGS) is a functional genomics tool that uses recombinant viruses to specifically downregulate the endogenous gene activity through plant innate silencing mechanisms called Post-Transcriptional Gene Silencing (PTGS) (Kirigia et al., 2014). VIGS has been widely employed as a tool to decipher the functions of several plants genes in biotic stress resistance (Kage et al., 2016; Manmathan et al., 2013; Scofield et al., 2005; Senthil-Kumar and Mysore, 2011). VIGS is a relatively easier technique to validate the gene(s) functions, compared to other functional validation approaches, as it doesn't involve plant regeneration protocol, which is problematic in various crop plants (Burch-Smith et al., 2004). VIGS is cost effective, less laborious, possess ability to silence either individual or multiple members of a gene family and a rapid method of assessment (usually 3-4 weeks from infection to silencing) (Burch-Smith et al., 2004). Due to the polyploid nature of wheat and high recalcitrance to *in vitro* regeneration, the functional characterization of wheat genes is lagging. Owing the simplicity and advantageous VIGS possess, it has become the system of choice to elucidate the gene functions in wheat (Burch-Smith et al., 2004; Campbell and Huang, 2010; Scofield et al., 2005). The resistance functions of three genes (*Lr21, Lr10 and Pm3b*) in wheat were elucidated employing VIGS (Scofield et al., 2005). The silencing of *Mlo* genes in wheat using VIGS conferred resistance against powdery mildew (Varallyay et al., 2012). A novel wall-associated kinase gene *TaWAK5* in wheat was silenced using VIGS to prove its involvement in imparting resistance against *R. cerealis* (Yang et al., 2014). Silencing of *WRKY53* and phenylalanine ammonia lyase in wheat reduced aphid resistance (Van Eck et al., 2010). The resistance function of wheat agmatine coumaroyl transferase (*TaACT*) gene was proved based on VIGS against FHB using resistant NIL (Kage et al., 2016).

CONNECTING STATEMENT FOR CHAPTER III

Chapter III presents a manuscript entitled "A transcription factor *TaMYBFhb5* in QTL-Fhb5 regulates downstream resistance genes to biosynthesize hydroxycinnamic acid amides and flavonoids conferring spikelet resistance against *Fusarium graminearum*". The authors are Hukkeri S, Karre S, Kushalappa AC, Charron JB and Raj Duggavathi. The manuscript will be submitted to a peer reviewed scientific journal for publication.

In the chapter II, a comprehensive review on Fusarium head blight (FHB) indicated a brief understanding on importance FHB resistance genotypes and their exploration in identifying the QTL against FHB disease resistance in wheat. Particularly, the wheat genotype Sumai3 has been used in developing the lines for both spikelet and rachis resistance against FHB disease. Enormous amounts of research have been carried out to understand the rachis resistance in wheat as comparted to spikelet resistance. More than 100 QTL have been identified for FHB resistance, of which QTL-Fhb5 is a major effect QTL for spikelet resistance derived from Sumai3 wheat cultivar. Hence, we explored the spikelet resistance mechanism based on semi-comprehensive metabolic profiling and dissecting the QTL-Fhb5 to identify the candidate genes. In the present study, the wheat near isogenic lines (NILs) carrying the QTL-Fhb5 alleles from Sumai3 were subjected to semi-comprehensive metabolic profiling to identify the mechanisms of resistance based on resistant related (RR) metabolites accumulation in resistant NIL (R-NIL), relative to the susceptible NIL (S-NIL). We observed high accumulation of RR metabolites, mainly pathogen- induced (PRr) and constitutive (RRC), from phenylpropanoid and flavonoid pathways. Also, the tightly linked flanking markers of QTL-Fhb5 were sequenced using NILs genomic DNA, based on Sanger sequencing method. Using the wheat reference sequences we carried out the primer walking from both the ends of the QTL-Fhb5. The annotation of consensus sequences obtained from nested amplicons revealed an R2R3 MYB transcription factor (TF) tagged to one of the flanking marker (Xgwm415). The metabolic profiling of TF virus induced gene silenced R-NIL and differential expression analysis of metabolic pathway genes (*R*) indicated that the *TaMYBFhb5* regulated downstream *R* genes involved in biosynthesizing RR metabolites, which in-turn reduced the fungal biomass accumulation in wheat.

CHAPTER III

A transcription factor *TaMYBFhb5* in QTL-Fhb5 regulates downstream resistance genes to biosynthesize hydroxycinnamic acid amides and flavonoids conferring spikelet resistance against *Fusarium graminearum*.

Hukkeri S[1], Karre S[1], Kushalappa AC[1], Charron JB[1] and Raj Duggavathi[2]

[1]Plant Science Department, McGill University, 21 111 Lakeshore Road, Ste. Anne de Bellevue, Quebec H9X3V9, Canada. [2]Animal Science Department, McGill University, Ste. Anne de Bellevue, Quebec, Canada H9X3V9

3.1 Abstract

Fusarium head blight (FHB) of wheat is of global importance due to its drastic impact on yield and mycotoxin contamination of grains. FHB resistance is quantitatively inherited and is controlled by several genes. In this study, the FHB resistance was assessed as resistance to spikelet infection, and resistance to spread of FHB among spikelets within spike through rachis. The metabolic profiling of near isogenic lines (NILs) of wheat carrying contrasting alleles for QTL-Fhb5 revealed the high accumulation of both phenylpropanoid and flavonoid resistance related (RR) metabolites. A significant difference in FHB disease severity was observed between resistant (R) and susceptible (S) NIL. The dissection of spikelet resistance genes in QTL-Fhb5 from wheat NILs revealed a new R2R3 MYB transcription factor encoding gene, *TaMYBFhb5*, which was polymorphic and also regulated downstream genes that biosynthesized hydroxycinnamic acid amides and flavonoids. The promoter analysis of downstream genes from both phenylpropanoid and flavonoid pathways, such as phenyl ammonia lyase (*PAL*), agmatine *p*-coumaroyl transferase (*ACT*) and chalcone synthase (*CHS*) interacted with *TaMYBFhb5* TF. The differential expression of these genes and accumulation of their biosynthetic RR metabolites

indicated that the *TaMYBFhb5* (GenBank: AHZ33834.1) TF is a key regulator of downstream genes that biosynthesized HCAA that are known to be involved in FHB resistance through cell wall reinforcement, while the flavonoids mainly functioned as phytoalexins. Upon silencing of *TaMYBFhb5* in the resistant NIL (R-NIL), both the fungal biomass and DON content were significantly increased in spikelets. Interestingly, the candidate genes from both phenylpropanoid and flavonoid metabolic pathways were down-regulated, reducing the abundances of respective RR metabolites. The *TaMYBFhb5* gene validated in the current study can be used to replace the susceptible genes in elite cultivars, if mutated, through genome editing to improve resistance against FHB.

3.2 Introduction

Fusarium head blight (FHB) caused by *Fusarium graminearum* Schwabe (Teleomorph: *Gibberella zeae* (Schwein) Petch), is one of the destructive and dreadful diseases of common wheat (*Triticum aestivum* L.). The disease significantly impacts on the economy but also on the health of animals, including humans due to mycotoxin contamination of food grains and animal feed (Gilbert and Tekauz, 2000; Luongo et al., 2010). The most commonly detected mycotoxin is deoxynivalenol (DON) (Sobrova et al., 2010). DON is generally detected in wheat spikelets at 36 and 48 hpi (hours post inoculation) (Kang and Buchenauer, 1999; Mirocha et al., 1997). These mycotoxins affect the cellular metabolism of the eukaryotic cells by affecting protein biosynthesis and hampering DNA function, and inducing apoptosis and programmed cell death in animals (Rocha et al., 2005). Hence, it is essential to understand the mechanism FHB resistance to develop cultivars with minimal mycotoxin accumulation , thus reducing the ill-effects on animal and human health.

FHB resistance is a quantitatively inherited trait in wheat and barley,implying several genes are involved in resisting the *Fusarium spp.* infection. More than 100 quantitative trait loci (QTL) across genotypes on different wheat chromosomes have been identified (Anderson et al., 2001; Bai and Shaner, 2004; Buerstmayr et al., 2009; Lemmens et al., 2005; Yang et al., 2005a). However, the resistance mechanisms governed by these QTL are yet to be revealed. Among the QTL identified for FHB spikelet resistance, QTL-Fhb5, QTL-Fhb1 and QTL-Fhb2 were validated across several populations (Liu et al., 2009). The validated QTL were further fine mapped to reduce their sizes through increased population size, a number of markers and

mutational breeding to identify the genes underlying these QTL (Collard et al., 2005). The fine mapping of QTL and synteny analysis based on the available genomic databases led to the identification of peroxisomal *acyl-coenzyme A oxidase 1* (*ACOX1*) in seabass (Wang et al., 2015). Similarly, *in-silico* analysis of FHB QTLs led to the identification of defense response, cellular detoxification, and immune regulation genes in wheat (Choura et al., 2016). The comparative genomics and *in-silico* analysis of 261 genes in plant species led to the identification of fatty acid biosynthesis candidates genes (Sharma and Chauhan, 2012). The availability of the genomic resources and databases in the recent past helped in identifying the three disease resistance genes against powdery mildew and leaf rust, based on map-based cloning in wheat (Keller et al., 2005). The comparative analysis between wheat physical and genetic maps using SSR markers revealed numerous expressed sequences tags (ESTs) that could be potential candidate genes (Sourdille et al., 2004). The QTL-Fhb5 has been precisely fine mapped to 0.3cM with 60% reduction in FHB incidence, mainly contributed to spikelet resistance (Xue et al., 2011).

The wheat spikelet resistance involves the interaction of fungal effectors and wheat cell response to the effector molecules released by *F. graminearum*. To understand the proteins secreted by *F. graminearum* during early infection stages of wheat cells, secretome analysis revealed upregulation of host putative enzymes, phytotoxins, and antifungal proteins (Brown et al., 2012). Plausibly, *F. graminearum* induces ion fluxes, oxidative burst, and expression of several signaling biochemical molecules, as well as, defense genes following its invasion (Ding et al., 2011).

The plant FHB resistance involves biochemical warfare against *F. graminearum* infection through the accumulation of biochemical molecules, such as phenolics, saponins, terpenoids, steroids, and proteins such as pathogenesis-related (*PR*) proteins (Bollina et al., 2010; Ferreira et al., 2007). The metabolo-proteomics studies gave a snapshot image of the plant response to pathogen attack through the accumulation of secondary metabolites biosynthesized by phenylalanine ammonia lyase (*PAL*) and chalcone synthase (*CHS*) genes (Hammond-Kosack and Jones, 1996). Among the secondary metabolites accumulated during the pathogen attack, hydroxycinnamic acid amides (HCAAs) and flavonoids exhibit antifungal activity as well as cell wall reinforcement function (Gunnaiah et al., 2012; Walters et al., 2001). Similarly, the

conjugated polyamines of HCAAs, p-coumaroyl-hydroxyagmatine in barley challenged with powdery mildew fungus and N-feruloyltyramine, N-caffeoyl tyramine in *Allium* species act as antifungal agents against *Fusarium culmorum* (Fattorusso et al., 1999; Sadeghi et al., 2013; Von Ropenack et al., 1998). Also, these plant HCAAs and flavonoid secondary metabolites were reported against biotic and abiotic stress in diverse crop species, including wheat (*Triticum aestivum* L), barley (*Hordeum volgare* L), rice (*Oryza sativa* L), maize (*Zea mays* L) and potato (*Solanum tuberosum* L) (Edreva et al., 2008; Gunnaiah and Kushalappa, 2014; Yogendra et al., 2015; Yogendra et al., 2014). Therefore, the phenylpropanoid and flavonoid metabolic pathways are highly conserved and involved in plant defense (Dixon et al., 2002; Shih et al., 2006). The biosynthesis of phenylpropanoids and flavonoids required two groups of genes; structural genes, which codes for enzymes that are directly involved in the biosynthetic reactions, and transcription factors encoding genes which regulate the expression of structural genes and accumulation of metabolites. Hence, the susceptibility and resistance of the host depends on the rapid detection of pathogen infection and activation of the defense mechanisms through reprogramming of cellular metabolism (Somssich and Hahlbrock, 1998).

The plant transcription factors (TFs) can be used as powerful tools in reprogramming of cellular metabolism either through activating or suppressing the downstream structural genes of the secondary metabolic pathways (Broun, 2004). The overexpression of *AtMYB12* in Arabidopsis regulated genes accumulating high abundance of polyphenols in fruits (Luo et al., 2008). The activation tagging of MYB transcription factor, mediated with viral enhancer sequence led to enhanced biosynthesis phenylpropanoids and flavonoids in Arabidopsis (Borevitz et al., 2000). These MYB TF are a large family of TFs accounted for multiple biological processes within plant kingdom (Riechmann et al., 2000; Rosinski and Atchley, 1998). The MYB TF family has two structural and highly conserved domains at the N-terminal region of the protein called the MYB domain (Stracke et al., 2001). The TFs are key factors that significantly regulate several downstream genes, following recognition of the pathogen, increasing the abundance of RR metabolites (Alves et al., 2013; Kushalappa et al., 2016a; Vom Endt et al., 2002). The HCAAs and flavonoids biosynthesis pathways appear to be under the control of MYC and MYB TF. The over expression of R2R3 MYB transcription factor gene (*VuMYB5a*) from grape (*Vitis vinifera*) in tobacco led to high accumulation of phenyl propanoid pathway related metabolites like, cyanidin-3-rhamnoglucoside and quercetin-3-

rhamnoglucosideside, tannins and lignin (Deluc et al., 2006). The polyamine biosynthesis was regulated by MYB8 in Tobacco (*Nicotiana attenuate*) (Onkokesung et al., 2012). Similarly, JA mediated biochemical resistance and co-expression of many defense genes was controlled by transcription factors (Eulgem et al., 2000; Vom Endt et al., 2002; Woldemariam et al., 2011). The plant defense mechanism also involves cascade of transcription factors (TFs), belonging to Zn finger family proteins, MYC (HLH), AP2, MYB and NAC, and most of these TFs have been associated with secondary metabolism, in various environmental cues (De Geyter et al., 2012).

In this study, the QTL-Fhb5 region was sequenced based on marker-walking, *in-silico* analysis, and synteny mapping was carried out. The QTL-Fhb5 associated flanking markers or primer walking and annotation of the QTL-Fhb5 sequence led to identification of the R2R3 MYB transcription factor encoding gene, designated as *TaMYBFhb5*. Interestingly, the latter gene was tagged with one of the flanking markers (Xgwm415) of QTL-Fhb5. An *in-silico* annotation of the fine mapped QTL-Fhb5 sequences revealed several genes involved in biotic stress resistance. The electrophoretic mobility shift analysis of phenylpropanoid and flavonoid metabolic pathways structural genes and *TaMYBFhb5* TF was studied to confirm their interactions. Further, the virus induced gene silencing (VIGS) of *TaMYBFhb5* gene in R-NIL was carried out to undersdant the effect of TF on regulation of phenylpropanoid and flavonoid pathways genes in wheat spikelets.

3.3 Materials and Methods

3.3.1 Plant production

The resistance (R) and susceptible (S) wheat NILs carrying contrasting alleles for QTL-Fhb5 were obtained from Agriculture and Agri-Food Canada, Winnipeg, Canada (Dr. Curt McCartney). These NILs were derived from a cross between 98B08*A111 and Kanata (BW263) (Somers et al., 2005). The donor parental line, 98B08*A111 is a double haploid line (DHL) carrying QTL-Fhb5 for spikelet resistance, which was derived from Sumai3 (Somers et al., 2003), and Kanata (BW263) is an elite cultivar (recurrent parent) largely grown in Western Canada. The NILs from BC_2F_6 populations with 93% recurrent parent genome were selected based on the heterozygous alleles for QTL-Fhb5 flanking microsatellite markers (Somers et al., 2005). The wheat NILs seeds were sown in seven and half inch pots, 4-5 seedlings of resistant

(R-NIL) and susceptible NIL (S-NIL) were grown and later, three seedlings per pot were maintained under greenhouse conditions with 16 hour daylight and 8 hour darkness, and relative humidity of 65 ± 5% at temperature 25 ± 2^{o}C. Plants were watered with regulated drip irrigation, based on the moisture status, and a slow releasing fertilizer 20-20-20=N-PK was applied at early seedling and booting growth stages.

3.3.2 Pathogen production and inoculation

The *F. graminearum* (teleomorph: *Gibberella zeae*), isolate Z-3639 (Proctor et al., 1995) culture was stored in glycerol at -80^{o}C. The glycerol stocks were prepared in multiple steps: Potato dextrose agar (PDA) plates were prepared using commercially available agar media and *Fg* mycelium plugs were placed onto the media for six-seven days at 19-20^{o}C. Fresh potato PDA media was poured into two ml tubes and the tubes were kept at 45 degree angle for 50-60 min. Freshly grown fungal mycelium plugs were placed into two ml tubes containing PDA media and kept at 19-20^{o}C for five-six days for mycelial growth. Freshly prepared and autoclaved 60% glycerol stock was poured (0.5-1.0 ml) onto the freshly grown fungal mycelial plugs and the tubes were stored at -80^{o}C until further use. The fresh cultures of *Fg* plugs from glycerol stocks were transferred onto rye-agar media plates. These plates were kept in 27^{o}C incubator for three-four days for enough mycelial growth. The mycelia grown plates were exposed to blue luminescent light for three days to obtain macroconidial spores and the macroconidial suspension were prepared just before the inoculation. The 10 µl of 10^{5}spores/ml concentration was used for inoculation. At 50% anthesis (GS=65) (Zadoks et al., 1974), spikelets were either individually inoculated with a syringe, and spikes were spray inoculated for disease severity and metabolites analysis experiments respectively. The plants were covered with transparent plastic bags to maintain high relative humidity, and the covers were removed at 48 hours post inoculation (hpi).

3.3.3 Disease severity assessment

The wheat NILs were grown separately for disease severity assessment under greenhouse conditions. A randomized complete block design with two genotypes (NILs) inoculated with one isolate of the pathogen and three replications over time were used. Each experimental unit consisted of 30 spikes. The spikelets were spray inoculated using Deluxe set 200, airbrush sprayer (Badger, IL, U.S) at GS=65. The disease severity was assessed as number of spikelets

diseased in a spike at 3, 6, 9, 12 and 15 days post inoculation (dpi). From this the proportion of spikelets diseased (PSD) per spike was derived, and from PSD the area under the disease progress curve (AUDPC) was calculated. The data were analyzed based on both students' *t*-test and ANOVA methods using SAS program (SAS Institute Inc., Raleigh, North Carolina).

3.3.4 Fungal biomass quantification based on real time quantitative PCR (qPCR)

This experiment was conducted as a randomized complete block design, with two genotypes, R-NIL and S-NIL, two inoculations, pathogen and mock, and five replicates over time. Plants were grown in greenhouse conditions and at 50% anthesis (GS=65) (Zadoks et al., 1974), two alternate pairs of spikelets in the mid region of spike were individually inoculated with macroconidial suspension (10 µl of spore suspension containing 10^5 spores ml-1) using an auto-dispenser syringe (GASTIGHT 1750DAD W/S, Hamilton, Reno, NV, USA) and covered with transparent plastic bags to maintain high relative humidity.The covers were removed at 48 hours post inoculation (hpi). At 72 hpi, inoculated spikelets, along with the alternate uninoculated spikelets, were harvested, immediately frozen in liquid nitrogen and stored at -80^{o}C until further use. The fungal biomass was quantified as a relative copy number of *Tri6_10* gene in spikelets inoculated with syringe (Kumar et al., 2015). The frozen spikelets of both R-NIL and S-NIL were ground and the genomic DNA was extracted using Qiagen kit (Qiagen Inc,Toronto, Ontario, Canada). The wheat *Actin* gene was used as housekeeping gene to amplify the genomic DNA of *Fg* infected samples. *Fg* specific *Tri6_10* gene primers were used along with the *Actin* gene. The *Actin* gene was amplified in all the replicates to normalize the quantity of genomic DNA based on band intensities and NanoDrop spectrophotometer (NanoDrop, Wilmington, DE, USA) readings. Further, the normalized genomic DNA from all three biological replicates was used for the real time quantitative polymerase chain reaction (qPCR) analysis to calculate the relative *Fg* gene transcript abundance within the wheat spikelets. The qRT-PCR was carried out for each biological replicates with three technical replicates. The relative gene copy number of *Tri6_10* gene was calculated based on Ct (Cycle threshold) values, to quantify the total fungal biomass from *Fg* colonized tissue using the $2^{-\Delta\Delta Ct}$ method (Livak and Schmittgen, 2001).

3.3.5 Metabolic profiling and data processing

The spikelets individually inoculated with spore suspension collected at 72 hpi, in the above study, were also used for metabolic profiling. Just before analysis, the spikelets were ground in liquid nitrogen using a mortar and pestle, metabolites were extracted using 60% aqueous solution of methanol, centrifuged and supernatant were used for analysis. An aliquot of extract were injected into LC-ESI-LTQ-Orbitrap (LC-HRMS) (Bollina et al., 2010). The abundance of peaks were subjected to *t*-test to identify treatment significant metabolites. A peak or metabolite with a higher abundance in a resistant than in a susceptible genotype were considered as a resistance related (RR) metabolite. A RR metabolite based on mock inoculations was considered as a constitutive (RRC = RM>SM) metabolite. A metabolite with significantly high abundance in the pathogen inoculated NIL than in mock inoculated NIL was considered as a pathogenesis related (PR) metabolite, in resistant (PRr = RP>RM) or susceptible (PRs = SP>SM) genotypes. A PRr metabolite in a resistant genotype with abundance greater than susceptible genotype inoculated with the pathogen was considered as an RR induced (RRI=(RP>RM) >(RP>SP)) metabolite. In addition, resistance indicator metabolites, such as DON and total DON converted to D3G (through enzymatic action) were identified. The RR metabolites were putatively identified with a compound name using different databases PlantCyc, METabolite LINk (METLIN), KNApSAcK and Kyoto encyclopedia genes, genomes (KEGG), Massbank, Lipid maps, Chemspider and chemsketch.

3.3.6 DNA extraction and QTL-Fhb5 flanking marker amplification

The wheat NILs seedlings were maintained in greenhouse conditions and leaf samples were collected and immediately frozen in liquid nitrogen. The leaf DNA was extracted based on CTAB method (Murray and Thompson, 1980) with some modifications. The 100mg of leaf samples were ground using a pestle and morter to make a fine powder and 800 µL of modified 2% CTAB buffer (2% CTAB, 0.1M Tris·HCl at pH 8.0, 20 mM EDTA at pH 8.0, 1.4M NaCl) was added. The mixture was transferred to 2.0 ml safe-lock eppendorf tubes. The tubes containing the samples were incubated in water a bath at 60^{o}C for 40 minutes. The tubes were inverted 2-3 times every 10 minutes. After cooling, 600µL of chloroform:isoamyl (24:1 v/v) alcohol was added. The tubes were shaken and centrifuged for 10 min at 13000 rpm using Eppendorf instrument (Cole-Parmer Instrument Company, LLC, US). The supernatant was

transferred to a new 1.5 mL tubes containing 400µL of 2-propanol and the tubes were kept at -20^{o}C for 10 min. Then tubes were centrifuged for 15 min at 13000 rpm and supernatant was discarded. The 500µL of ethyl alcohol was added to each tube and centrifuged for 1.0 min to remove the chlorophyll pigments and other proteins. The precipitated DNA pellet was air dried for 8-10 hours.

We used the microsatellite markers mapped on to the QTL-Fhb5 for PCR amplification (Suzuki et al., 2012; Xue et al., 2011; Yang et al., 2005b). PCR was performed using the plant genomic DNA of R-NIL, S-NIL and Sumai3. The 50µL PCR solution comprising of 1µL of the DNA template (about 30ng), 1.0 Unit of Taq polymerase: Pfu enzyme in a ratio of 9:1µL, 1x buffer, 1.5mM $MgCl_2$, 200µL of each dNTP, 5.0 picomoles of primers. Thermocycler conditions used were an initial 94^{o}C for 5 min; 35 cycles of 95^{o}C for 1 min, 57^{o}C, for 1 min, and 72^{o}C for 2 min and final 72^{o}C extension for 10 min using eppendorf thermocycler, and then 10µL PCR products were separated on agarose gel and detected in Eppendorf gel documentation unit and the remaining PCR product was column purified (Qiagen kit) for the further TA-cloning.

3.3.7 Cloning, transformation and sequencing of genes

The column purified PCR products of *TaMYBFhb5* TF gene, Xgwm304, Xgwm415 and metabolic pathway structural genes phenylalanine ammonia lyase (*PAL*), agmatine coumaroyl transferase (*ACT*), and chalcone synthase (*CHS*) and their promoters were ligated using the TA-cloning kit (Bio Basic Inc.). The ligated products were transformed into *E.coli* competent cells (DH5alpa) (NEB Inc.) using the heat shock method (https://www.addgene.org/plasmid-protocols/bacterial-transformation/). The positive colonies were selected based on the blue-white color indications as the LB plates used antibiotic (ampicillin) selection and 100mM IPTG (Isopropyl β-D-1-thiogalactopyranoside) and 40mg/ml X-Gal (bromochloroindoxyl galactoside). The white colonies were screened using M13 forward and reverse primers for further confirmation. The positive colonies were grown overnight in the LB broth and plasmids were extracted using Qiagen MiniPrep kit. The isolated plasmid was sequenced using Sanger's dideoxy method, Applied Biosystem's platform at the Genome Quebec-McGill Innovation Center. The glycerol stocks of *E.coli* plasmid containing genes and flanking markers were prepared and stored in -80^{o}C until further use.

3.3.8 Flanking marker primer walking and *TaMYBFhb5* TF phylogenetic analysis

The validated QTL-Fhb5 flanking markers were selected to carry out the primer walking. The resistant and susceptible NILs genomic DNA was extracted along with Sumai3 genotype. The polymerase chain reaction (PCR) was carried out using LongAmp *Taq* polymerase (NEB Inc.). The amplified product was cloned using TA cloning vector and sequenced through Sanger di-deoxy method at the Genome Quebec-McGill Innovation Center. The marker sequences from QTL-Fhb5 amplicons were removed using VecScreen (NCBI). The sequences were aligned onto the 5A chromosome sequences retrieved from NCBI database (Chinese spring genome) and UK454 wheat reads from Dr. Gary Barker (University of Bristol, UK). The regions aligned with the flanking markers were used as anchors for selecting the reference sequences covering QTL-Fhb5 to design the primers for the second round of PCR amplification. The sequenced amplicons were annotated using FGeneSH. Further, BLASTn and BLASTp analysis were carried out for all the sequences. The phylogenetic analysis was carried out for the *TaMYBFhb5* with the published sequence of wheat (Chinese spring), barley, rice, sorghum, *brachypodium* and *arabidopsis* MYB homologs. The sequences were aligned using ClustlW algorithm of the MultAlign software package, and the trees were prepared using neighbor-joining method. Bootstrap values were calculated from 1000 replicates of the tree. The sequences of model crops were retrieved from the Plant TF database (http://planttfdb.cbi.pku.edu.cn/).

3.3.9 *In-silico* annotation of QTL-Fhb5 using a 5A chromosome sequence from NCBI database

The tightly linked SSR markers, Xgwm304 and Xgwm415 flanking the FHB spikelet resistance QTL-Fhb5 on chromosome 5AS of wheat, were amplified using Sumai3 wheat genomic DNA. Both the flanking markers were sequenced based on Sanger di-deoxy method at Genome-Quebec McGill Innovation Centre. The marker Xgwm304 is renamed as Xgwm304_Ta5A_QTL (GenBank: KF226136) and Xgwm415 as Xgwm415_Ta5A_QTL (GenBank: KF226135). These flanking marker sequences were used to BLAST search the wheat 5A chromosome contigs. The QTL-Fhb5 fine mapped genomic regions were retrieved from NCBI site (http://www.ncbi.nlm.nih.gov/genome/?term=Triticum%20aestivum). The retrieved genomic regions were annotated using AUGUSTUS user interface software (http://augustus.gobics.de/). Further, the retrieved sequences were annotated using FGeneSH

genes prediction algorithm (http://www.softberry.com). The Blast2GO software was employed for gene ontology (GO) and homology analysis of the predicted genes (https://www.blast2go.com/). The flanking markers of the fine mapped regions and annotated gene sequences were used for the synteny mapping among *Oryza sativa*, *Brachypodium distachyon*, *Sorghum bicolor* and *Triticum aestivum* chromosomes.

3.3.10 *TaMYBFhb5* transcription factor protein expression and purification

The E-coli plasmid containing *TaMYBFhb5* TF gene were digested using restriction enzymes (EcoR-I and BamH-I) and the eluted gene fragment was cloned into expression vector (pTrcHis-B) of *E.coli* competent cells (BL21) from New England Biolabs Inc. The transformation and expression of protein from *TaMYBFhb5* was carried out according to the protocol explained in NEB kit. The expressed protein was isolated using PrepEase Histidine-Tagged protein purification kit (Affymetrix). The isolated protein was purified through dialysis. Dialysis buffer was prepared using TrisHCL (50mM), sodium chloride (150mM) and dithiothreitol, DTT (1mM) at pH 7.6-8.0. The isolated crude protein was transferred into regenerated cellulose tubular membrane (Membrane Filtration Products, Inc.). The dialysis was carried out on magnetic stir plate by immersing the cellulose membrane into dialysis buffer with magnetic stirrer bead for 5 hours.

3.3.11 Electrophoretic mobility shift assay (EMSA) and *in-silico* analysis of nuclear localization signal and auto-docking of *TaMYBFhb5* TF

The multiplexed electro mobility shift assay was carried out with *TaMYBFhb5* protein and promoters of structural genes. The promoter sequences of downstream metabolic pathway structural genes (*ACT*, *CHS* and *PAL*) were amplified and purified using PCR product purification kit (Bio Basic Inc.). EMSA reaction was set using purified *TaMYBFhb5* TF protein (3µg) and purified PCR product (40ng/µl) with 10X binding buffer. For 5ml stock of 10X binding buffer we used 100mM TrisHCl (pH 7.5), 10mM EDTA, 1M KCL, 1mM DTT, 50% (w/v) glycerol, 0.1BSA (mg/ml). The reaction was kept at room temperature for 45-50 minutes. The EMSA reactions were used to run on both poly-acrylamide (PAGE) and 6% agarose gels to see the interactions. The *in-silico* analysis of nuclear localization analysis for nuclear localization signal (NLS) in *TaMYBFhb5* TF was carried out using the PLACE software (Higo et

al., 1998). The *TaMYBFhb5* protein 3-dimentional (3D) structure was predicted using Phyre[2] web interface tool (Kelley et al., 2015). The top hit domain (c3zqcG) was searched in protein database (PDB) using RCSB web interface (http://www.rcsb.org/pdb/home/home.do). The 3D models for structural genes promoter DNA sequences were carried out to develop the B-DNA using Modelit software (Munteanu et al., 1998). The protein-DNA interactions were docked using NPDock web docking server (Tuszynska et al., 2015). The top hits in the docking analysis were visualized using PyMOL (Schrodinger, 2015). The software's visual molecular dynamics (VMD) and Virtual screening (VS) lab were used for the analysis of docking poses for *TaMYBFhb5* TF (PDB: 3ZQC) as well as to study the interaction of ligands (*PAL*, *ACT* and *CHS* prompters sequence) with the target protein (Cerqueira et al., 2011; Humphrey et al., 1996). The target protein 3ZQC PDB file was loaded into the VMD. The VS lab was launched from VMD main page extension. The 3 ligands were loaded into VS lab using the input option. The autodock parameters used for the aligning the active site grid were: X:58.166, Y:38.224, Z:50.382. The predicted protein was used to see the interacting components within the promoters of downstream structural genes.

3.3.12 Virus induced gene silencing of *TaMYBFhb5* TF

The barley stripe mosaic virus (BSMV) constructs were obtained (USDA). The *TaMYBFhb5* gene fragment specific to wheat chromosome 5A short arm that was non-homologous to other copies in the 5B and 5D chromosomes was selected. Selecting *TaMYBFhb5* TF fragment (277bp) from the 3' end of the gene was another very important step. Because, usually the sequences towards the 3' end of the genes are very specific to each gene. Particularly, the R2R3 MYB gene families have domains highly conserved towards the 5' end of the genes. The *TaMYBFhb5* TF fragment was cloned into pSL038-1 (gamma) vector. All the vectors, such as pSL038-1 , pSL039-1 (PDS), pBSMV (Alpha42) and pBSMV (beta42.sp1) were linearized using specific restriction enzyme and *in-vitro* transcription (Scofield and Brandt, 2012). The vector with the phytoene desaturase (PDS) gene was used to see the silencing efficiency based on chlorophyll depigmentation (photobleaching, positive control) at 3 days post swabbing of the constructs. The construct (pSL038-1) with *TaMYBFhb5* gene fragment was swabbed on five spikes and the flag leaf of R-NIL at early anthesis stage.The experiment was conducted as a randomized complete block design in greenhouse conditions, with one R-NIL silenced or non-

silenced, inoculated with pathogen or mock-solution, with three replications over time. The spikelets were inoculated at 50% anthesis (growth stage, GS=65) (Zadoks et al., 1974) using *F. graminearum* spore suspension (10ul) 10^5 spores per ml concentration) or mock-solution (10ul). The pathogenesis related (PR) metabolites in R-NIL silenced and R-NIL non-silenced were determined based on higher abundance in non-silenced R-NIL pathogen inoculated than silenced R-NIL (RnP>RsP).

3.3.13 Gene expression analysis

The spikelet samples collected at 48 hpi, from the fungal biomass and metabolome quantification experiment was used to assess gene expression (section: 3.3.4 and 3.3.5). Total RNA was isolated from spikelets inoculated with *Fg* from both R-NIL and S-NIL. The RNA was extracted using Qiagen RNAeasy plant mini kit (Qiagen) and care was taken to avoid the genomic DNA contamination. Total RNA (1µg) was reverse transcribed in a 20-µL reaction using iScript cDNA synthesis kit (BioRad, On, Canada). To remove the RNA templates, cDNA was treated with RNAse. Freshly, prepared cDNA was quantified using NanoDrop1000 spectrophotometer (NanoDrop, Wilmington, DE, USA). Total 20µL Polymerase chain reaction (PCR) was carried out by using diluted (20 nanograms per microliter) cDNA, 10 picomoles of primers (Forward and Reverse), 2X PCRmix (Froggabio Life Sciences, NY) at standard annealing temperature. Normalized cDNA was used to carry out the quantitative real-time PCR based on iQSYBR Green supermix (BioRad) using CFX384TM Real-Time System (BioRad, ON, Canada).

3.4 Results

3.4.1 Disease severity

***Spikelet disease severity*:** The FHB disease severity, in both R-NIL and S-NIL, was assessed as PSD, following spray inoculation of spikelets. The spikelets of both the NILs showed necrotic spots at 3dpi, however, there after the spread of necrotic regions and bleaching of adjacent spikelets was much faster in S-NIL (Figure 3.1). The disease severity based on proportion of spikelets diseased (PSD) at 9 dpi was significantly higher in NIL-S ($P < 0.001$). The area under the disease progress curve (AUDPC), over 21 dpi, was also significantly ($P < 0.004$) higher in S-NIL as compared to R-NIL (Figure 3.2).

3.4.2 *Fusarium graminearum* virulence factor DON and fungal biomass accumulation

The *F. graminearum* indicator metabolite or virulent factor (DON) accumulation was significantly different between the R-NIL and S-NIL (Figure 3.3A). Significant difference was observed in DON to D3G conversion in R-NIL. The DON accumulated in S-NIL was 1.33 mg kg^{-1} and in R-NIL was 0.98 mg kg^{-1}. Interestingly the VIGS of *TaMYBFhb5* in R-NIL showed nearly 3.5 fold increase in DON accumulation as compare to non-silenced R-NIL (Figure 3.3B). Further, *F. graminearum* fungal biomass was more than two fold high after the silencing of *TaMYBFhb5* in R-NIL, which clearly supported that this reduction was due to RR metabolites accumulation, further confirming the control of these genes by *TaMYBFhb5* TF (Figure 3.4).

3.4.3 The spikelets of resistant and susceptible NILs varied in RR metabolites

Metabolic profiling of R-NIL and S-NIL spikelets at 72 hpi revealed a total of 2643 consistent peaks in all the replicates. Among these, 931 peaks were identified as resistant related induced (RRI) with more than one fold change. Among these, 21 were putatively identified as RRI and 91 as PRr metabolites. Similarly, among the 1763 resistant related constitutive (RRC) peaks that were detected with more than one fold change across the treatment, only 48 were putatively identified with a compound name (Table. 3.1, Appendix of the Table A3.1).

3.4.4 QTL-Fhb5 dissection through marker walking and synteny mapping discovered *TaMYBFhb5* gene

The QTL-Fhb5 tightly associated flanking markers (Xgwm415 and Xgwm304) were consistently linked to the spikelet resistance phenotype in different studies and subsequently the latter were used for fine mapping of QTL-Fhb5 to 0.3cM (Xue et al., 2011). Therefore, we sequenced these flanking markers and submitted the sequences to the NCBI database (Xgwm415_Ta5a_QTL with GenBank: KF226135 and Xgwm304_ Ta5a_QTL with GenBank: KF226136). The flanking marker sequences were used as a starting point, or anchors, for amplifying the QTL-Fhb5. The sequences retrieved through PCR amplification and sequencing revealed that the flanking marker (Xgwm415_Ta5a_QTL) was tagged to a DNA binding R2R3 MYB transcription factor gene *TaMYBFhb5* (GenBank: AHZ33834.1). The QTL-Fhb5 sequences were retrieved using tightly linked flanking markers sequences and *in-silico* annotation of QTL-Fhb5 sequences revealed the R2R3 MYB transcription factor gene along with

several biotic stress resistance genes (Appendix Table A3.2). The phylogenetic and conserved domain analysis of the *TaMYBFhb5* using PROSITE web interface confirmed the helix-turn-helix features of DNA binding and MYB type domains (http://prosite.expasy.org/). The Xgwm415 marker was tagged to the *TaMYBFhb5* TF gene (Figure 3.5). Further, the *TaMYBFhb5* gene tagged flanking marker association was confirmed by aligning the reference sequences of Chines Spring sequence from NCBI database (AEOM01037456.1) and the 5A genome progenitor *Tritucum urartu* scaffold (scaffold5558) (Appendix Figure A3.1) and transcriptome genome assembly (*Triticum urartu* UCW_Tu-k55_contig_10394). The QTL-Fhb5 flanking markers were lying within physical bin 5AS 1-0.40-0.75 of wheat chromosome 5A (La Rota and Sorrels, 2004; Sourdille et al., 2004).

The genetic to physical distance varies based on the recombination frequencies and gene richness of the regions in wheat chromosomes (Gill et al., 1996a; Gill et al., 1996b). Therefore, we assumed the fine mapped region of QTL-Fhb5 was as little as 0.3cM must be less than 1.0 mega base pairs (Mbp) and hence, we used tightly linked markers to sequence in wheat NILs used in the study and aligned the marker sequence onto the 5A reference chromosome. The retrieved 5A region *In-silico* annotation revealed several putative candidate genes (Appendix Table A3.2). Among the predicted genes the R2R3 MYB transcription factor encoding gene was also present. The *TaMYBFhb5* had two introns and two exons (Figure 3.5). The comparison of physical and genetic maps data from GrainGenes (http://wheat.pw.usda.gov/cgi-graingenes/report.cgi?class=locus;name=Centromere-5A), along with *in-silico* annotated genes from QTL-Fhb5, revealed *TaMYBFhb5* gene conservation across the species (Figure 3.6). Additionally, the predicted QTL-Fhb5 genes showed homology to orthologous genes in rice chromosome 12, sorghum 8 and Brachypodium 4, confirming the synteny with wheat 5AS (La Rota and Sorrells, 2004). The *TaMYBFhb5* allele was compared with the other two alleles of hexaploid wheat to see the sequence variation and we found several single nucleotide polymorphisms (SNPs). The cDNA sequence of *TaMYBFhb5* gene in R-NIL and S-NIL revealed the SNP between B and D alleles (Appendix Figure A3.2).

3.4.5 Transcriptional regulation of phenylpropanoid and flavonoid pathway genes

The *TaMYBFhb5* TF is known to regulate the phenylpropanoid metabolic pathway. The mapping of high fold change RR metabolites onto the KEGG secondary metabolic pathways

indicated several biosynthetic *R* genes. The *PAL* which is a key enzyme for both phenylpropanoid and flavonoid pathways. Similarly the downstream structural genes of phenylpropanoid and flavonoid pathways, such as *CHS* and *ACT* genes promoter regions carries R2R3 MYB interacting domains and hence, the latter were transcriptionally regulated by *TaMYBFhb5* TF. (Figure 3.7).

Further, the *in-silico* analysis for nuclear localization signal (NLS) domain in *TaMYBFhb5* revealed that the presence of six base pairs (CCWACC or CCTACC) known for nuclear localization (ID: MYBPZM, S000179). These base pairs had similar hits for the core of the consensus maize *P* (myb homolog) binding site, where the myb-homologous *P* gene regulates the phlobaphene pigmentation in maize floral organs by directly activating flavonoid biosynthetic genes (Grotewold et al., 1994). This further confirmed that the structural genes from both phenylpropanoid and flavonoid pathways can be transcriptionally regulated through *TaMYBFhb5* TF.

3.4.6 Virus induced *TaMYBFhb5* gene silencing confirmed its role on downstream gene regulation

The efficiency of virus induced gene silencing (VIGS) of *TaMYBFhb5* was confirmed based on the phytoene desaturase (PDS) gene responsible for green pigmentation in plants (Figure 3.8). The high accumulation of phenylpropanoid and flavonoid pathways key enzymes encoding structural genes, such as *PAL, CHS* and *ACT* transcripts was observed at 72 hpi of pathogen between R-NIL and S-NIL (Figure 3.9). Similarly, the *TaMYBFhb5* gene also showed high expression in R-NIL as compared to S-NIL and R-NIL silenced (Figure 3.10). The downstream gene expression in silenced R-NIL also indicated the reduction of relative transcript abundance in spikelets collected 72 hpi of *F. graminearum* (Figure 3.11).

Further, the electro mobility shift analysis (EMSA) based on the interactions between *TaMYBFhb5* TF and the promoter sequence of key candidate genes (*PAL, ACT* and *CHS*) from secondary metabolic pathway indicated the shift in the mobility of the interacted products in both polyacrylamide and agarose gels (Figure 3.12). This implies the promoter sequences of downstream genes of phenylpropanoid and flavonoid pathways carries the *TaMYBFhb5* TF interacting domains and hence, transcriptionally regulated during *Fusarium spp*. initial infection.

The *in-silico* analysis of *TaMYBFhb5* TF matching protein data base (PDB) file (3ZQC) with model dimensionsof (Å):X:58.166, Y:38.224, Z:50.382 from RCSB (http://www.rcsb.org) also confirmed the structural genes interactions active amino acid residues within *TaMYBFhb5* TF (PDB:3ZQC) with phenylpropanoid and flavonoid pathways enzymes (Figure 3.13).

3.4.7 Virus induced *TaMYBFhb5* gene silencing confirmed its role in the accumulation of RR metabolites

The transit suppression of *TaMYBFhb5* TF expression in R-NIL led to the disappearance of several phenylpropanoid and flavonoid pathway metabolites during *F. graminearum* infection. This may be because the key metabolic pathway enzymes encoding genes, such as *PAL*, *CHS* and *ACT* were also downregulated. The RR metabolites identified upon pathogen inoculation mainly, phenylpropanoid group metabolites; podophyllotoxin (3.8 FC), podorhizol beta-D-glucoside (2.5 FC), syringin (1.5 FC) and malvidin 3-diglucoside (1.5 FC) were significantly lower in silenced R-NIL compared to non-silence R-NIL (Table 3.2). Similarly, flavonoids; kanzonol I (3.4 FC), 4-O-alpha-Cadinylangolensin (3.3 FC), peonidin 3-galactoside-5-glucoside (1.9 FC), diosmin (2.0 FC) and cyanidin 3-lathyroside (1.5 FC), Terpenoids; convallasaponin A (2.1 FC), 10-Deoxygeniposidic acid (1.6 FC) and secologanin (1.7 FC), Lipids and Fatty acids; 1-dodecanoyl-2-heneicosanoyl-glycero-3-phosphate (10.7 FC), 1α,25-dihydroxy-23-azavitamin D3 / 1α,25-dihydroxy-23-azacholecalciferol (9.5 FC), C-12 NBD-dihydro-Ceramide (17.7 FC), sorbitan palmitate (8.7 FC), N,N-(2,2-dihydroxy-ethyl)arachidonoylamide (7.9FC), N-palmitoyl phenylalanine (6.5 FC) and 3,-Oxohexadecanoic acid glycerides (4.6 FC) were significantly low in silenced R-NIL spikelets ($P<0.05$).

3.5 Discussion

The advancement in the molecular breeding technologies and statistical analysis helped plant breeders to associate the phenotypic observations with genotypic variations. In wheat, more than 100 FHB resistances QTL were identified, but the underlying genes are largely unknown. The well-defined and fine mapped QTL-Fhb5 was dissected based on primer walking. Interestingly, one of the tightly associated markers was tagged with a R2R3 MYB transcription factor, designated as *TaMYBFhb5*. This was functionally characterized using wheat NILs, derived from Suami3 genotype, with contrasting alleles against spikelet resistance.

3.5.1 QTL-Fhb5 dissection led to the discovery of a MYB TF

The QTL-Fhb5 was fine mapped between tightly linked flanking markers Xgwm305 and Xgwm 415 to 0.3 cM and these markers were lying within the deletion bin map 5AS1-0.45-0.75 (Sourdille et al., 2004; Xue et al., 2011). The primer walking method has been employed in sequencing the long stretch of DNA (Griffin and Griffin, 1993; Sverdlov and Azhikina, 2005). The availability of genomic databases and advancement in in bioinformatic tools in the recent past helped *in-silico* annotation of unknown genome. The QTL-Fhb5 flanking markers based primer walking technique led to identification the R2R3 MYB transcription factor in the current study, designated as *TaMYBFhb5* TF. An *in-silico* annotation of the entire QTL-Fhb5 region revealed several genes including the *TaMYBFhb5* . Interestingly, the *TaMYBFhb5* gene was tagged to one of the flanking marker Xgwm 415 (Xgwm415_Ta5A_QTL, GenBank: KF226135). This indicates the QTL-Fhb5 is a hot spot for FHB disease resistance genes. The primer walking technique with automation and low redundancy, has given a fruitful result in identifying the gene and reducing the time required by other methods, such as molecular marker assisted fine mapping and mutation breeding approaches (Voss et al., 1993).

3.5.2 *TaMYBFhb5* regulates hydroxycinnamic acid amide RR metabolite biosynthetic genes

The hydroxycinnamic acid amides (HCAAs), a phenylpropanoid, enforce the cell walls around infection site to contain the pathogen initial infection (Gunnaiah and Kushalappa, 2014; Gunnaiah et al., 2012). The current study also detected several HCAAs metabolites with high fold change accumulation such as, 4-coumaroylputrescine, N-caffeoylputrescine, 4-coumaroyl agmatine, 4-coumaroyl-3-hydroxyagmatine and syringin (Table 3.1). The transient gene silencing of *TaMYBFhb5* led to a decrease in the accumulation of these metabolites in R-NIL (Table 3.2) Therefore, the regulatory function of TFs greatly helped in understanding the key genes involved in the biosynthesis of resistance metabolites in the secondary metabolic pathways (Broun et al., 2006). However, the TFs generally regulate several downstream genes and a chromatin immunoprecipitation (ChIP) study would be needed to reveal all the downstream genes regulated by this TF (Singh et al., 2002). We also found high fold induction (27.46, $P<0.001$) of 4-coumaroyl-3-hydroxyagmatine as a PRr metabolite in R-NIL, as opposed to S-NIL. A higher level of accumulation of *p*-coumaroyl-hydroxyagmatine has also been reported upon *Erysiphe graminis* f. sp. *hordei* inoculation in barley near-isogenic lines, which showed *in-*

vitro and in-vivo antifungal activities (Von Ropenack et al., 1998). Accumulation of several HCAAs in both wheat and barley following *F. graminearum* infection have been reported (Gunnaiah and Kushalappa, 2014; Gunnaiah et al., 2012). Several antifungal metabolites reported in the earlier studies, like p-coumaric acid, methyl jasmonate, feruloyl quinic acid were also detected in the current study (Bollina et al., 2010; Kumaraswamy et al., 2011b).

3.5.3 *TaMYBFhb5* also regulated flavonoid metabolic pathway genes

Our study reports regulation of *PAL* and *CHS* genes through *TaMYBFhb5* TF to accumulate RR flavonoids metabolites. In the R-NIL the flavonoid metabolites such as 3,3"-binaringenin, 8-prenylnaringenin, Cyanidin 3-(*p*-coumaroyl)-glucoside and Isoorientin 2"-O-rhamnoside were highly accumulated, relative to S-NIL. An EMSA assay revealed interaction of *TaMYBFhb5* with the promoter sequence of downstream metabolic pathway genes: *PAL, ACT* and *CHS* (Figure 3.12). Similarly, the R2R3 MYB TFs are well known in regulating the phenylpropanoid and flavonoid metabolites following biotic stresses (Ambawat et al., 2013; Holl et al., 2013). The single MYB8 controlled the accumulation polyamides by regulating several hydroxycinnamoyl co-A genes in *Nicotiana attenuata* (Onkokesung et al., 2012).

3.5.4 *TaMYBFhb5* regulated downstream genes that biosynthesized RR metabolites, which suppressed the accumulation of fungal biomass

There was a direct correlation between host resistance based on PSD (Figure 3.2) and the total fungal biomass accumulation in the pathogen infected tissues (Figure 3.4). This also, associated with a higher accumulation of the mycotoxin, DON, in S-NIL than in R-NIL (Figure 3.3). In our study, the R-NIL suppressed both DON and fungal biomass as compare to S-NIL. However, following silencing of *TaMYBFhb5* the fungal biomass accumulation in R-NIL was increased by more than two fold, implying that the resistance allele of *TaMYBFhb5* has a direct role in FHB resistance. Furthermore the associated reduction in candidate RR metabolites and also reduction in the expression of biosynthetic genes confirmed the mechanism by which this TF controlled FHB resistance.

Table 3.1. Fusarium head blight resistance related metabolites identified from the spikelets of wheat NILs carrying QTL-Fhb5, resistant and susceptible alleles, following *F. graminearum* or mock inoculations.

m/z Value Observed	**Metabolites**	**FC®**	**Database ID©**
Mass (Da)	**Phenylpropanoids**	**FC®**	**Database ID©**
148.0524	*trans*-Cinnamate	1.37** (PRr)	PlantCyc:DIHYDROCOUMARIN;KEGG:C00423
164.0473	m-coumaric acid	4.17** (PRr)	**METLIN :305**
178.0630	Coniferaldehyde	2.79*** (PRr)	PlantCyc:CONIFERYL-ALDEHYDE;KEGG:C02666, **McGill MD C00002728**
234.1368	4-Coumaroylputrescine	38.81** (PRr)	HMDB:HMDB33461;Metlin:2371; LIPIDMAPS:LMFA01090008;pUBcHEM:4983;**In silico, (Muroi et al., 2009)**
250.1317	N-Caffeoylputrescine	11.92*** (PRr)	KEGG:C03002;**METLIN:3380**
276.1586	4-coumaroyl agmatine	126.05*** (PRr) 1.21** (RRI)	PlantCyc :N-4-GUANIDINOBUTYL-4-HYDROXYCINNAMAMID; ChEBI:58644 ;KEGG:C04498 ;PubChem:25245514;**METLIN :43471;In silico(Gunnaiah et al. 2012)**
292.1535	4-coumaroyl-3-hydroxyagmatine	27.46*** (PRr)	PlantCyc:CPD-12237; KEGG:C11633;METLIN:64338
326.1002	4-O-beta-D-Glucosyl-4-hydroxycinnamate	1.23*** (PRr)	KEGG:C04415
344.1471	Dihydroconiferyl alcohol glucoside	1.67*** (PRr)	PlantCyc:CPD-82;METLIN:41168;KEGG:C11652;GUN:2012
372.1420	Syringin	8.65* (PRr)	PlantCyc:CPD-63;KEGG:C01533;**METLI**

			N:64181
Mass (Da)	**Lipids and Fatty Acids**	**FC®**	**Database ID©**
130.0630	6-oxohexanoate	1.30** (PRr)	PlantCyc:6-OXO-HEXANOATE;KEGG:C06102;HMDB:HMDB12882
182.0790	L-iditol	1.96*(PRr) 1.42*(RRC)	PlantCyc:CPD-369;KEGG:C01507;HMDB:HMDB11632;**MASSBANK:PR100483**
200.1412	2-hydroxy-10-undecenoic acid	1.39* (RRC)	LIPIDMAPS:LMFA01050164;METLIN:
278.2246	Crepenynate	1.57* (PRr)	PlantCyc:CREPENYNATE;KEGG:C07289
310.2297	14'-apo-beta-Carotenal	1.22* (RRC)	KEGG:C06734:LIPIDMAPS:LMPR01070297
312.2301	12,13-dihydroxyoctadeca-9,15-dienoate	1.12*** (PRr)	PlantCyc:CPD-13092;KEGG:C04717; **MASSBANK:UT000064**
328.2250	2,3-Dinor-8-iso prostaglandin F1alpha	1.68* (PRr)	KEGG:C14795
328.2613	Avocadene Acetate	1.28* (RRI)	METLIN:43512;HMDB:31043
375.2773	N-Arachidonoyl-L-Alanine	1.45* (RRC)	METLIN:64920;LIPIDMAPS:LMFA08020153
392.2021	(6RS)-22-oxo-23,24,25,26,27-pentanorvitamin D3 6,19-sulfur dioxide adduct	1.26* (RRC)	LIPIDMAPS:LMST03020008
416.3142	2-(Trimethylsilyl) Oxy-Hexadecanoic Acid Trimethylsilyl Ester	1.49* (RRC)	MASSBANK:JP000609
537.1060	Phenanthridine-2-carboxylic acid	2.06*** (PRr)	KEGG:C11471
572.2962	Phosphatidylinositol lyso	1.66***(PRr) 1.47*(RRC)	**MASSBANK:UT001490**
698.3514	Corchorusoside A	1.22* (RRC)	METLIN:88745:HMDB:HMDB32823
Mass (Da)	**Aromatic compounds and**	**FC®**	**Database ID©**

	Flavonoids		
300.1209	Salidroside	1.39* (RRC)	PlantCyc:CPD-13354;KEGG:C06046;**METLIN : 44847**
316.0794	2,5-dihydroxybenzoate 2-O-β-D-glucoside	1.37** (RRC)	PlantCyc:CPD-12663
326.1453	Acepromazine	2.56* (RRC)	METLIN:85533
330.0951	1-O-Vanilloyl-beta-D-glucose	1.42* (RRC)	KEGG:C20470
340.1311	8-prenylnaringenin	1.35*** (PRr)	PlantCyc:CPD-9440
400.1376	Zuclopenthixol	1.51** (RRC)	METLIN:3109
504.2032	Chlorhexidine	1.25* (RRC)	KEGG:C06902;**METLIN:1720**
514.3308	2-((4-Dodecylphenyl)azo)-4-(2,4-xylylazo) resorcinol	14.02* (RRC)	PubChem:110018
542.1210	3,3"-binaringenin	1.42* (RRC)	KEGG:C09758;METLIN:47514;LIPIDMAPS:LMPK12040001
566.1424	Poriolide	1.63* (RRC)	LIPIDMAPS:LMPK12140226;METLIN:52714
586.1320	Prunin 6"-O-gallate	1.34* (RRC)	LIPIDMAPS:LMPK12140244
594.1585	Isoorientin 2"-O-rhamnoside	1.47** (RRC)	KEGG:C04024;PlantCyc:VITEXIN-2-O-BETA-D-GLUCOSIDE
595.1452	Cyanidin 3-(p-coumaroyl)-glucoside	2.44*** (PRr) 1.98*(RRC)	PlantCyc:CPD-7866;KEGG:C12095;
595.1660	Pelargonidin-3,5-diglucoside	1.38*** (PRr)	PlantCyc:CPD-7137;KEGG:C08725;**MASSBANK:PR100645**
760.2579	Epimedoside	1.62** (RRC)	LIPIDMAPS:LMPK12112021
770.2058	Pelargonidin 3-(6"-ferulylglucoside)-5-glucoside	1.35*** (PRr)	METLIN:46811;LIPIDMAPS: LMPK12010044
782.2068	Pelargonidin 3-(6"-p-coumarylglucosi	2.67* (RRC)	METLIN:46814;LIPIDMAPS:LMPK12010047

	de)-5-(6'''-acetylglucoside)		
Mass (Da)	**Unclassified Metabolites**	**FC®**	**Database ID©**
152.0685	Xylitol	1.74** (PRr)	KEGG:C00379
165.0790	L-phenylalanine	1.21*** (PRr)	PlantCyc:PHE;KEGG:C00079;**METLIN:28**
204.0899	L-tryptophan	1.85*** (PRr)	KEGG:C00078;**MASSBANK:PR100498**
214.1200	Methyl 2-diazoacetamidohexonate	1.91*** (PRr)	KEGG:C01223
224.1412	(-)-jasmonic acid methyl ester	1.36* (RRC)	PlantCyc:CPD1F-2;KEGG:C11512;LIPIDMAPS:LMFA02020010;**MASSBANK:PR100748**
226.1569	Dihydrojasmonic acid, methyl ester	1.36* (RRI)	METLIN:43916
230.0192	D-ribulose-5-phosphate	1.23*** (PRr)	KEGG:C00199;**METLIN : 159**
234.1620	Zealexin A1	1.27* (RRC)	PlantCyc:CPD-13573
260.0202	D-Galactose 6-sulfate	2.75*** (RRC)	KEGG:C01067
282.2433	Tropane	3.44*** (RRC)	PubCHem:4157
313.1889	Heliotrine	1.69*** (PRr)	KEGG:C10324
334.1125	Asp Ser Asn	1.27** (RRI)	METLIN:16742
343.0903	DIBOA-β-D-glucoside	1.25** (PRr)	PlantCyc:CPD-13811;KEGG:C15772
346.1264	Aucubin	1.62* (RRC)	KEGG:C09771;LIPIDMAPS:LMPR0102070006;METLIN:41151
360.1420	7-deoxyloganate	1.93*** (PRr) 1.42*(RRC)	PlantCyc:CPD-9981;KEGG:C11636
390.1526	Loganin	1.44** (RRC)	PlantCyc:LOGANIN;KEGG:C01433;MASSBANK:C01433
406.2396	Calcium undecylenate	8.61* (RRC)	PubChem:14865
436.2590	1-oleyl-2-lyso-phosphatidate	2.09** (RRC)	PlantCyc:L-1-LYSOPHOSPHATIDATE;**METLIN:5432**;HMDB:HMDB07855
458.1424	2'-(E)-Feruloyl-3-(arabinosylxylos	1.47* (RRC)	METLIN:86818;HMDB:HMDB30230

	e)		
532.3764	Pentanoic acid ester	32.28*** (PRr)	PubChem: 157226 ChemSpider: 138374
544.2632	Perindopril glucuronide	1.44* (RRC)	METLIN:1796

* *t*-test significance at $P<0.05$, ** *t*-test significance at $P<.01$, *** *t*-test significance at $P<.001$

® FC(Fold change) calculation: were based on relative intensity of metabolites, RRC(Resistance related constitutive) = RM/SM, PRr (Pathogen related in resistant NIL) = RP/RM, RRI(Resistance related induced) = (RP/RM)/(SP/SM); RP: resistant NIL with pathogen inoculation, RM: resistant NIL with mock inoculation, SP: susceptible NIL with pathogen inoculation, SM: susceptible NIL with mock inoculation.

©Database ID in bold is the fragmentation match

Table 3.2. List of resistant related (RR) metabolites identified in R-NIL non-silenced versus silenced upon *Fusarium graminearum* inoculation.

m/z value observed	Metabolites	AME[a]	FC [b]	Database ID[c]
Mass (Da)	**Phenylpropanoids**			
164.04	m-Coumaric acid	1.0	1.2***	305
372.14	Syringin	0.2	1.5***	64181
386.12	1-O-Sinapoyl-β-D-glucose	0.0	1.2**	64184
414.13	Podophyllotoxin	1.2	3.8***	2039
578.19	Podorhizol beta-D-glucoside	0.7	2.5*	68647
580.21	(+)-Syringaresinol O-beta-D-glucoside	1.0	1.5***	68660
596.14	Okanin 4'-(6"-p-coumarylglucoside)	2.1	1.6***	51962
654.17	Malvidin 3-diglucoside	0.9	1.5**	47140
800.23	Malvidin 3-rutinoside-5-glucoside	1.0	1.2***	47147
Mass (Da)	**Flavonoids**			
435.21	Kanzonol I	4.0	3.4***	HMDB40606
468.12	Catechin-4-ol 3-O-beta-D-galactopyranoside	5.0	1.2**	47415
475.28	4-O-alpha-Cadinylangolensin	1.6	3.3***	LMPK12160053
502.11	Apigenin 7-(2"-acetyl-6"-methylglucuronide)	1.9	1.2***	48807
580.14	Cyanidin 3-lathyroside	0.4	1.5***	46863
608.17	Diosmin	0.1	2.0**	3676

624.16	Peonidin 3-galactoside-5-glucoside	1.1	1.9***	46997
Mass (Da)	**Lipids and Fatty acids**			
661.48	1-dodecanoyl-2-heneicosanoyl-glycero-3-phosphate	5.1	10.7*	LMGP10010062
416.31	1α,25-dihydroxy-23-azavitamin D3 / 1α,25-dihydroxy-23-azacholecalciferol	3.7	9.5***	LMST03020070
368.37	Lignoceric acid	0.8	3.6***	420
197.99	Dihydroxyacetone Phosphate Acyl Ester	1.4	3.1***	62468
336.30	7,7-dimethyl-5,8-Eicosadienoic Acid	1.2	2.3***	34670
498.21	Iridodial glucoside tetraacetate	2.0	2.1	41171
294.22	13-Keto-octadeca-9Z,11E-dienoic acid	1.5	2.0***	34474
214.16	12-hydroxy-10-dodecenoic acid	1.1	1.9***	35534
310.21	9-hydroperoxy-10E,12,15Z-octadecatrienoic acid	0.9	1.5***	35356
660.47	C-12 NBD-dihydro-Ceramide	2.9	17.7***	44980
401.29	Sorbitan palmitate	3.3	8.7***	HMDB29887
390.30	N,N-(2,2-dihydroxy-ethyl)arachidonoylamide	3.0	7.9***	LMFA08020028
402.30	N-palmitoyl	3.0	6.5***	LMFA0802

	phenylalanine			0091
360.25	3-Oxohexadecanoic acid glycerides	2.6	4.6***	HMDB3984 9
405.11	2-(4-Chloro-3,5-dimethylphenoxy)-N-(2-phenyl-2H-benzotriazol-5-yl)-acetamide	2.6	3.3***	C11561
358.13	10-Deoxygeniposidic acid	0.0	2.8***	64051
382.38	pentacosanoic acid	0.9	2.3***	4209
316.26	2,3-dihydroxy stearic acid	1.1	2.1***	35462
284.27	Stearic acid	0.5	1.2**	189
Mass (Da)	**Terpenoids**			
580.35	Convallasaponin A	4.8	2.1***	67250
388.13	Secologanin	0.1	1.7***	41147
358.12	10-Deoxygeniposidic acid	1.0	1.6***	64051
388.13	Secologanin	0.2	1.2***	41147
Mass (Da)	**Miscellaneous**			
193.15	Solanone (Ketone)	4.1	27.9***	88390, HMDB3235 5
254.10	N-D-Glucosylarylamine (Amide conjugate)	1.7	7.8***	C03142
141.04	2-Aminomuconate 6-semialdehyde(Amide conjugate)	0.1	3.5***	3248
478.29	Glycerophospho-N-Oleoyl Ethanolamine (Ester)	4.1	3.3***	45335
198.04	Vanillylmandelic acid (Aminoacid conjugate)	4.0	2.8***	697
344.25	1,2-Dioctanoyl-sn-glycerol (Polyol)	0.9	2.6***	414

398.14	S-Adenosyl-L-methionine (SAMe) (Aminoacid conjugate)	5.0	1.6***	3289
290.12	Argininosuccinic acid(Aminoacid conjugate)	1.4	1.4***	389
174.05	Shikimic acid (Shikimate)	0.2	1.2***	338

* *t*-test significance at P<0.05, ** *t*-test significance at P<.01, *** *t*-test significance at P<.001

[a]Accurate mass error (AME) calculation: ((Observed mass - Exact mass)/Exact mass)*10^6)

[b]FC (Fold change) calculation: were based on relative abundances of RR metabolites between silenced and non-silenced samples upon pathogen inoculation = RNIL non-silenced (RnP)/silenced (RsP).

[c]Database ID = KEGG (starts with "C"), Human Metabolome Data Base (HMDB), numerical value indicates METLIN ID and LIPID metabolites and pathways strategy (LMAPS).

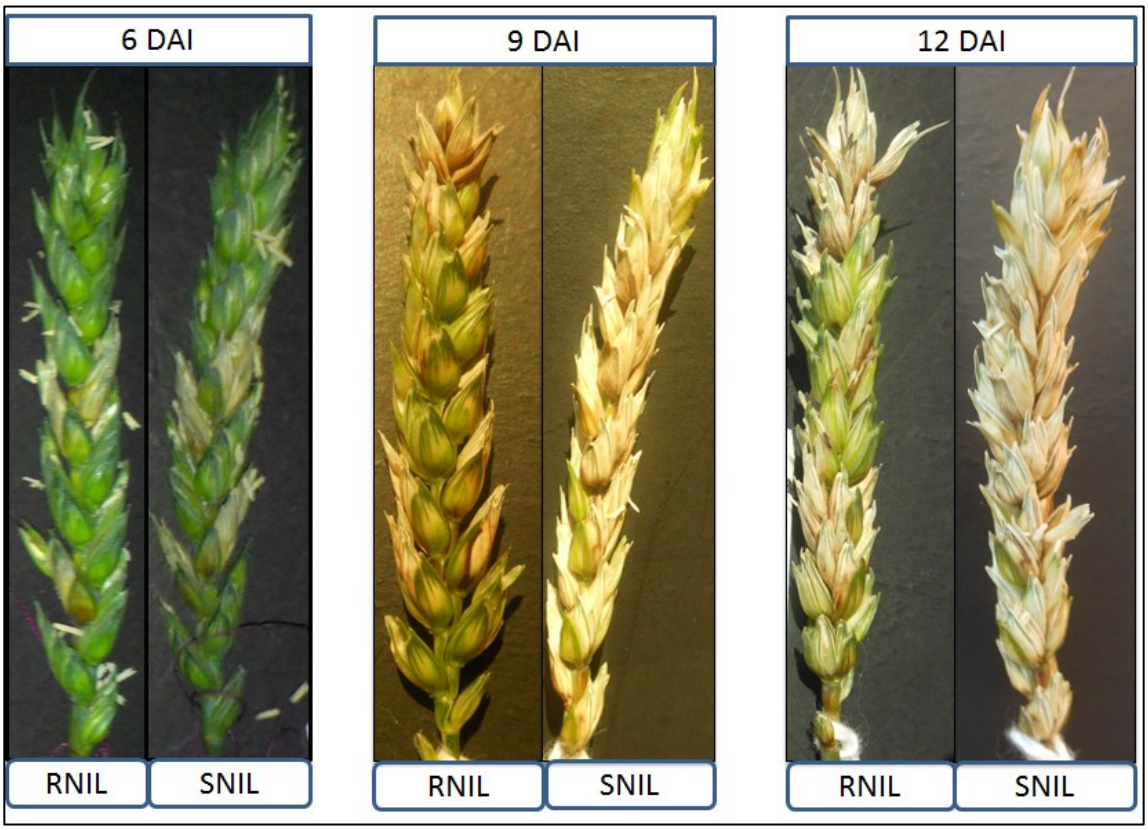

Figure 3.1. The disease severity was assessed following point inoculation with *Fusarium graminearum* (*Fg*). Disease symptoms observed in spikes at 6, 9, and 12 days post inoculation (dpi) of wheat NILs carrying resistant and susceptible alleles of QTL-Fhb5. Where, R-NIL= resistant near isogenic line, S-NIL=susceptible near isogenic line.

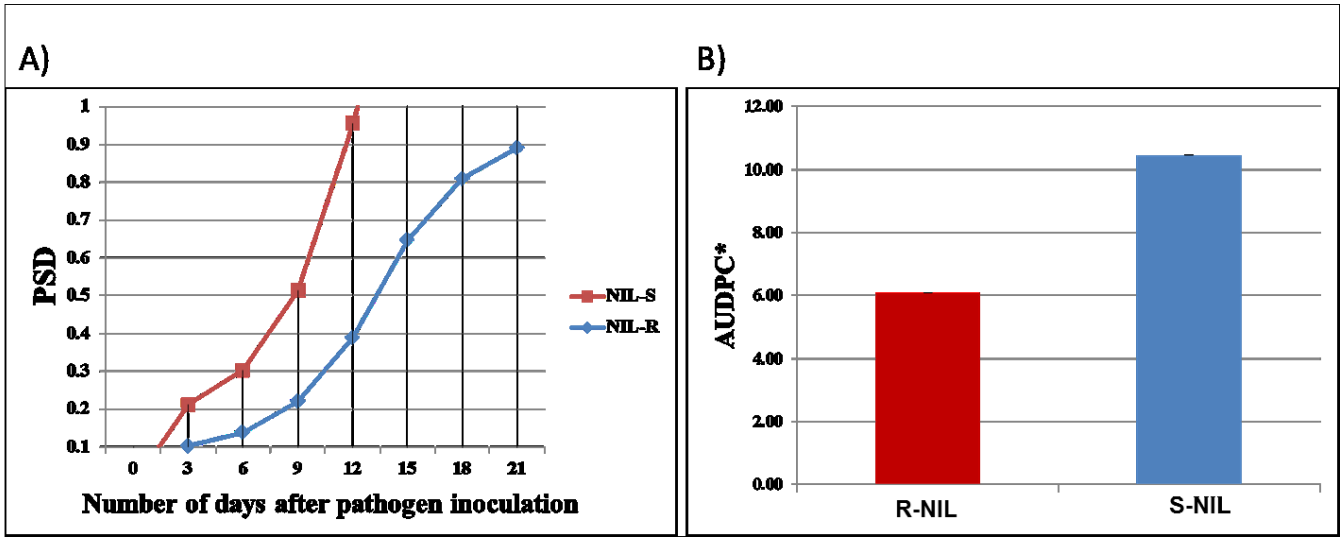

Figure 3.2. Disease severity was assessed based on visual observations, following spray inoculation with *Fusarium graminearum*; A) Proportion of spikelets diseased (PSD, significant at $P<0.001$ at 9 dpi); B) Area under disease progress curve (AUDPC* significant at $P< 0.004$), calculated based on every 3 d observations until 21 dpi. Where**,** R-NIL= resistant near isogenic line, S-NIL= susceptible near isogenic line.

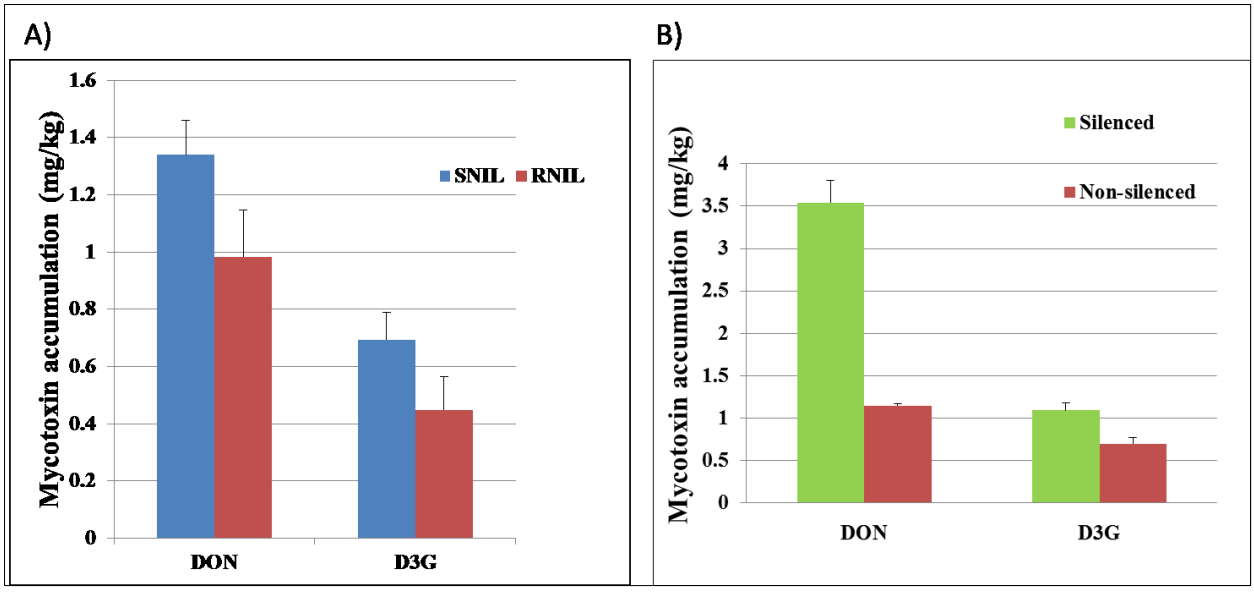

Figure 3.3 Accumulation of *Fusarium graminearum* pathogen indicator (RI) metabolite and its conversion within wheat near isogenic lines (NILs) carrying resistant and susceptible alleles of *TaMYBFhb5*. A) Mycotoxin accumulation between R-NIL and S-NIL after 72 hpi; B) Mycotoxin accumulation in silenced and non-silenced R-NIL at 72 hpi, based on individual spikelet inoculation. Where, R-NIL= resistant near isogenic line, S-NIL= susceptible near isogenic line, DON= deoxynivalenol, D3G=DON-3-o-glucoside.

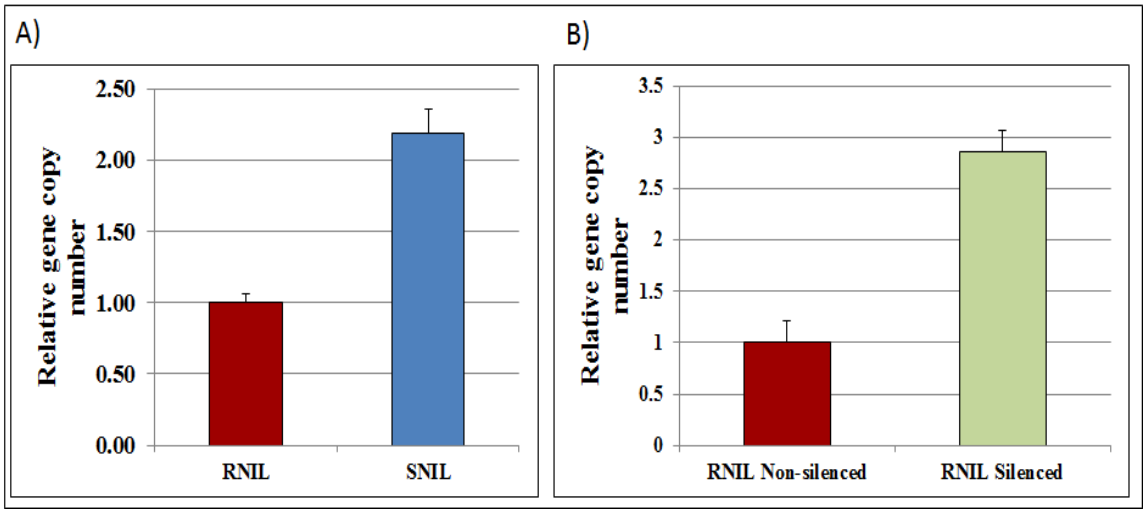

Figure 3.4. Fungal biomass quantification based on quantitative real time PCR (RT-qPCR) using *Fusarium graminearum* gene (*Tri6_10*) specific primers, between 5A R-NIL and S-NIL spikelet samples collected 72 hours post inoculation (hpi), following individual spikelet inoculation of two alternate pairs. Where, R-NIL= resistant near isogenic line carrying resistant allele for *TaMYBFhb5* gene, S-NIL= susceptible near isogenic line carrying susceptible allele for *TaMYBFhb5* gene.

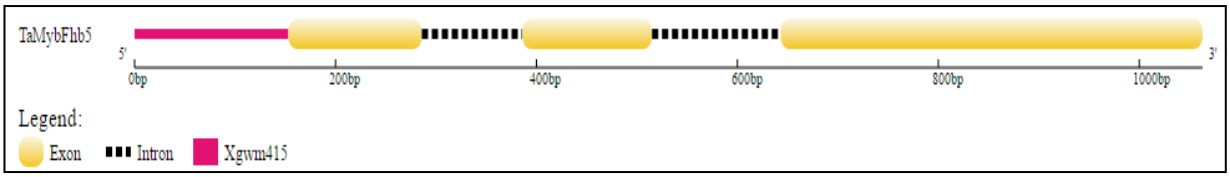

Figure 3.5 Schematic representations of *TaMYBFhb5* TF gene structure and flanking marker Xgwm415 tagged at 5' end.

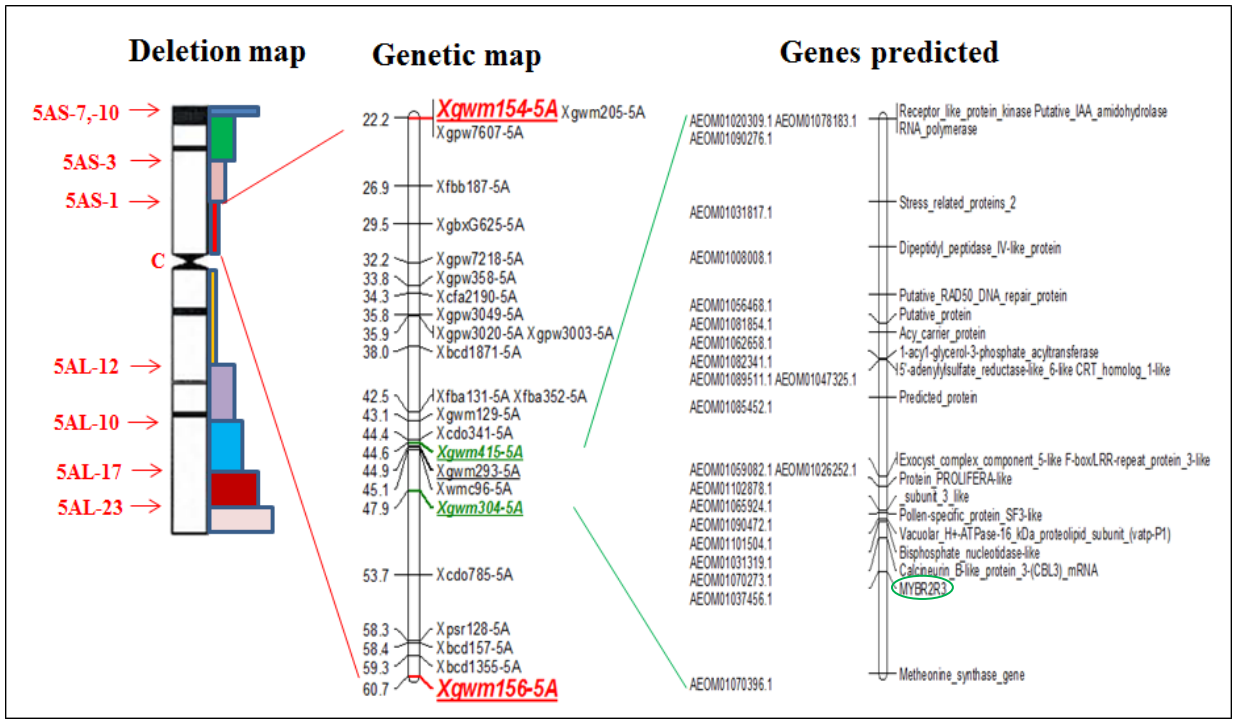

Figure 3.6. Comparative mapping of wheat QTL-Fhb5 genetic and physical maps encompassing *TaMYBFhb5* gene. The markers in red and green color were consistently associated with the QTL-Fhb5. The *TaMYBFhb5* gene lying between green color flanking markers (0.3cM) was found within the deletion bin 5AS-1(http://wheat.pw.usda.gov/cgi-bin/westsql/bin_candidates.cgi?bin=5AS1-0.40-0.75). Left side for deletion map are bin numbers; Left side for genetic map=linkage distance (cM); Left side for gene predicted= NCBI IDs. The predicted genes have synteny with Brachypodium, rice, sorghum, barley, Arabidopsis and wheat.

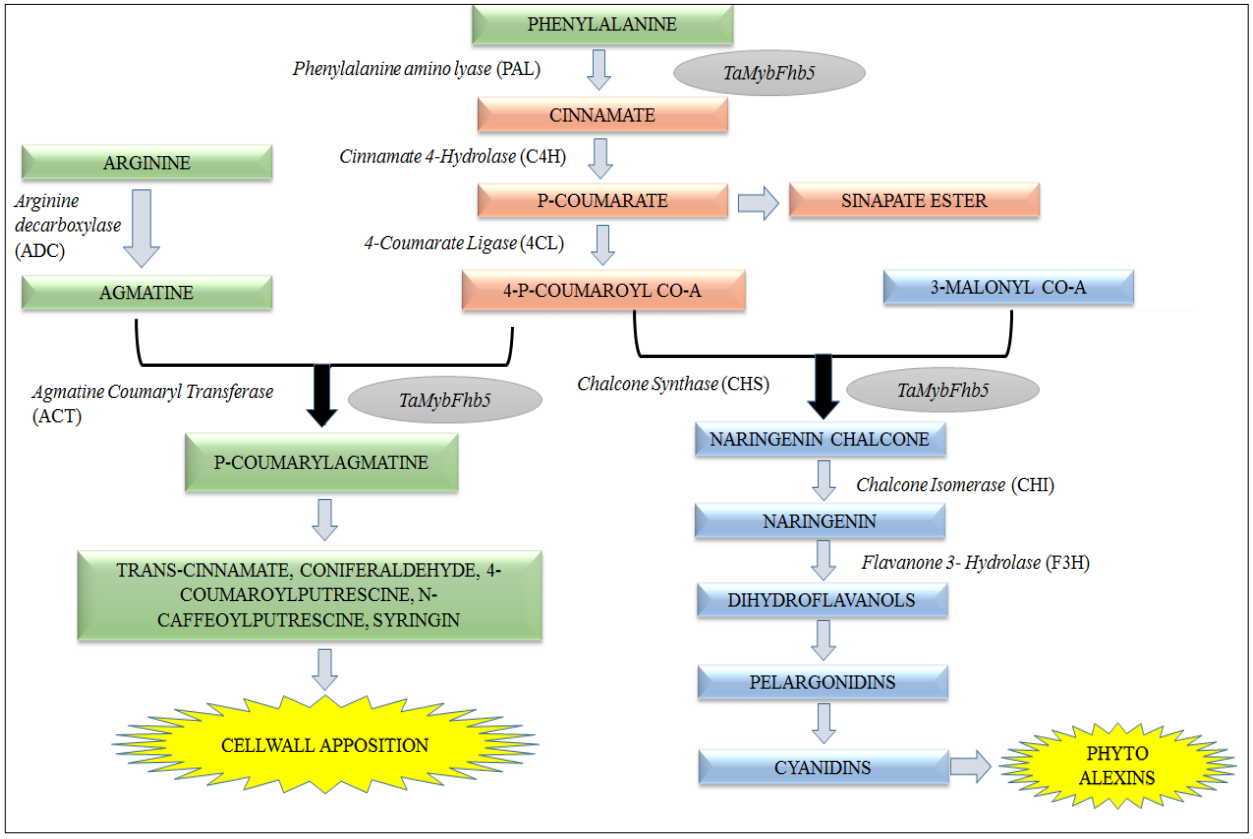

Figure 3.7. Schematic representation of resistance related metabolites mapped on to KEGG pathway and major phenylpropanoid and flavonoid gene regulation through *TaMYBFhb5* gene.

Figure 3.8. Virus induced gene silencing of phytoen desaturase (PDS) gene in resistant near isogenic line (R-NIL) spikelets carrying *TaMYBFhb5* gene at 6 days post inoculation (dpi). Where, BSMV:PDS = BSMV carrying fragment of PDS gene (Scofield et al., 2005); BSMV:00 = BSMV without PDS fragment.

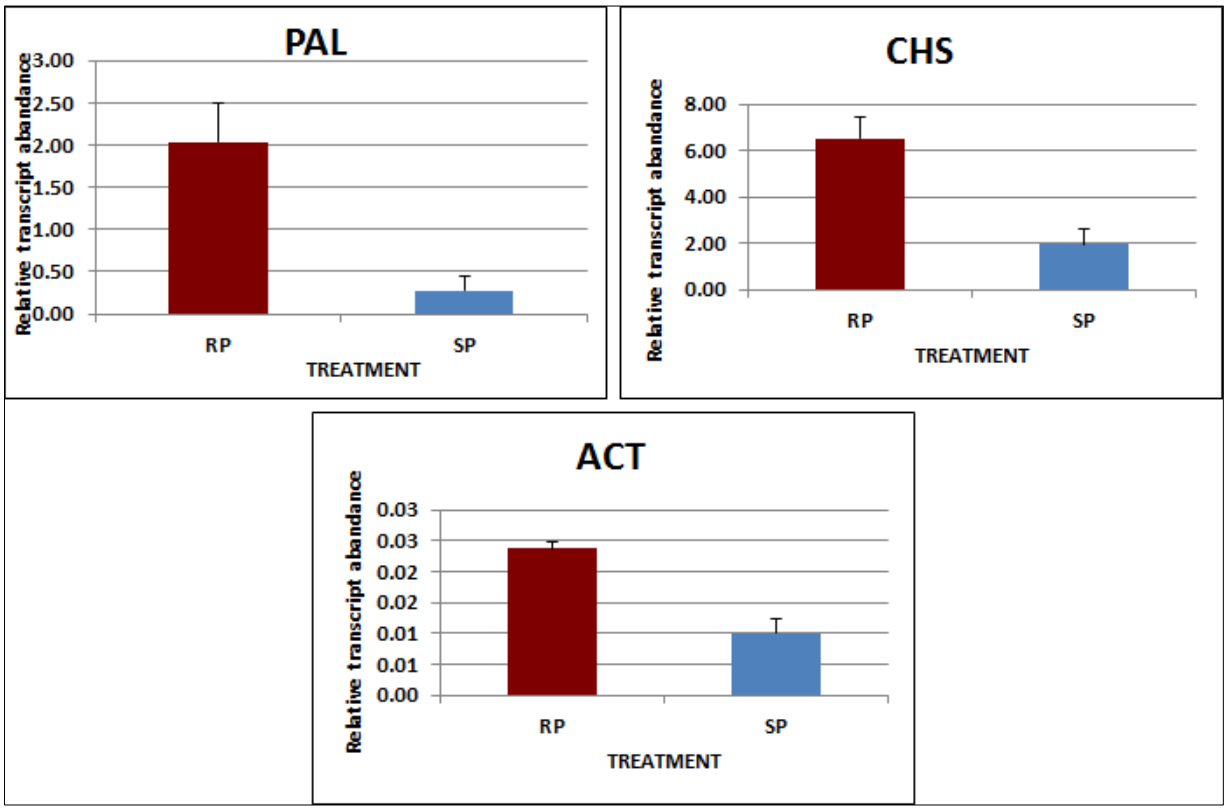

Figure 3.9 Differential expression analysis of structural genes, *PAL, ACT* and *CHS* at 72 hpi of *Fusarium graminearum*. Where, RP=resistant near isogenic line (NILs) inoculated with pathogen, SP= susceptible NIL inoculated with pathogen.

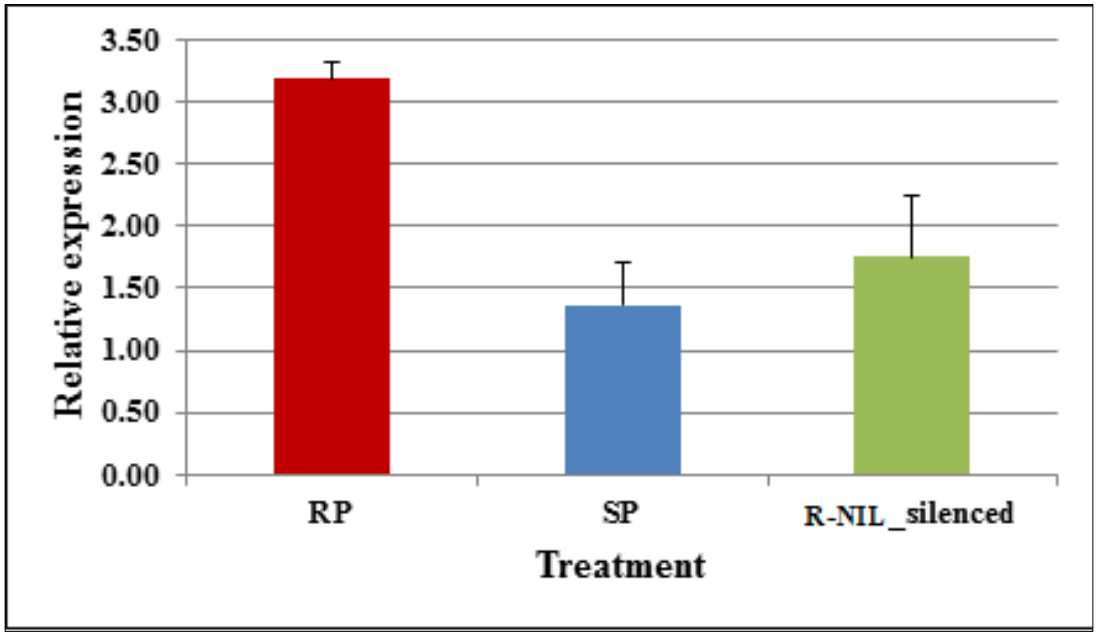

Figure 3.10. Differential expression of *TaMYBFhb5* between R-NIL and S-NIL 72 hpi of *Fusarium graminearum*. Where, RP=resistant near isogenic line (NILs) inoculated with pathogen, SP= susceptible NIL inoculated with pathogen, R-NIL_silenced= *TaMYBFhb5* transcription factor silenced in resistant near isogenic line (NILs) inoculated with pathogen.

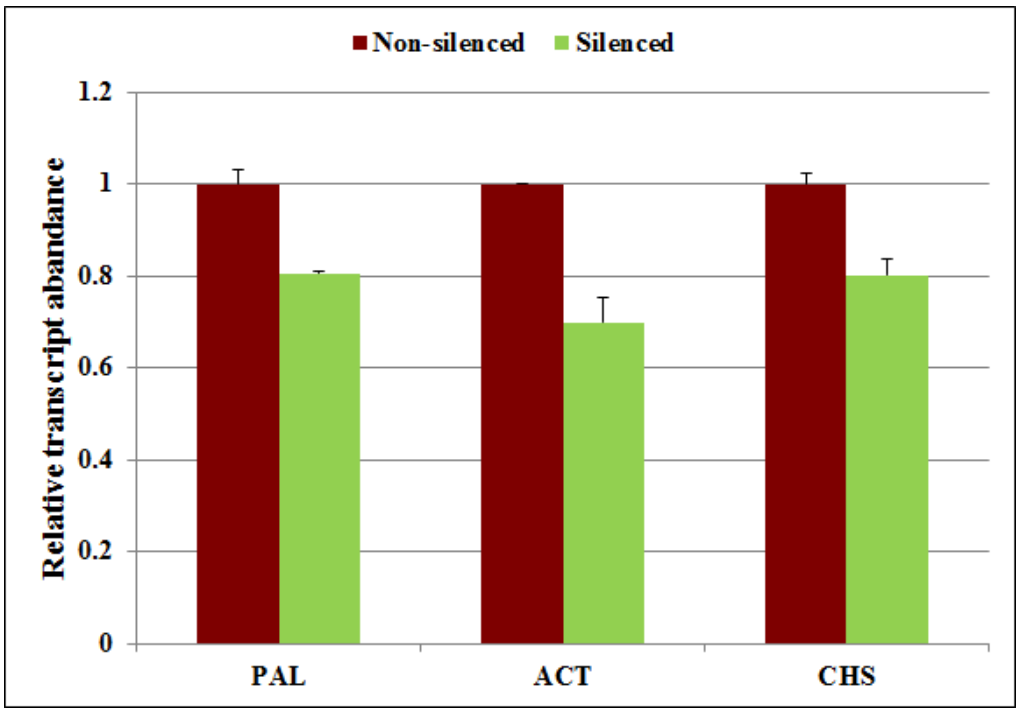

Figure 3.11. Differential expression analysis of host structural genes after silencing the *TaMYBFhb5* gene in wheat R-NIL. Where, PAL=phenylalanine ammonia lyase, *ACT*=agmatine coumaroyl transferase and *CHS*=chalcone synthase genes.

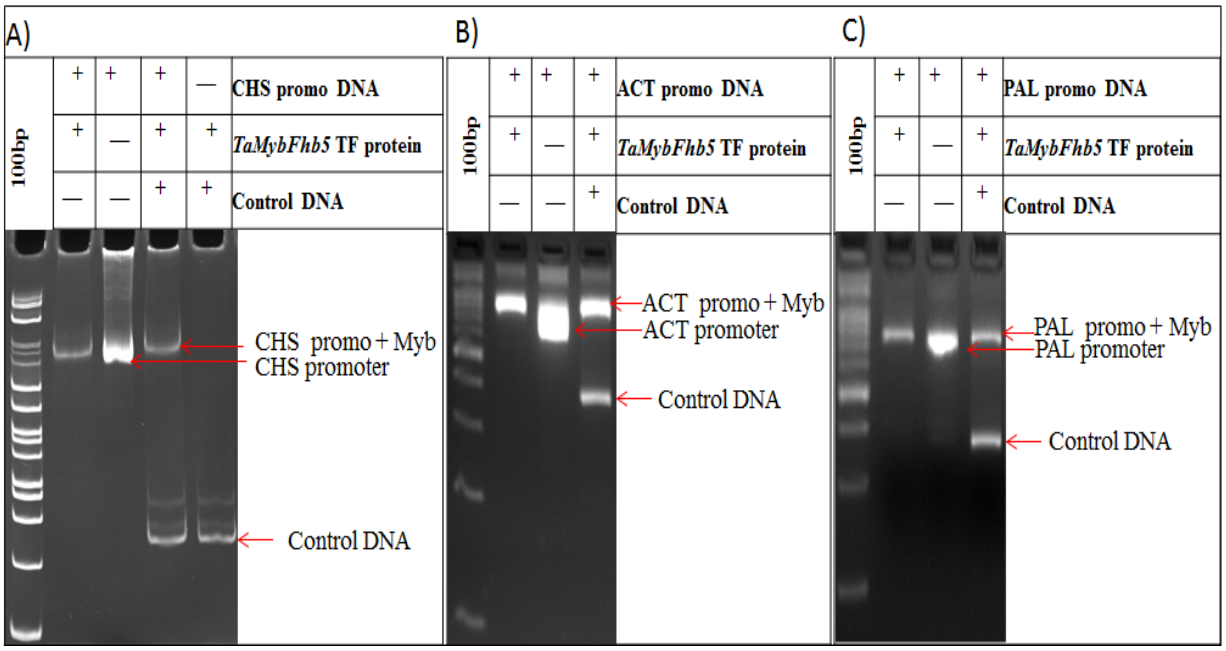

Figure 3.12. The *TaMYBFhb5* interaction with promoter regions of downstream genes; A) chalcone synthase (*CHS*) 8% PAGE, B) agmatine coumaroyl transferase (*ACT*) 4% Agarose gel, C) phenylalanine ammonia lyase (*PAL*), 4% Agarose gel.

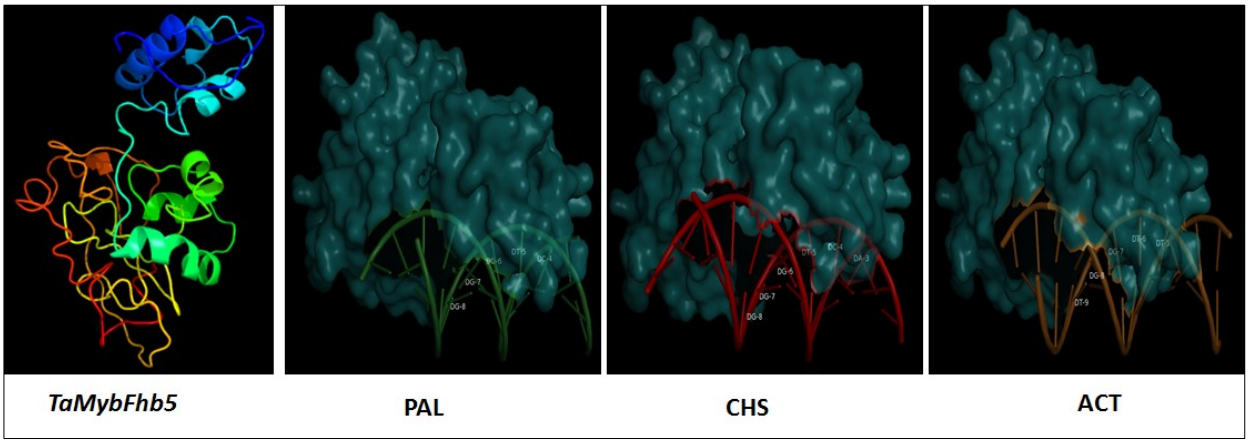

Fig 3.13 Post-docking interactions between the active site residues of the *TaMYBFhb5* (3ZQC) with ligands, *PAL*, *CHS* and *ACT* DNA sequences. The 3ZQC is depicted in surface view and ligands as a stick in the binding pocket.

CONNECTING STATEMENT FOR CHAPTER IV

Chapter IV, is a manuscript entitled "The *TaMYBFhb5* transcription factor from wheat QTL-Fhb5 regulates downstream resistance related metabolite biosynthetic enzymes encoding genes in Sumai3 during *Fusarium graminearum* infection" prepared by Shivappa Hukkeri, Udaykumar K and Ajjamada C. Kushalappa and Dion Y. The manuscript will be submitted to a peer reviewed scientific journal for publication.

The metabolome profiling of spikelets from R-NIL and S-NIL of wheat s in the third chapter revealed the RR metabolites accumulated during *Fusarium spp.* pathogenesis belongs to the phenylpropanoid and flavonoid pathways. In the third chapter, we have identified a transcription factor (*TaMYBFhb5*) from wheat near isogenic lines (NILs) carrying QTL-Fhb5 derived from Sumai3 genotype, regulating the three key enzymes encoding genes from phenylpropanoid and flavonoid pathways, such as, phenylalanine ammonia lyase (*PAL*), chalcone synthase (*CHS*)and amatine coumoroyl transferase (*ACT*). With the advent of systems biology several genes and gene functions are being revealed and attempts are being made to improve plants by pyramiding several functional genes based on genome editing. The objective of this study was to provide an indirect proof of controlling several genes by silencing the single significant FHB resistance R2R3 MYB transcription factor (*TaMYBFhb5*) gene, which would significantly reduce FHB resistance level in silenced conditions. Hence, the latter gene can be used in future replacement of non-functional alleles in susceptible genotype s to enhance FHB resistance without taking the risk of stacking the several resistance genes. The wheat genotype, Sumai3 is known to carry resistance for both resistance initial infection and resistance to sprread within the rachis. Hence, current was envisaged to study the effect of *TaMYBFhb5* TF gene silencing through virus induced gene silencing (VIGS) in Sumai3 wheat genotype. The silencing of *TaMYBFhb5* gene not only significantly increased the FHB disease with high fungal biomass, this was also associated with reduced downstream metabolic pathway genes expression and accumulation of resistance related (RR) secondary metabolites. The expression of the key RR metabolites biosynthetic enzymes encoding genes except *ACT* gene, such as, phenylalanine ammonia lyase (*PAL*) and chalcone synthase (*CHS*) were significantly reduced. This result validates the function of *TaMYBFhb5* TF gene during FHB disease resistance mechanism in wheat.

CHAPTER IV

The *TaMYBFhb5* gene from wheat QTL-Fhb5 regulates downstream resistance related metabolite biosynthetic enzymes encoding genes in Sumai3 during *Fusarium graminearum* infection

Hukkeri S[a], Udaykumar K[a], Ajjamada C. Kushalappa[a] and Dion Y[b]

[a]Plant Science Department, McGill University, 21 111 Lakeshore Road, Ste-Anne-de-Bellevue, Quebec H9X3V9, Canada. [b]Centre de recherché sur les grains inc., 740, chemin Trudeau, Saint-Mathieu-de-Beloeil, QC J3G0E2, Canada.

4.1 Abstract

Plants experience several biotic and abiotic stresses during growth and development stages. Fusarium head blight (FHB) disease of wheat (*Triticum aestivum* L.) is one of the major biotic stresses in warm and humid climatic conditions. The plants respond to such environmental cues majorly through cellular regulatory mechanisms. The gene families mainly involved in the regulation of downstream RR metabolite biosynthetic genes are: MYB, MYC, WRKY and NAC transcription factors (TFs). The wheat R2R3 MYB TF gene *TaMYBFhb5,* localized in the quantitative trait loci (QTL) Fhb5 was induced upon *Fusarium graminearum* infection of near isogenic lines (NILs). The metabolic profiling of *TaMYBFhb5* gene silenced and non-silenced NILs spikelets revealed the latter as a master switch in regulating both phenyl propanoid and flavonoid related metabolites accumulation against *F. graminearum,* resulting in reduced fungal biomass accumulation. Sumai3 is a genotype with several FHB resistance genes. The objective of this study was to prove if silencing of a large resistance effect *TaMYBFhb5* gene in Sumai3 would reveal significant reduction in resistance effects. Such a confirmation would give us a hope that in commercial cultivars if the same gene is mutated and nonfunctional, then, replacing it with the functional gene discovered here would significantly increase the resistance effects of the cultivar. The metabolic profiling of silenced and non-silenced *TaMYBFhb5* gene in Sumai3 genotype revealed the accumulation of several terpenoids and lipids in addition to phenylpropanoids and flavonoids, as identified in our previous study based on NILs. The differential expression analysis of key genes from phenylpropanoid and flavonoid pathways,

coding for phenylalanine ammonia lyase (*PAL*) and chalcone synthase (*CHS*) indicated significantly reduced transcripts accumulation, along with associated accumulation of low abundance of their respective biosynthetic metabolites. These were also associated with increased disease severity, fungal biomass and also DON mycotoxin accumulation produced by *F. graminearum*. We provide here compelling evidence that the functional FHB resistance gene, *TaMYBFhb5,* is an excellent candidate for the replacement of a non-functional gene in susceptible commercial cultivars.

4.2 Introduction

Wheat (*Triticum aestivum* L.) is a staple and economically important crop, contributing nearly 30% of the world edible dry matter and nearly 60% of the world energy intake in several developing countries (Jaradat, 2011). Biotic and abiotic stresses are the major constraints for wheat production around the globe, particularly in developing countries and hence, the international co-operation is essential to reduce the factors affecting wheat production (Kosina et al., 2007). Fusarium head blight (FHB) is devastating disease in wheat and barley caused by *Fusarium graminearum* (Telomorph: *Gibberella zeae*, (Schwein) Petch). The FHB disease severity and mycotoxin contamination frequency is mainly dependent on wet and warm weather conditions (Dong et al., 2016; McMullen et al., 1997). Apart from yield loss, FHB disease degrades the grain quality by accumulating mycotoxins. The mycotoxin deoxynivalenol (DON) produced by *F. graminearum* is a known virulence factor for pathogenicity (Proctor et al., 1995) and also highly toxic to animals fed with mycotoxin contaminated fodder and feed (Pestka and Smolinski, 2005).

The first line of defense mechanism in plant systems involves biochemical signal transduction during biotic or abiotic stress. To understand the various secondary metabolites induced against FHB resistance, a non-targeted metabolomics of various crops was carried out in wheat (Dhokane et al., 2016; Gunnaiah and Kushalappa, 2014; Gunnaiah et al., 2012; Hamzehzarghani et al., 2005; Hamzehzarghani et al., 2008), barley (Bollina et al., 2010; Kumar et al., 2016; Kumaraswamy et al., 2011a), cereals (Atanasova-Penichon et al., 2016; Gauthier et al., 2015) and maize (Campos-Bermudez et al., 2013). The non-targeted metabolic analysis of wheat NILs carrying QTL-Fhb5 against FHB spikelet resistance also revealed RR metabolites in phenylpropanoid and flavonoid metabolic pathways. Similarly, FHB RR metabolites were

reported in wheat (Gunnaiah and Kushalappa, 2014; Kage et al., 2016) and barley (Bollina et al., 2010; Kumaraswamy et al., 2012). Therefore, the crux of the FHB resistance mechanism depends on the type of genetic source cultivars carrying FHB resistance genes and RR metabolites.

FHB resistance involves mainly spikelet resistance against initial infection (Type I) of *F. graminearum* and rachis resistance against spread of *F. graminearum* infection (Type II). Therefore, selecting genomic regions within the wheat genome associated with FHB resistance phenotype and identifying resistance genes through molecular markers association studies play a critical role (Somers et al., 2005). More than 100 FHB quantitative trait loci (QTLs) were identified on all 21 chromosomes of wheat associated with FHB resistance, some were consistent across the different environmental conditions (Buerstmayr et al., 2009). Among the major QTLs identified, 3B and 5A showed high FHB disease resistance in wheat lines carrying each QTLs and more effective when both the QTLs were combined within the wheat lines (Lemmens et al., 2005; Miedaner et al., 2006; Miedaner, 1997). However, these QTLs contain several genes. Transferring the FHB resistance QTLs into susceptible wheat lines was a difficult task, as they were associated with negative linkage drag effect (Collard and Mackill, 2008). However, the advancement in genomic sequencing and availability of cereal model crops genomes databases helped in comparative mapping to unravel the hot spot regions of the wheat genome.

The comparative genomic analysis was used to identify the genes collinearly existing between rice and wheat 2D chromosomes with the function of FHB resistance (Handa et al., 2008). Similarly, the physical mapping between rice and wheat chromosome 5 using molecular markers on the deletion lines revealed that parts of the rice chromosomes 9, 11 and 12 are syntenous, and the physical location of flowering time genes (*Vrn*) and grain hardiness (*Ha*) of wheat were determined (Sarma et al., 2000). The QTL on the 5AS chromosome explained 60% of phenotypic variance in spikelet resistance (Xue et al., 2011). Though, the QTL-Fhb5 has shown additive effects along with 3BS, genes governing spikelet resistance were not revealed (Cai, 2016; Schweiger et al., 2013; Suzuki et al., 2012). In our previous study (Chapter III), we reported the list of genes encompassed within QTL-Fhb5 along with a *TaMYBFhb5* TF gene, responsible for FHB resistance related metabolic pathway genes regulation.

The plant MYB transcription factors are key regulators for both cytoplasmic and nuclear gene expression and metabolic responses against biotic and abiotic stresses in plant cells (Ambawat et al., 2013; Dubos et al., 2010; Wang et al., 2016; Xie et al., 2014; Zhang et al., 2012). The R2R3 MYB gene in wheat (*TaPIMP1*) regulated the expression of both disease resistance (*Bioilaris sorokiniana*) and drought stress related genes. The downstream genes including *TaPIMP1* were initially triggered through abscisic acid (ABA) and salicylic acid (SA) metabolites (Zhang et al., 2012). Another study showed R2R3 MYB genes, *MYB28* and *MYB29* regulated the biosynthesis of aliphatic glucosinolates (GLS) secondary metabolites, which are known for antioxidant and antimicrobial activities (Hirai et al., 2007). Therefore, MYB transcription factors play an important role in growth and development stages of plants and also, in defense mechanism against biotic and abiotic stress.

The hemi-biotrophic nature of *F. graminearum* triggers plant innate immunity through *R* receptor genes expression and plant defense related phytohormones like jasmonic acid (JA), salicylic acid (SA) and ethylene (ET) accumulation during colonization (Ding et al., 2011; Qi et al., 2016). Wheat genotype s (Nyubai and Sumai3), at 72 hours post inoculation (hpi) with *F. graminearum*, showed over expression of PR proteins and phenylpropanoid secondary metabolites (Gunnaiah et al., 2012). The oxidative burst during pathogen infection induces the expression of pathogenesis-related (PR) proteins as a defense mechanism in plant cells (Conrath et al., 2002). The PR genes, 1 to 5, were highly expressed following *F. graminearum* inoculation in wheat (Kruger et al., 2002; Pritsch et al., 2000). Further, *F. graminearum* evolution in host preferential expression of genes during the pathogenesis makes it more difficult to understand the resistance mechanism (Harris et al., 2016). Whole genome transcriptomic analysis of Sumai3 revealed the cell wall associated peroxidase and proteases gene expression at 7 days post inoculation (dpi) (Kosaka et al., 2015). The metabolo-proteomic analysis of NILs derived from Nyubai genetic background wheat lines at 72 hpi of *F. graminearum* showed the high accumulation of hydroxycinnamic acid amides (HCAA) and flavonoids accumulation and peroxidase gene expression (Gunnaiah et al., 2012).

In our previous study the wheat NILs carrying QTL-Fhb5 showed differential expression of phenylpropanoid and flavonoid pathway genes, such as phenylalanine ammonia lyase (*PAL*), chalcone synthase (*CHS*) and agmatine coumaroyl transferase (*ACT*), which were positively

regulated by *TaMYBFhb5* (Chapter III). The objectives of the present study was to silence the TF *TaMYBFhb5* in Sumai3 wheat v, which is known to have several FHB resistance genes and mechanisms of resistance. To obtain a proof-of-concept that silencing of one significant FHB resistance gene (*TaMYBFhb5*) would have significant effect on FHB disease severity and fungal biomass accumulation. Our present study provided substantial evidence on significant increase in FHB disease severity and fungal biomass accumulation and decrease in RR metabolites accumulation following *TaMYBFhb5* gene silencingin Sumai3. This suggests, the effect of *TaMYBFhb5* gene on a series of RR metabolic pathway enzymes encoding genes necessary during FHB resistance.

4.3 Materials and Methods

4.3.1 Plant materials

The Chinese wheat genotype Sumai3 seeds were obtained from Agriculture and Agri-Food Canada, Winnipeg, Canada (Dr. C. McCartney). Sumai3 is well known resistant genotype around the world for FHB disease resistance. Seeds were sown in 7.5 inch pots filled with Agro mix PV20 (Fafard, QC, Canada). The equal number of plants (three) per pot were maintained after germination. The greenhouse conditions were maintained at temperature 25 ± 2^{o}C, with 16 hour daylight and 8 hour darkness, and relative humidity of 60 ± 10%. Plants were watered using drip irrigation with controlled water droplets based on the moisture status and slow releasing fertilizer 20-20-20=N-P-K was applied two weeks post germination of seeds and during early booting stage.

4.3.2 VIGS constructs, wheat *TaMYBFhb5* TF gene cloning and inoculation

The transient suppression of the *TaMYBFhb5* TF gene through barley stripe mosaic virus (BSMV) vectors was carried out as described byScofield et al., (2005). The α, β and γ BSMV vectors used for VIGS assay were obtained from Dr. Scofield (USDA). The *TaMYBFhb5* gene fragment (277bp) was cloned into the third partite (γ vector, Psl038-1). The BSMV vectors inoculum was prepared in 1:1:1; α (Alpha42):β (beta42.sp1):γ(Psl038-1) ratio, respectively. The FES buffer containing sodium pyrophosphate, Bentonite and Celite was prepared fresh and sterilized before swabbing. The Celite material in FES buffer helps course rubbing the leaf and spikes to allow the virus particles to enter the plant system. Equal proportions of BSMV vectors

(3µl) and 7µl of inoculum and abrasive FES buffer was mixed. The flag leaves and spikes were rub-inoculated with phytoene desaturase (PDS) at growth stage 55 (1/2 of head emerged from flag leaf) (Zadoks et al., 1974). FES plus BSMV empty constructs were used as negative control (BSMV:00).

4.3.3 *Fusarium graminearum* macroconidia production

The *F. graminearum*, isolate Z-3639 (Proctor et al., 1995) was grown on potato dextrose agar (PDA) plates for four to five days and later, mycelial plug were transferred onto rye media plate. These rye plates were exposed to UV blue light for 3-4 days to produce macroconidia. Plates were flooded with water and the macroconidial concentration was adjusted to 10^5 spores ml^{-1}, using haemocytometer.

4.3.4 VIGS construct and *F. graminearum* inoculation

The wheat plants previously swabbed with VIGS constructs were transferred to growth chambers at growth stage 55 (Zadoks et al., 1974). They were maintained at temperature 25 ± 1^oC, with 16 hour daylight and 8 hour darkness, and relative humidity of 60 ± 10%. At growth stage 65 two alternate pairs of spikelets (one pair at the bottom and one pair at the middle of the spike) were inoculated with 10µl of the spore suspension per spikelet using a syringe (GASTIGHT 1750DAD W/S, Hamilton, Reno, NV, USA). The inoculated spikes were covered with transparent polythene bags sprayed with sterile water to maintain sufficient moisture for macrospore germination and the bags were removed at 72 hpi.

4.3.5 Metabolic profiling

The wheat spikes inoculated with *Fusarium spp.* macrospores were collected at 72 hpi. The harvested spikes were immediately stored in -80 degree freezer until further use. The spike region containing alternative two pairs of inoculated, along with uninoculated spikelets were cut off, the spikelets and rachis were separated. The samples were separately ground using a sterile pestle and mortar. The metabolites were extracted using 70% methanol. An aliquot of 10µl of extract was injected into liquid chromatography and high resolution mass spectrometry (LC-HRMS: LC-ESI-LTQ-Orbitrap at the Institut de recherches cliniques de Montreal facility at the University of Montreal). The output raw files on metabolite peaks were converted to .CDA files

to read in MZmine 2 software (Pluskal et al., 2010). The abundance of peaks were determined for Sumai3 silenced inoculated with pathogen (RsP) and Sumai3 nonsilenced inoculated with pathogen (RnP). The metabolites that were higher abundance in a non-silenced Sumai3 pathogen inoculated than silenced Sumai3 (RnP>RsP) were considered as pathogenesis related (PR) metabolites.

4.3.6 RRI metabolic pathway genes differential expression analysis

The samples of the Sumai3 silenced and non-silenced spikelets and rachis samples collected at 72 hpi were used for differential gene expression analysis through quantitative real time PCR (qRT-PCR). The genes regulated by *TaMYBFhb5* TF, such as chalcone synthase (*CHS*), phenylalanine ammonia lyase (*PAL*) and agmatine coumaroyl transferase (*ACT*) were amplified and normalized on agarose gel based on band intensities along with the housekeeping *actin* gene. Total RNA was isolated from Sumai3 silenced and non-silenced spikelets inoculated with *F. graminearum* using Qiagen RNAeasy plant mini kit (Qiagen). The extracted total RNA (1µg) was reverse transcribed in a 20µL reaction using iScript cDNA synthesis kit (BioRad, On, Canada). To remove the untranscribed RNA templates, cDNA was treated with RNAse. Freshly prepared cDNA was quantified using the NanoDrop 1000 spectrophotometer (NanoDrop, Wilmington, DE, USA). Total 20µL Polymerase chain reaction (PCR) was carried out by using diluted (20 nanogram per microliter) cDNA, 10 pico-moles of primers (Forward and Reverse), 2X PCRmix (Froggabio Life Sciences, NY) at standard annealing temperature. Normalized cDNA was used to carry out the qRT-PCR based on iQ SYBR Green supermix (BioRad) using CFX384TM Real-Time System (BioRad, ON, Canada). The relative gene expression compared to housekeeping *actin* gene using $2^{-\Delta\Delta Ct}$ method (Livak and Schmittgen, 2001).

4.3.7 *Fusarium graminearum* biomass assessment

The two pairs of inoculated spikelets, along with two uninoculated pairs of spikelets, collected at 72 hpi were used to extract the genomic DNA using Qiagen kit (Qiagen Inc, Toronto, Canada). The extracted DNA was quantified and normalized using the Nano drop instrument (Thermo Scientific, Canada). The primers specific to *Fusarium spp*. (*Tri6_10*) and galactose oxidase (*GaO*) were used for polymerase chain reaction (PCR) amplification. PCR was performed using the genomic DNA of Sumai3 silenced and non-silenced samples to normalize

the DNA concentration based on the band intensities. The 50µL PCR solution comprising of 1µL of the DNA template (nearly 30ng), 1.0 Unit of Taq polymerase, 1x buffer, 1.5mM MgCl2, 200µL of each dNTP, 5.0 Picomoles of forward and reverse *Tri6_10* and *GaO* primers. Thermocycler conditions used were an initial 94^{o}C for 5 min; 35 cycles of 95^{o}C for 1 min, appropriate annealing temperature for 1 min, and 72^{o}C for 2 min and final 72^{o}C extension for 10 min using eppendorf thermocycler. The amplified product was analyzed for band intensities using 2% agarose gel electrophoresis. Further, the real time quantitative PCR (qPCR) was carried out using appropriate annealing temperature to see the *Fusarium spp. Tri6_10* and *GaO* gene copy numbers within the pathogen inoculated samples. The wheat *actin* gene was used as a housekeeping gene to calculate the *Fusarium graminearum* specific gene copies within Sumai3 (Kumar et al., 2015).

4.4 Results

4.4.1 Effect of transient suppression of *TaMYBFhb5* gene in Sumai3 on downstream gene expression

The PDS gene suppression within the Sumai3 genotype was clearly seen at three days post swab inoculation of the VIGS constructs, due to PDS genes photobleaching effect (Figure 4.1). The photobleaching effect was used as indirect method to confirm the suppression of target gene (*TaMYBFhb5*) expression through VIGS within the plant system. Further, the low expression of *TaMYBFhb5* was observed within silenced compared to non-silenced Suamai3 spikelets (Figure 4.2). The phenotypic appearance of disease spread through the rachis in silenced Sumai3 was supported with very low expression of *TaMYBFhb5* TF.

4.4.2 Disease severity based fungal biomass in spikelets

The phenotypic appearance of disease spread to uninoculated spikelets through the rachis was more visible in *TaMYBFhb5* silenced than in nonsilenced Sumai3 spikes at 72 hpi (Figure 4.3). The *Fusarium spp.* specific galactose oxidase (*GaO*) gene copies of in silenced Sumai3 spikelets were higher than in non-silenced spikelets (Figure 4.4A). Interestingly, the phenotypic appearance of disease on the rachis in silenced Sumai3 spikes was further evidenced with high fold accumulation of fungal biomass. Whereas, the relative abundance of *Fusarium spp.* specific *Tri6_10* gene copies were 2.5 fold greater in silenced than non-silenced rachis (Figure 4.4B).

Furthermore the abundance of DON toxin produce by *F. graminearum* was also higher in non-silenced than in silenced. These findings clearly demonstrated that the silencing of *TaMYBFhb5* significantly affected the resistance in Sumai3. The *Fusarium spp.* virulence factor DON accumulation was significantly different between the Sumai3 silenced and non-silenced spikelets (Figure 4.5). The DON accumulated in Sumai3 silenced spikelets was 8.01 (mg kg-1) and in non-silenced spikelets was 6.92 (mg kg-1). Interestingly, both fungal biomass and DON accumulations were higher in silenced spikelets compared non-silenced spikelets of Sumai3.

4.4.3 Effects of *TaMYBFhb5* gene silencing on downstream phenylpropanoid and flavonoid pathway metabolite biosynthetic genes.

The downregulation of *PAL* and *CHS* gene expression was observed in Sumai3 *TaMYBFhb5* gene silenced and non-silenced spikelets and rachis (Figure 4.6A and 4.6B). However, the transcripts abundance in the rachis was much lower compared to spikelets of silenced and non-silenced Sumai3. This result further confirmed the earlier claim of *TaMYBFhb5* TF as main switch for expression of *PAL* and *CHS* genes during *Fusarium spp.* pathogenesis. The electro mobility shift assay (EMSA) also indicated in the earlier chapter III that the promoters of *PAL*, *CHS* and *ACT* were having *TaMYBFhb5* binding domain. However, we did not observe a significant difference in differential expression of the *ACT* gene after *TaMYBFhb5* gene silencing in both spikelets and rachis of Sumai3.

4.4.4 Effects of silencing of *TaMYBFhb5* gene on RR metabolites accumulation

The significant RR metabolic profiles between *TaMYBFhb5* TF silenced and non-silenced Sumai3 were listed in Table 4.1. A total of 648 consistent peaks were detected in all the replications. The metabolite peaks absent in silenced and present in non-silenced samples were considered here as qualitative metabolites. We observed 50 qualitative peaks that were absent in silenced Sumai3 spikelets. Among the total number of peaks detected only 71 pathogen induced RR metabolites were statistically significant between the silenced and non-silenced spikelets of Sumai3. These RR metabolites were calculated to be in higher abundance in Sumai3 non-silenced than in silenced pathogen inoculated spikelets. A total of 29 metabolites were identified with putative chemical names, having accurate mass error (AME < 5) with known metabolic

database ID (Table 4.1). These RR metbolites were mapped to sikimate and mevolanate pathways (Figure 4.7).

4.5 Discussion

The resistance in wheat against *F. graminearum* is complex and is polygenic, meaning FHB is controlled by more than one gene. The resistance in plants against pathogen stress is due to hierarchies of genes, including regulatory genes that regulate the downstream genes, which biosynthesize the RR proteins and RR metabolites. Transcription factors play a major role in regulating the downstream biosynthetic genes, affecting expression of resistance (Kushalappa et al. 2016a). Our previous study (Chapter III) identified a TF *TaMYBFhb5* as the key gene localized in QTL-Fhb5, which controls a significant amount of resistance in NILs. The resistance was mainly due to the regulation of phenylpropanoid and flavonoid metabolites. This gene can be used in genome editing, if nonfunctional in commercial cultivars, to improve FHB resistance. In this study, we provide compelling evidence that this gene would be able to improve FHB resistance in commercial cultivars, by silencing this gene in a cultivar which is known to have several resistance mechanisms and genes. When the *TaMYBFhb5* was silenced in the genotype Sumai3, not only the disease severity significantly increased, but also this was associated with higher *F. graminearum* biomass and associated DON toxin, which is generally equivalent to pathogen biomass. *TaMYBFhb5* TF regulated, as reported earlier, the gene expression of the key metabolic enzymes phenylalanine ammonia lyase (*PAL*) and chalcone synthase (*CHS*) which were significantly reduced following silencing of the TF and then inoculation with *F. graminearum*. The latter genes play major roles in the biosynthesis of RR metabolites that restrict the spread of the pathogen from the inoculated spikelet to the neighboring spikelets through rachis. The R2R3 MYB TFs are known to regulate the downstream genes during biotic and abiotic stress. The accumulation of flavonoids and glycosides was observed during pathogen infection and abiotic stress in poplar tree and were regulated through R2R3 MYB (*MYB134*) TF gene (Mellway et al., 2009). Following silencing of the *TaMYBFhb5* gene, the expression of key genes encoding phenylalanine ammonia lyase (*PAL*) and chalcone synthase (*CHS*) were downregulated by 2.6 and 2.5 folds in the rachis (Figure 4.6). However, there was no significant difference in *ACT* gene expression in Sumai3 silenced spikelets and rachis. It is possible that this gene is complimented by other transferase genes in in Sumai3.

The *Fg* inoculated spikelets, after *TaMYBFhb5* silencing, had a significantly reduced amount of RR metabolites. The abundances of cell wall reinforcing RR metabolites such as 5-O-feruloylquinic acid, N-Caffeoylputrescine, 1-O-Sinapoyl-beta-D-glucose, p-Coumaroylagmatine, coumarins and coniferin were significantly reduced when *TaMYBFhb5* was silenced. Also, the abundances of flavonoids such as, isoscoparine, apigenin 7-O-[beta-D-apiosyl-(1->2)-beta-D-glucoside] and apigenin were also decreased in spikelets of Sumai3 when silenced as compared non-silenced. In addition to these, surprisingly there were very high fold decrease in the accumulation of RR metabolites of the terpenoid pathway such as, hyperforin, alpha-Tocopherolquinone, alpha-Tocopherolquinone and cathasterone. Also some lipids such as 1-eicosyl-2-(13Z,16Z-docosadienoyl)-glycero-3-phosphate (60.85 FC) and 5-alpah-Cholestan-3-Alpa-YL Benzoate (6.45 FC) were also significantly reduced after silencing. We also observed very high fold decrease in several unidentified RR metabolites accumulations in silenced Sumai3 spikelets. These RR metabolites, in general, act as phytoalexins and/or as cell wall reinforcing to suppress pathogen progress in plant, thus limiting FHB (Gunnaiah et al., 2012).

The decrease in the abundances of diverse groups of RR metabolites, following silencing of *TaMYBFhb5,* indicated that this gene is regulating more than one RR metabolic pathway. The TFs are known to regulate several downstream genes. However, in our study only a few key downstream gene expression analysis were conducted. A more elaborate study based on chromatin immunoprecipitation (ChIP) analysis is required to identify all the downstream genes regulated by the MYB TFs (Nie et al., 2009; Stadhouders et al., 2012).

In summary, the *TaMYBFhb5* localized in QTL-Fhb5 is controlling not only the spikelet initial infection resistance, but also rachis resistance to reduce the spread of pathogen through rachis. The *TaMYBFhb5* regulates the key downstream genes in major metabolic pathways known for biotic stress resistance. Hence, this gene can be used to replace nonfunctional genes in susceptible commercial cultivars to enhance FHB resistance, through genic marker assisted breeding or through gene editing based on CRISPR-Cas9 systems.

Table 4.1. List of resistant related (RR) metabolites identified from *TaMYBFhb5* non-silenced versus silenced Sumai3 spikelet upon *Fusarium graminearum* inoculation.

m/z value observed	Metabolites	AME[a]	FC [b]	Database ID[c]
Mass (Da)	**Phenylpropanoids**			
342.13	Coniferin	1.4	1.83**	C00761
298.16	Coumarins	1.3	1.80*	C09281
276.16	p-Coumaroylagmatine	1.4	1.68***	C04498
386.12	1-O-Sinapoyl-beta-D-glucose	0.7	1.29*	C01175
250.13	N-Caffeoylputrescine	0.6	1.14*	C03002
368.11	5-O-Feruloylquinic acid	1.4	2.52***	C02572
Mass (Da)	**Fatty acids**			
310.29	Prostanoic acid	2.3	1.91***	C02064
244.20	2S-Hydroxytetradecanoic acid	1.9	1.60**	C13790
256.24	Hexadecanoic acid	1.3	1.37**	C00249
256.24	Hexadecanoic acid	1.4	1.31**	C00249
298.25	2-Oxooctadecanoic acid	2.5	1.12*	C00869
Mass (Da)	**Flavonoids**			
462.12	Isoscoparine	1.2	2.65*	C05990
564.15	Apigenin 7-O-[beta-D-apiosyl-(1->2)-beta-D-glucoside]	1.5	1.49***	C04858
270.05	Apigenin	2.0	1.13***	C01477
Mass (Da)	**Terpenoids**			
536.39	Hyperforin	3.9	74.18**	HMDB30463
446.38	alpha-Tocopherolquinone	5.0	32.08*	HMDB34408
382.38	Pentacosanoic acid	2.3	8.49***	HMDB36843
432.36	Cathasterone	3.9	6.92***	C15790
490.37	Barringtogenol C	1.6	1.62**	C08931
414.12	Asperuloside	1.0	1.54**	C09769
360.14	7-Deoxyloganate	1.1	1.38***	C11636
406.15	Ipolamiide	1.0	1.35***	C09784
308.27	Sclareol	2.1	1.29*	C09183
Mass (Da)	**Miscellaneous**			
770.62	1-eicosyl-2-(13Z,16Z-docosadienoyl)-glycero-3-phosphate	3.8	60.85***	LMGP10020068
492.39	5-alpah-Cholestan-3-Alpa-YL Benzoate	5.0	6.45***	C34H52O2
141.04	2-Aminomuconate semialdehyde	0.5	1.89***	C03824

222.07	6-Acetyl-D-glucose	1.9	1.87***	C02655
332.07	1-O-Galloyl-beta-D-glucose	1.7	1.77***	C01158
272.23	16-Hydroxypalmitate	2.3	1.21***	C18218

* *t*-test significance at $P<0.05$, ** *t*-test significance at $P<.01$, *** *t*-test significance at $P<.001$

[a]Accurate mass error (AME) calculation: ((Observed mass - Exact mass)/Exact mass)*10^6

[b] FC(Fold change) calculation: were based on relative abundances of metabolites between silenced and non-silenced samples upon pathogen inoculation = Suami3 non-silenced (RnP)/silenced (RsP).

[c]Database ID = KEGG (starts with "C"), Human Metabolome Data Base (HMDB) and LIPID metabolites and pathways strategy (LMAPS).

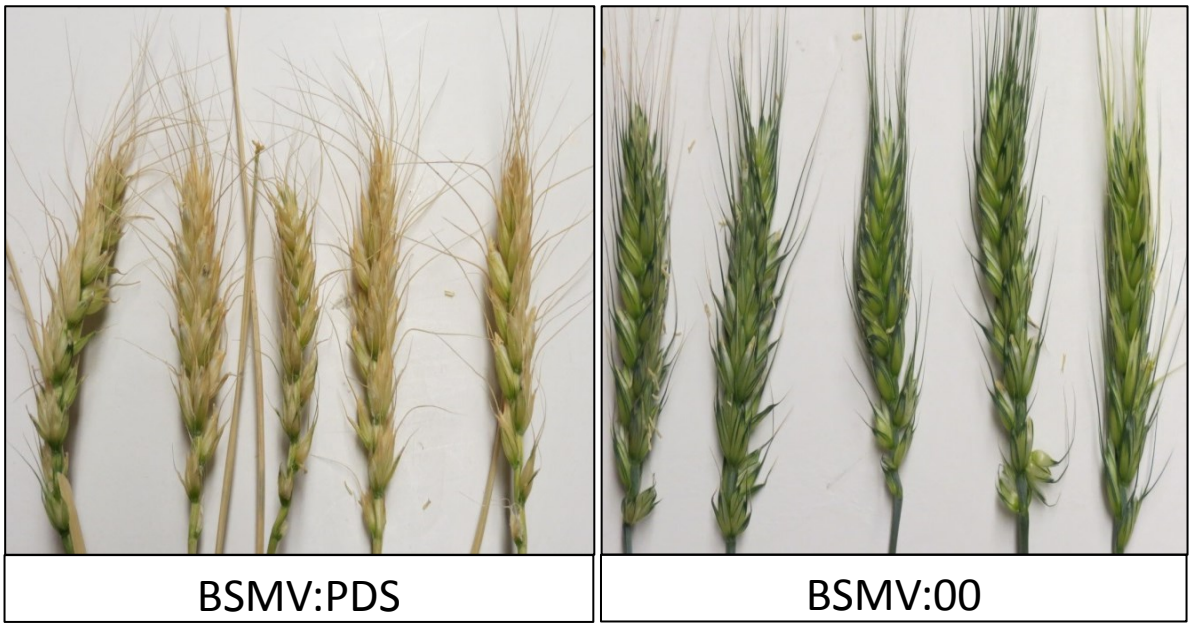

Figure 4.1: Virus induced gene silencing of phytoen desaturase (PDS) gene in Sumai3 spikelets at 6 days post inoculation (dpi). Where, BSMV: PDS = BSMV carrying fragment of PDS gene (Scofield et al., 2005); BSMV:00 = BSMV without PDS fragment.

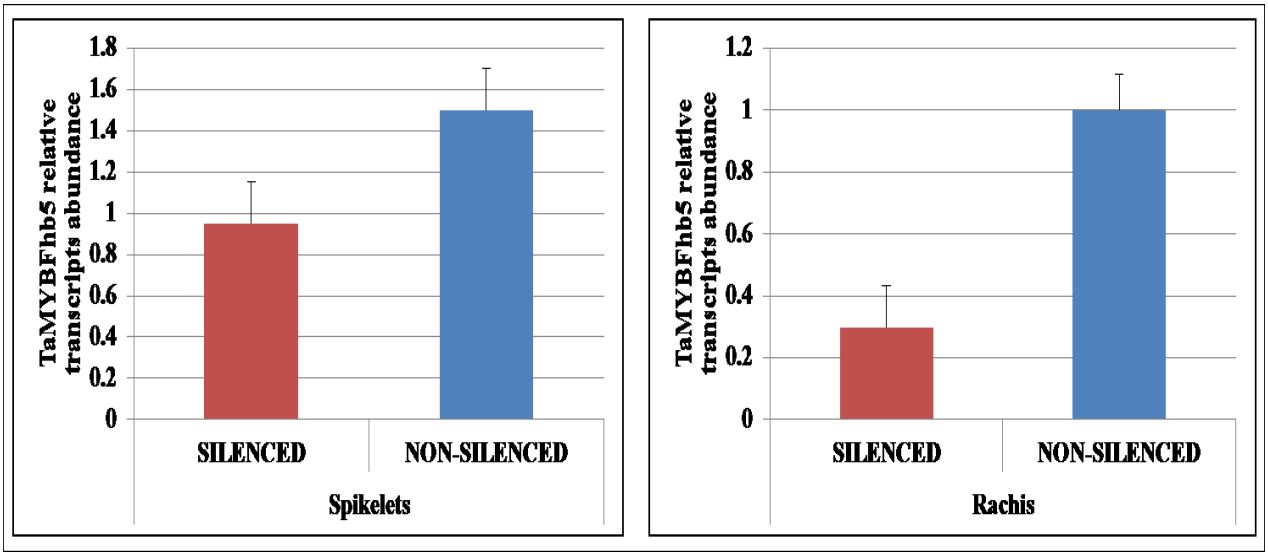

Figure 4.2: *TaMYBFhb5* gene differential expression between silenced and non-silenced Sumai3 spikelet's and rachis. The relative transcript abundance of *TaMYBFhb5* gene was calculated using wheat actin as housekeeping gene at 72 hpi.

Figure 4.3: Disease symptoms of *TaMYBFhb5* transcription factor gene silenced sumai3 spikelets inoculated with *Fusarium graminearum* after 72 hpi. The red arrow mark indicates the spread of disease seen only in rachis of the silenced spikes and not in nonsilenced spikes.

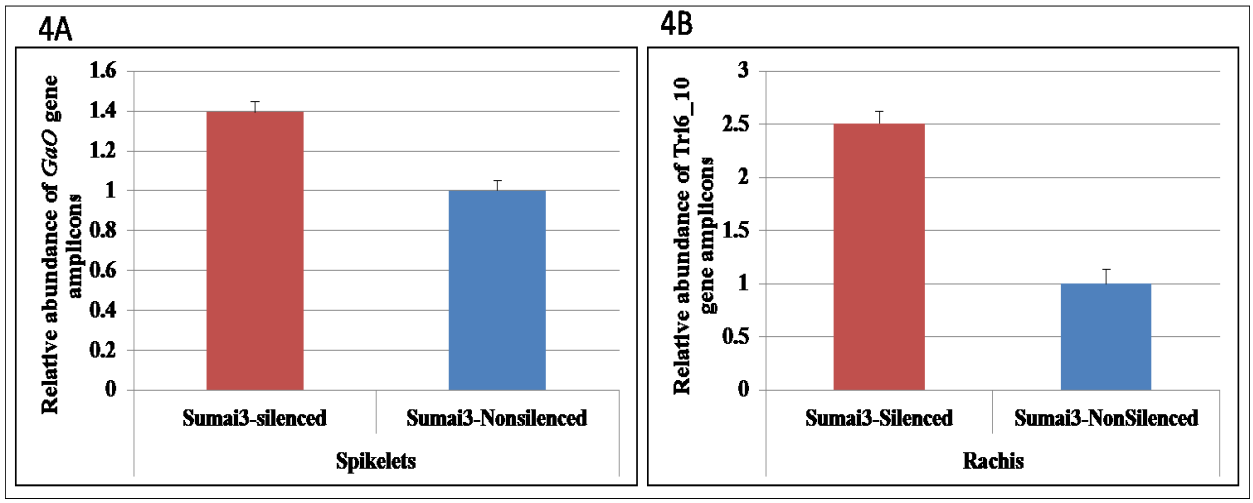

Figure 4.4: *Fusarium graminearum* fungal biomass quantified in Sumai3 silenced and non-silenced spikelets, two pairs of inoculated along with two uninoculated pairs, and rachis in the region of inoculation at 72hpi. 4A) the relative gene copy number of *GaO* in spikelets. 4B) the relative gene copy number of *Tri6_10* in rachis.

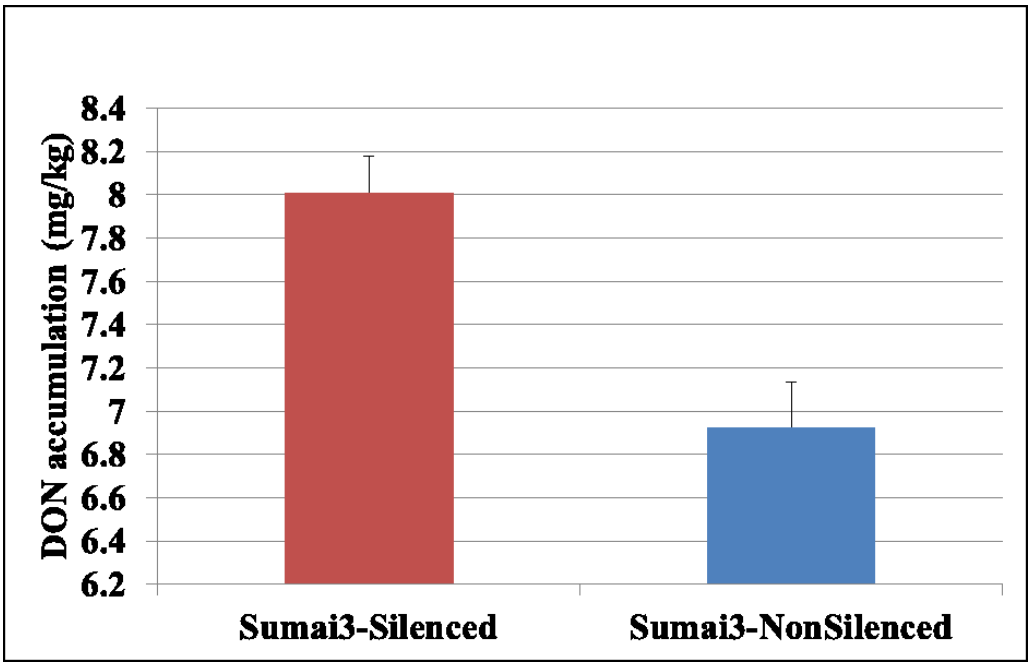

Figure 4.5: Accumulation of *Fusarium graminearum* resistance indicator (RI) metabolite, deoxy nivalenol (DON) within Sumai3 *TaMYBFhb5* gene silenced and non-silenced spikelets at 72 hpi.

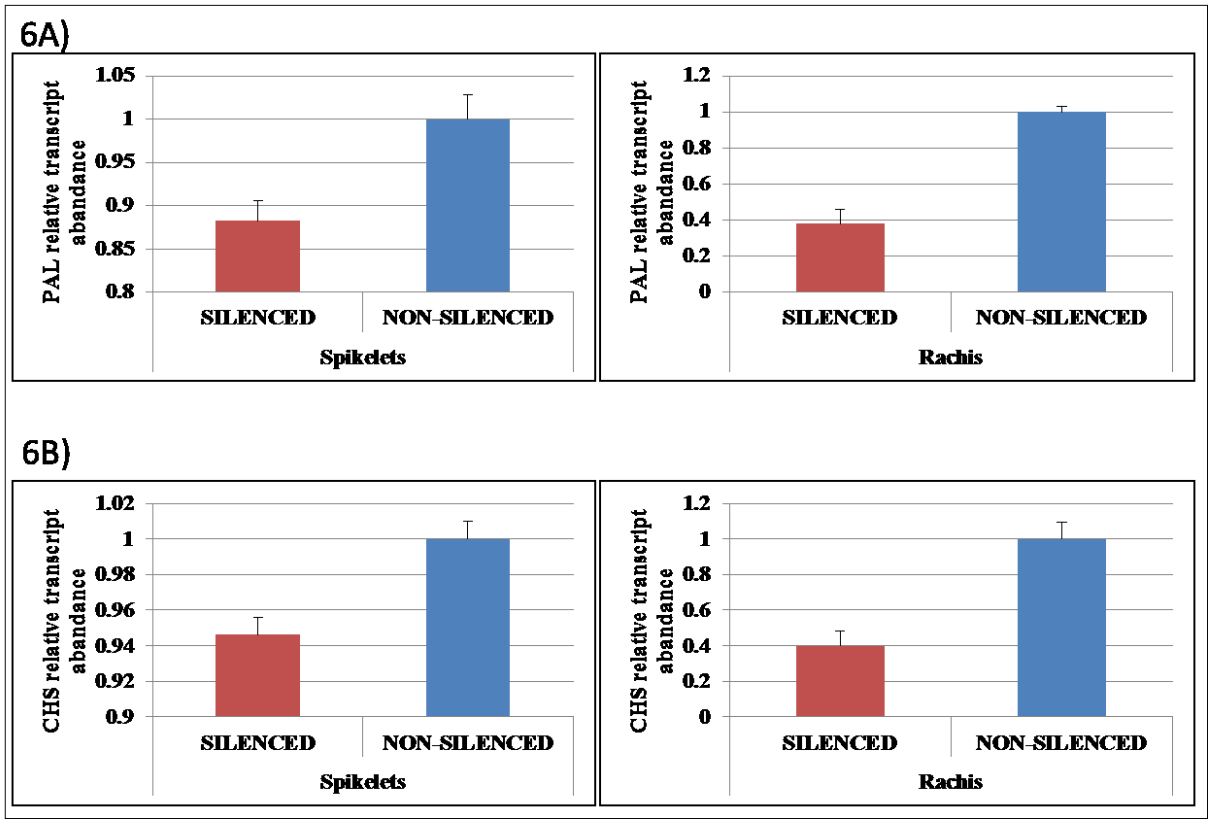

Figure 4.6: Metabolic pathway genes relative transcript abundances in Sumai3 *TaMYBFhb5* gene silenced and non-silenced spikelets and rachis. 6A) Differential expression of structural gene, *PAL* at 72 hpi of *Fusarium graminearum* in spikelets. 6B) Differential expression of structural gene *CHS* at 72 hpi of *Fusarium graminearum* in rachis.

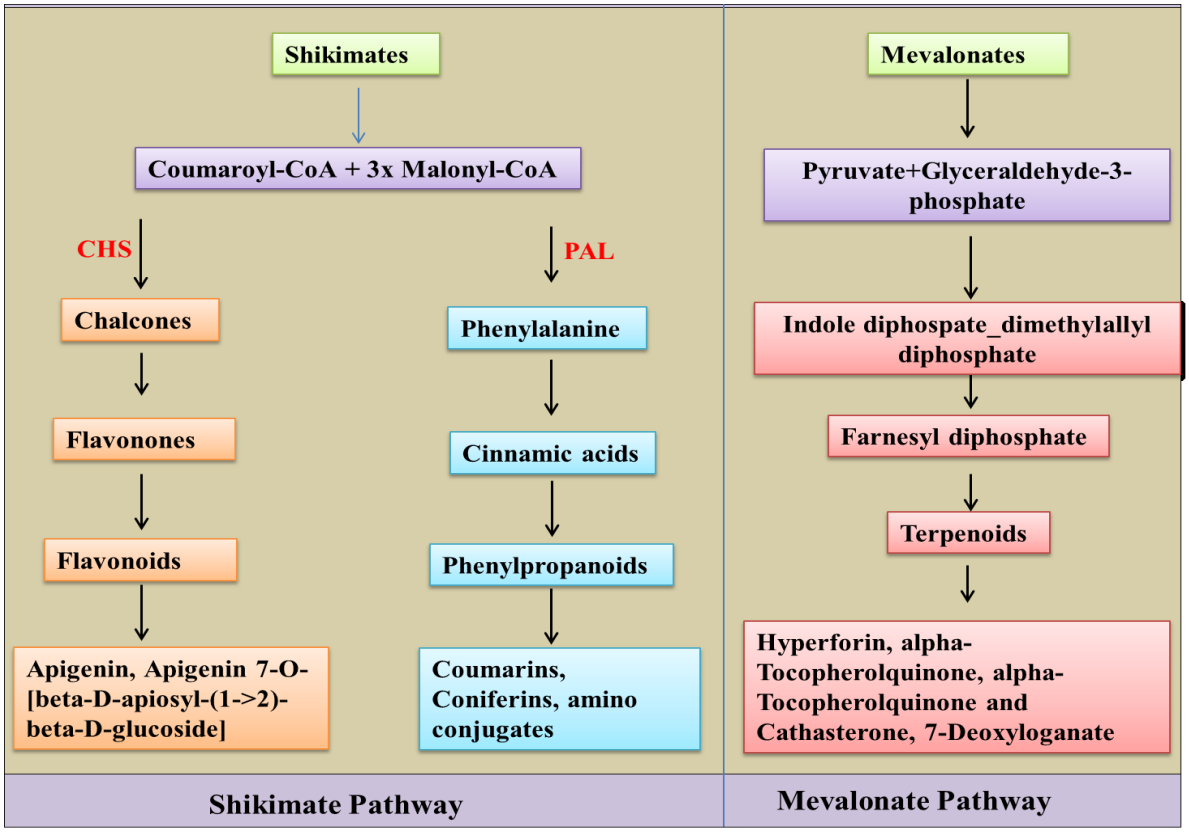

Figure 4.7: Schematic representation of RR metabolites induced upon *Fusarium graminearum* infection in Sumai3 *TaMYBFhb5* gene non-silenced and silenced were mapped on to KEGG pathways. The phenylpropanoids and flavonoids were derived from the shikimate pathway and terpenoids were derived from mevalonate pathway.

CONNECTING STATEMENT FOR CHAPTER V

In chapter III and IV, the semi-comprehensive metabolomics and functional analysis of *TaMYBFhb5* gene in of wheat NILs and Sumai3 revealed the association of phenylpropanoid and flavonoid pathway genes in both FHB spikelet and rachis resistance. To understand the role of mycotoxins in FHB resistance, evaluation of host response against DON nonproducing *Fusarium spp.* is essential. Accordingly the role of trichothecenes, including DON, on spikelet resistance to initial infection was explored, using two isolates of *F. graminearum*, one trichothecene producing wild type (isolate Z-3639) and another mutant lacking trichothecene production (isolate ZGT40). A resistant (Sumai3) and a susceptible (Roblin) wheat genotypes were used to explore the role of DON as a virulence factor, and host response against wild and mutant isolates of *F. graminearum* during pathogenesis.

Chapter V presents a manuscript entitled "Identification of spikelet resistance related metabolites and host resistance (*R*) genes in wheat following *Fusarium graminearum* infection". The authors are Hukkeri S. Ji L. and Kushalappa A.C. The manuscript will be submitted to a peer reviewed journal for publication.

In the current study, a Chinese spring wheat genotype resistant to FHB, Sumai3, and a relatively susceptible genotype, Roblin, were inoculated with *F. graminearum* mutant and wild isolates, under greenhouse conditions, and metabolites were profiled. A semi-comprehensive metabolome analysis of spikelets at 72 hours post inoculation (hpi) of pathogens revealed high accumulation of secondary metabolites falling into three major metabolic pathways, namely phenylpropanoid, flavonoid and lipids. The wild pathogen with capacity to produce the trichothecenes in Sumai3 showed less accumulation of deoxynivalenol (DON) in spikelets of Sumai3 as compared to Roblin. Further, the fungal biomass quantified based on real time PCR also revealed that the *Fusarium spp.* biomass accumulation was higher in Roblin than in Sumai3. However, the disease symptoms observed at 48 hpi on spikelets indicated no significant differences in the proportion of diseased spikelets. Further, we explored the biosynthetic genes of RR metabolites that accumulated in higher abundance in the resistant than in the susceptible genotype. Mapping of these metabolites in the metabolic pathways led to a few important hub metabolic pathway genes and these were: *T. aestivum* acyl glycerol-3 phosphate acyltransferase (*TaAGPAT*) and *T. aestivum* serine threonine protein kinase (*TaSTPK*) and also, the genes

associated with FHB disease resistance in wheat and barley were selected as candidate resistance genes (*R*) and these were: *T. aestivum* basic helix-loop-helix (*TabHLH*), a MYC transcription factor, and pathogenesis related protein1 (*TaPR1*) and taumatine like protein (*TaTLP*) genes. The higher fold change in expression of these *R*-genes in the resistant, relative to the susceptible genotype, supported their co-regulation with biosynthetic RR metabolites.

CHAPETR V

Identification of spikelet resistance related metabolites and host resistance (*R*) genes in wheat following *Fusarium graminearum* infection

Hukkeri S[a], Ji L[a] and Kushalappa AC[a]

[a]Plant Science Department, McGill University, 21 111 Lakeshore Road, Ste-Anne-de-Bellevue, Quebec H9X3V9, Canada.

5.1 Abstract

Fusarium graminearum (*Fg*) is one of the most common and destructive pathogens that cause Fusarium head blight (FHB) in wheat. Apart from yield reduction, food grains contamination with mycotoxins, especially deoxynivalenol (DON) that causes animal and human health hazards, is a serious concern. This study explored the interactions between wheat genotypes and trichothecene producing wild (*FgT*) and nonproducing mutant (*Fgt*) isolates of *Fg* pathogen for spikelet resistance. An increase in the number of resistance related induced (RRI) metabolites and a decrease in fungal biomass and DON accumulation in spikelets of wheat Sumai3 relative to Roblin was observed. The majority of significantly abundant RR metabolites detected were: *phenylpropanoids*: p-coumaroylagmatine, N-caffeoylputrescine, trans-cinnamic acid, arctigenin, fucoumarinic acid glucoside, and methoxycinnamic acid amides, syringin; *Lipids and fatty acids*: D-glucosyldihydrosphingosine, 2,5-dimethyl-2E-tridecenoic acid, 9-oxononanoic acid, 25,26,27-trinorcholecalciferol, dodecanedioic acid, 2,5-dimethyl-2E-tridecenoic acid and 9,10-dibromo-stearic acid, and *flavonoids*: naringenin related, 6-benzoylaminoflavonone. A higher expression of host *R* genes such as, *T. aestivum* acyl glycerol-3 phosphate acyltransferase (*TaAGPAT*), pathogenesis related protein1 (*TaPR1*) and taumatine like protein (*TaTLP*) in Sumai3 than in Roblin was observed following *Fg* inoculation.

The roles of these RR metabolites and *R* genes in FHB resistance, as evidenced based on disease severity, trichothecene mycotoxins accumulation, and fungal biomass are discussed.

5.2 Introduction

Fusarium head blight (FHB), caused by *Fusarium graminearum* Schwabe (Teleomorph: *Gibberella zeae* (Schwein) Petch), is a destructive disease in wheat, owing to high yield losses and also contamination of grains with mycotoxins (McMullen et al., 1997). Grain contamination with mycotoxins such as deoxynivalenol (DON), 3-acetyl Deoxynivalenol (3A-DON), 15-acetyl Deoxynivalenol (15A-DON), nivalenol (NIV) and zearalenone (ZON) are the major health concerns (Bai and Shaner, 1994). Particularly, the mycotoxin DON, a virulence factor produced by *FgT*, inhibits the protein bio-synthesis in plants and animals (Rocha et al., 2005). The disruption of *Tricodiene synthase* gene *Tri5*- (*Fgt*) showed reduced virulence in wheat seedlings and winter rye (Proctor et al., 1995). However, the resistance mechanism against *Fusarium spp.* infection is yet to be revealed. Plants have evolved different mechanisms to resist *Fusarium spp.* infection and spread, like changing florets morphology (Andersen, 1948), true resistance through host resistance gene expression (Dixon and Harrison, 1990) and biochemical resistance (Kushalappa and Gunnaiah, 2013). The host biochemical resistance mainly involves resistance related (RR) secondary metabolite and RR protein (formerly known as pathogenesis related (PR) proteins) accumulation. Hence, exploring the network of secondary metabolic pathways are essential to identify the key structural genes involved in the FHB resistance mechanism. Based on metabolomic analysis, several RR metabolites, such as p-coumaric acid, syringin, sinapaldehyde, catechin, phenylalanine and jasmonic acids were consistently detected in wheat and barley across FHB disease resistance studies (Bollina et al., 2011; Gunnaiah et al., 2012; Kumaraswamy et al., 2011). Accumulation of RR metabolites, from the chemical groups such as, coumaric acids, amino acids and fatty acids have been reported upon *FgT* isolate (99-15-35) inoculation of Sumai3 (Hamzehzarghani et al., 2005). Inoculation of *FgT* isolate had higher fold change in abundances of RR metabolites such as *p*-coumaric acid, coumarin, sinapaldehyde and jasmonic acid, whereas the inoculation of *Fgt* had higher fold changes of phenylalanine, cinnamic acid, sinapoyl alcohol and catechin metabolites in barley (Kumaraswamy et al., 2011b). Further, the metabolic profiling of the wheat rachis, following *FgT* and *Fgt* inoculation revealed a higher fold change in metabolites accumulation, such as syringyl rich monolignols, glucosides

and antifungal flavonoids in *FgT* than in *Fgt* (Gunnaiah and Kushalappa, 2014). Another study on *Brachypodium* showed phosphoglycerol and phospholipids accumulation, meaning the cell membrane also plays an important role during biotic stress defense or disease symptom development (Allwood et al., 2006). The *FgT* isolate suppressed fatty acids accumulation as compared to *Fgt* isolate, in both black (resistant) and yellow (susceptible) barley implying downregulation of fatty acid biosynthetic pathway genes by DON (Kumaraswamy et al., 2011), which is a known potent inhibitor of eukaryotic protein biosynthesis machinery (Nishiuchi et al., 2006). DON is phytotoxic and kills the host cells by activating ROS (H_2O_2) (Bushnell et al., 2010). Thus, plausibly DON, is activating the stress signaling RR metabolites and ROS in spite of the inhibitory function at advanced stages. Similar to RR metabolites, several *R* genes were also differentially expressed, such as, peroxidase, taumatine like proteins, UDP-glucosyltransferase, and phenylalanine ammonia lyase in wheat (Foroud et al., 2012; Jia et al., 2009; Steiner et al., 2009). Therefore, a thorough analysis of RR metabolites is essential to better understand the FHB resistance mechanisms.

In the present study, metabolic profiling of Sumai3 and Roblin wheat genotypes, based on liquid chromatography and high resolution mass spectrometry (LC-HRMS) was carried out. This experiment was conducted by inoculating trichothecene producing Z-3639 (*FgT*) and non-producing ZGT40 (*Fgt*) isolates of *F. graminearum*. These RR metabolites and *R* genes were analyzed for interactions based on *in-silico* predictions. The selected candidate genes such as: *T. aestivum* acyl glycerol-3 phosphate acyltransferase (*TaAGPAT*), pathogenesis related protein1 (*TaPR1*) and taumatine like protein (*TaTLP*) were studied by expression analysis and interactions with the RR metabolites.

5.3 Materials and Methods

5.3.1 Plant materials and growth conditions

A FHB resistant genotype, Sumai3 and a moderately susceptible and early maturing genotype, Roblin were used. The seeds of these wheat genotypes were obtained from Agriculture and Agri-Food Canada, Winnipeg, Canada (Dr. C. McCartney). Five seeds of Sumai3 or Roblin were sown in 7.5 inch pots filled Agro mix PV20 (Fafard, QC, Canada) and three plants per pot were maintained after germination. The greenhouse conditions were maintained at temperature

25 ± 2°C, with 16 hour daylight and 8 hour darkness, and relative humidity of 70 ± 10%. Plants were watered regularly based on the moisture status. The slow releasing fertilizer 20-20-20=N-P- K was applied two weeks post germination of seeds and also during early booting stage.

5.3.2 *Fusarium graminearum* macroconidia production

The *F. graminearum* (teleomorph*: Gibberella zeae*), trichothecene producing wild isolate Z-3639 (*FgT*) and non-producing mutant isolate GZT40 (*Fgt*) (Proctor et al., 1995), USDA, USA) cultures were maintained in glycerol stocks at -80°C on potato dextrose agar (PDA) media (DIFCO Laboratories Detroit, Michigan, USA). The glycerol stocks were prepared with freshly grown fungal mycelium plugs and stored in -80°C refrigerator until further use. The fresh culture of *Fg* plugs from glycerol stocks were transferred onto rye-agar media plates for spore production. A seven-day-old culture was used to obtain the macroconidial suspension as described by Bollina et al., (2010).

5.3.3 Macroconidia inoculations, metabolic profiling and data processing

The Sumai3 and Roblin spikelets were inoculated at 50% anthesis (growth stage, GS=65) (Zadoks et al., 1974) using *Fg* spore suspension or mock-solution. The two pairs of spikelets in the mid region of five spikes, per replication, were inoculated with *FgT* or *Fgt* macroconidial suspension, or sterile water for mock. An auto-dispenser syringe (GASTIGHT 1750DAD W/S, Hamilton, Reno, NV, USA) was used to dispense 10 µl of spore suspension containing $1x10^5$ macroconidia ml^{-1} and covered with transparent plastic bags sprayed inside with water to maintain a saturated atmosphere, and the covers were removed at 48 hours post inoculation (hpi) and samples were collected at 72 hpi.

The metabolic profiling experiment consisted of two genotypes (Sumai3 and Roblin), three inoculations (*FgT*, *Fgt* and mock solution) in five biological replicates. At 72 hpi the spikelets were harvested, immediately frozen in liquid nitrogen and stored at -80^{0}C until further use. The frozen spikelets were ground in liquid nitrogen using a mortar and pestle; metabolites were extracted using 60% aqueous solution of methanol (v/v) (Bollina et al., 2010). An aliquot of extract was injected into liquid chromatography and high resolution mass spectrometry (LC-HRMS =LC-ESI-LTQ-Orbitrap, Thermo Fisher, Waltham, MA, USA). The raw output data files were converted to .CDF files using Xcalibur 1.2 software (Thermo Scientific^{TM}) and the

monoisotopic masses were detected using MZmine 2.1 software (Pluskal et al., 2010). The metabolites were identified with compound names using different databases METabolite LINk (METLIN), KNApSAcK, HMDB and Kyoto encyclopedia genes and genomes (KEGG) (Kushalappa and Gunnaiah, 2013).

5.3.4 Identification of resistance related (RR) and resistance indicator (RI) metabolites

The monoisotopic masses for each peak/ion were subjected to paired t-test between RP*FgT* Vs RM, SP*FgT* Vs SM, RP*Fgt* Vs RM, SP*Fgt* Vs SM, where RP = resistant (Sumai3) pathogen and SP is susceptible (Roblin) pathogen, inoculated with *FgT* or *Fgt*; and M = mock (sterile water). The statistical significance for paired *t*-test was fixed at $P < 0.05$. The peaks with higher abundance in the resistant than in the susceptible genotype were considered as resistance related (RR) metabolites. The RR metabolites based on mock inoculations were considered as resistance related constitutive (RRC) metabolites, if the abundance of RM>SM. A metabolite with significantly higher abundance in the pathogen inoculated genotype than in mock-solution inoculated was considered as a pathogenesis related (PR=RP>RM) metabolite. A PR metabolite in resistant genotype (Sumai3) with abundance greater than that in susceptible genotype (Roblin) inoculated with pathogen were considered as RR induced (RRI). The putatively identified metabolites were mapped on to existing plant metabolic pathways to identify their biosynthetic genes. The *Fusarium spp.* secondary metabolites, such as deoxynivalenol (DON), 15-O-Acetyl-DON and total DON (DON+15-ADON) that were converted to DON-3-β-glucopyranoside (D3G), were considered as resistance indicator metabolites and their abundances were calculated based on DON standard curves (Bollina et al., 2011).

5.3.5 Multivariate analysis and hierarchical cluster analysis (HCA) of resistance related metabolites

A total of *FgT*=393 and *Fgt*=593 significant peaks based on *t*-test were subjected to hierarchical cluster analysis (HCA) and canonical discriminant (CANDISC) analysis to classify the treatments based on canonical scores using PROC GLM procedures of SAS (SAS 9.4, http://www.sas.com/en_ca/home.html).

5.3.6 Disease severity assessment

Disease severity was assessed based on a randomized complete block design experiment with two genotypes (Sumai3 and Roblin), inoculated with *FgT* isolate, in three replicates over time. Spikelets were spray inoculated at 50% anthesis with macroconidial suspension using an airbrush (Model: Badger 200.3). The experimental units consisted of 30 spikes. The number of spikelets diseased in a spike was recorded at three day intervals and experiment was conducted until 21 days post inoculation (dpi). The data collected from three to 21 dpi were used for calculating the proportion of spikelets diseased (PSD = number of spikelets diseased/total number of spikelets in a spike), from which the area under the disease progress curve (AUDPC) were calculated.

5.3.7 Fungal biomass quantification based on qPCR

Two alternate pairs of spikelets inoculated, along with two uninoculated pairs, samples collected for metabolites extraction (section 2.3), at 72 hpi after *FgT* and *Fgt* inoculations, were used to estimate the fungal biomass. The *Fusarium* species specific primer of the *galactose oxidase* (*GaO*) gene was used for quantifying the fungal biomass. The primer sequences and NCBI gene IDs are given in Appendix Table A5.1. The frozen spikelets of both Sumai3 and Roblin were ground and the genomic DNA was extracted using Qiagen kit. The *Fg* species specific *Gao* gene primers were used along with the wheat housekeeping *Actin* gene to amplify the genomic DNA of *Fg* and wheat. The *Actin* gene was amplified in all the replicates to normalize the quantity of genomic DNA based on band intensities and NanoDrop spectrophotometer (NanoDrop, Wilmington, DE, USA) quantification. Further, normalized genomic DNA from all the three biological replicates was used for real time quantitative polymerase chain reaction (qPCR) analysis to calculate the relative *Fg* gene copy numbers (Kumar et al., 2015). The relative gene copy number of the *Gao* gene was calculated based on Ct (Cycle threshold) values, to quantify the total fungal biomass within the *FgT* colonized tissue based on $2^{-\Delta\Delta Ct}$ method (Livak and Schmittgen, 2001).

5.3.8 Discovery of resistance genes and expression: cDNA synthesis, quantitative real-time PCR and Semi-quantitative PCR

The candidate host resistance genes (*R*), such as *T. aestivum* pathogenesis related protein1 (*TaPR1*), *T. aestivum* taumatine like protein (*TaTLP*), *T. aestivum* serine threonine protein kinase (*TaSTPK*), MYC transcription factor, *T. aestivum* basic helix loop helix (*TabHLH*), and *T. aestivum* acyl glycerol-3 phosphate acyltransferase (*TaAGPAT*) were selected based on their expression during *F. graminearum* infection in wheat and barley (Bernardo et al., 2007; Dhokane et al., 2016; Geddes et al., 2008; Kage et al., 2016; Mackintosh et al., 2007). The gene expression was conducted based on quantitative real time PCR (qRT-PCR). Total RNA was isolated from spikelets of three replicates of Sumai3 and Roblin genotypes point inoculated with *FgT* and *Fgt* at 72 hpi. For RNA extraction, Qiagen RNAeasy plant mini kit (Qiagen) was used and the genomic DNA contamination was reduced to a minimum by treating with DNAase I before cDNA synthesis. Total RNA (1µg) was reverse transcribed in a 20µl reaction using iScript cDNA synthesis kit (BioRad, On, Canada). To remove the RNA templates, cDNA was treated with RNAse. Freshly, prepared cDNA was quantified using NanoDrop 1000 spectrophotometer (NanoDrop, Wilmington, DE, USA). Total 20µl Polymerase chain reaction (PCR) was carried out by using diluted (20 nanogram per microliter) cDNA, 10 pico-moles of primers (Forward and Reverse), 2X PCRmix (Froggabio Life Sciences, NY) at appropriate annealing temperature. Each gene was amplified in five sets of reactions using standard annealing temperatures for 40 cycles. Sets of PCR tubes were removed at 20, 25, 30, 35, 40th cycles after one minute extension at 72^{o}C, and kept on ice. Finally, the latter were transferred to a PCR thermocycler and kept for 12 minutes final extension at 72^{o}C. Amplified PCR products were checked in 2.5 percent normal agarose gel. The aliquot of cDNA was used for qRT-PCR based on iQ SYBR Green supermix (BioRad) using CFX384TM Real-Time System (BioRad, ON, Canada).

5.4 Results

5.4.1 Disease severity and fungal biomass accumulation in spikelets

FHB disease severity on spikelets of Sumai3 and Roblin was quantified as the proportion of spikelets diseased following spray inoculation with the wild pathogen *FgT*. Spikes inoculated with the mutant pathogen (*Fgt*) did not show any symptom spreading to adjacent spikelets (Gunnaiah and Kushalappa, 2014). The disease severity based on the proportion of spikelets diseased (PSD) at 21 dpi was 0.98 in Roblin, whereas in Sumai3 the PSD was 0.51 (Figure. 5.1A and 5.1B). The increase in PSD in Roblin at 21 dpi may also be due to the spread of pathogen

through the rachis to the next spikelet, whereas the genotype Sumai3 has high rachis resistance. The area under disease progress curve (AUDPC) also significantly ($P < 0.01$) varied between genotype s, and it was 9.2 and 14.4, in resistant and susceptible genotypes, respectively.

Sumai3 and Roblin spikelets were point inoculated with both trichothecene producing (*FgT*) and non-producing (*Fgt*) isolates of *Fg* and fungal biomass were assessed at 72 hpi. The quantitative real-time quantitative PCR (qPCR) at 72 hpi spikelets showed significantly lower amount of *FgT* biomass in Sumai3 (0.21) than in Roblin (6.79) spikelets. Whereas, these differences were relatively small between Sumai3 (0.97) and Roblin (1.24), when the *Fgt* isolate was inoculated (Figure. 5.1C). However, the amount of fungal biomass in Sumai3 between *FgT* and *Fgt* inoculations wwas not significantly different ($P<0.05$) based on ANOVA, but Roblin showed significance for fungal biomass accumulation. This indicated that the *FgT* isolate, capable of producing trichothecene, empowered the pathogenesis as compared to *Fgt* isolate, meaning DON may have induced more resistance genes or RR metabolites having antifungal activity in Sumai3 then Roblin (Hamzehzarghani et al., 2005; Paranidharan et al., 2008).

5.4.2 Trichothecenes accumulation in wheat spikelets inoculated with *Fg* isolates

The trichothecenes DON and 15ADON are known as virulence factors for *Fg* pathogenesis. The accumulation of these trichothecenes was analyzed in spikelet samples collected at 72 hpi. Expectedly, DON and 15ADON were detected only in *FgT* isolate inoculated spikelets of Sumai3 and Roblin, but not in *Fgt*, confirming that *Fgt* lacks the ability to produce these trichothecenes. The concentration of DON was significantly ($P < 0.05$) higher in Roblin spikelets (2.27 mg kg-1) than in Sumai3 spikelets inoculated with *FgT* (0.73 mg kg-1). However, the total DON produced (TDP=DON+D3G+15ADON) and proportion of DON converted (PDC) did not show any significant difference between the genotype s, indicating that the DON detoxification is common to both the genotypes (Appendix Figure A5.1).

5.4.3 Spikelet resistance related metabolites in Sumai3

Metabolic profiling was carried out in the spikelets of resistant (Sumai3) and susceptible (Roblin) genotypes at 72 hpi of *FgT* and *Fgt* isolates along with a mock inoculation control. A total of 2595 and 2544 consistent peaks were detected, in all the treatments involving *FgT* and *Fgt* inoculations, respectively. Among these, a total of 129 (23 putatively identified) peaks were

resistant related constitutive (RRC) and 246 (88 putatively identified) were resistant related induced (RRI) metabolites (Table 5.1).

The RRI metabolites, such as flavonoids, glycerophospholipids and fatty acids were found only in *FgT* inoculated spikelets of Sumai3 and Roblin. Four phenylpropanoid pathway RRI metabolites, such as trans-cinnamic acid, 2-methoxycinnamic acid, O-methoxyhydrocinnamic acid, and furocoumarinic acid glucoside were found in *FgT* inoculated samples. In addition, arctigenin, podorhizol beta-D-glucoside, p-coumaroylagmatine and N-caffeoylputrescine were detected only in Sumai3. Among the RRI and RRC identified metabolites, only seven were common between *FgT* and *Fgt* inoculated spikelets and also, only one common metabolite (trans-cinnamic acid) from phenyl propanoid metabolic pathway was observed in *FgT*, *Fgt* and mock inoculated spikelets of Sumai3 and Roblin genotypes (Table 5.1; Figure. 5.2A, 5.2B). The metabolites detected only in *FgT* and *Fgt*, but not in mock inoculated spikelets of resistant and susceptible genotypes, were termed as RRI qualitative metabolites induced upon *FgT* (*RRI_FgTq*) and *Fgt* (*RRI_Fgtq*) inoculations.

A total 60 *RRI_FgTq* and 122 *RRI_Fgtq* consistent peaks were detected across the samples. Out of 60 *RRI_FgTq* and 122 *RRI_Fgtq* 11 *RRI_FgTq* and 14 *RRI_Fgtq* were identified as putative metabolites based on MS/MS fragmentation match. All the RR metabolites induced following inoculation of *FgT* and *Fgt* in Sumai3 and Roblin spikelets indicated the activation of both phenylpropanoid and flavonoid pathways and also, lipid pathways, which include terpenoids and fatty acids (Figure. 5.3).

5.4.4 Constitutive resistant related (RRC) metabolites in Sumai3 spikelets

Among the 127 significant (P<0.05) RRC metabolites detected, 23 were putatively identified based on monoisotopic masses, accurate mass error (AME) of less than 5 ppm and fold change of more than 1.0 (Table 5.1). More number of RRC metabolites belonged to lipids, alkaloids and glucose conjugated amino acids. There were two phenylpropanoid metabolites: trans-cinnamic acid and syringaresinol O-beta-D-glucoside, and one metabolite from each of flavonoid (6,8-Di-DMA-chrysin) and fatty acid (Stearidonic acid) groups. Also, one stilbenoid (piceatannol) and jasmonic acid (dihydro-jasmonic acid methyl ester) were found as RRC metabolic group.

5.4.5 Resistant related induced (RRI) metabolites in Sumai3 spikelets, following inoculation of trichothecene producing (*FgT*) and nonproducing (*Fgt*) isolates

A total of 120 (47 putatively identified) RR metabolites induced by *FgT* isolate and 107 (16 putatively identified) induced by *Fgt* isolate were detected (Table 5.1). Among the *FgT* induced metabolites, 17 fatty acids, seven carbohydrates and five phenylpropanoid, one hydroxycinnamic acid amides, four flavonoids, five lipids, four terpenoids and four metabolites belongs to an unclassified group were identified as RRI metabolites. Among *Fgt* induced RRI metabolites four belonged to phenylpropanoids, three terpenoids, three amino-acids, one lipid, one carbohydrate, two alkaloids and two to an unclassified group. Surprisingly, not a single fatty acid and flavonoid metabolite was identified as RRI_*Fgt*. Only one phenylpropanoid and four hydroxycinnamic (HCAA) acids namely: furocoumarinic acid glucoside, O-methoxyhydrocinnamic acid and trans-cinnamic acid were identified as RRI_*FgT*. Four phenylpropanoids: such as arctigenin, podorhizol beta-D-glucoside, p-coumaroylagmatine and N-caffeoylputrescine were identified as RRI_*Fgt*. Four flavonoids, such as, 6-bezoylaminoflavanone, naringenin 7-O-(2",6"-di-O-alpha-rhamnopyranosyl)-beta-glucopyranoside, and salicyl alcohol hexoside, whereas, *Fgt* infected spikelets did not show any flavonoids among the identified metabolites. Four terpenoids, gnidicin and S-japonin were identified as RRI_*FgT*, compare to three RRI_*Fgt* terpenoids and secologanin. One amide (1, 2-dithiolane-3-pentanamide) and one ester (di-trimethylsilyl 2-dodecenedioate) were found only on *FgT* isolate inoculated spikelets of resistant and susceptible genotypes. Out of total 60 qualitative metabolites (RRI_*FgTq*), only 11 were identified in *FgT* inoculated samples and 14 were identified among 64 RRI_*Fgtq* metabolites in *Fgt* isolate inoculated samples. Interestingly, several carbohydrates related metabolites such as, ribose; sucrose and 6-acetyl-D-glucose were induced only in *FgT* isolate inoculated spikelets of Sumai3. Three alkaloids: heliotrine, valeroidine and caffeine, were identified in each *FgT* and *Fgt* isolate inoculated spikelets of Sumai3. Three amino-acids were accumulated only in *Fgt* inoculated spikelets with more than 2.0 fold change. Also, one lipid (10-oxodecanoate) and one succinic acid (butoctamide hydrogen succinate) were found in *Fgt* inoculated spikelets of Sumai3, suggesting these metabolites are having the resistance function.

5.4.6 Clustering of observations based on multivariate analysis of peak abundances

A total of 393 and 506 significant ($P < 0.05$) peaks, consistent among all the treatments were subjected to canonical discrimination analysis to identify groups. The CAN1 successfully separated the peaks based on genotype and CAN2 separated the peaks based on treatments in both *FgT* and *Fgt* inoculated spikelets of Sumai3 and Roblin. Further, the scatter plot analysis based on the CAN loading (L) revealed 18 high loading metabolites to CAN1, explaining the genotype resistance function (Appendix Figure A5.2). Among 18, only seven metabolites were identified using METLIN database with less than 5 ppm error, such as caffeoylputrescine (metabolite loading $L \geq 0.86$), 8E-heptadecenedioic acid ($L \geq 2.34$), p-coumaroyl agmatine ($L \geq 3.4$), 9-10-dihydroxy octadecanedioic acid ($L \geq 0.96$), dihydroferulic acid 4-o-glucuronide ($L \geq 1.2$), secologanin ($L \geq 0.7$) and (-)-12-hydroxy-9,10-dihydrojasmonic acid ($L \geq 0.32$) in *FgT* inoculated samples. Whereas, galactosylglycerol ($L \geq 0.28$), 13-epi-12-oxo-phytodienoic acid ($L \geq 0.33$), 4-coumaroyl-2-hydroxyputrescine ($L \geq 1.5$) and secologanin ($L \geq 1.3$) RR metabolites were loaded to CAN2 for *Fgt* inoculated samples with lower loading values. The metabolites with high loading ($L \geq 0.5$) explain the genotype resistance or pathogen inoculation functions. The hierarchical cluster analysis clearly discriminated between resistant and susceptible genotypes, following *FgT* and *Fgt* inoculations.

5.4.7 Association of upregulated host genes with resistant related metabolites in Sumai3

The uniform expression of the wheat housekeeping gene *Actin* was observed across the treatments and replications. The differential expression of host genes such as *T. aestivum* pathogenesis related class-1 gene (*TaPR1*), *T. aestivum* basic helix-loop-helix *MYC* gene (*TabHLH*), *T. aestivum* taumatine like protein gene (*TaTLP*), *T. aestivum* acyl glycerol 3-phosphate acyltransferase gene (*TaAGPT*), *T. aestivum* serine threonine protein kinase (*TaSTPK*) was observed at 30, 35, 40 cycles of PCR (Figure. 5.4A). Among the *R* gene selected for the differential expression analysis, only *TaPR1*, *TaTLP* and *TaAGPAT* genes showed high differential expression between Sumai3 and Roblin genotypes (Figure. 5.4B). Whereas, *TabHLH* and *TaSTPK* did not show significant differences at the transcripts expression levels. Further, interaction between differentially expressed genes and RR metabolites was seen using web interface softwares, STRING/STITCH (http://string-db.org/). Interestingly, the *TaAGPAT* gene had very strong interaction (thick bonds indicate strong interactions) with *phosphatidate*

cytidylyltransferase of Arabidopsis (AT4G22340; high combined association score of 0.974), *phospholipid/glycerol acyltransferase* (AT5G60620; 0.959) and glycerol-3-phosphate metabolite (0.959). It is possible that these genes are associated with the large number of fatty acids and glycerol-phosphate metabolites detected in *FgT* inoculated spikelets of Sumai3 (Figure 5.5; Table 5.1). Similarly, the *TaTLP* gene also had very strong interaction with *pectate lyase* family protein (AT3G53190; score 0.758), leucine-rich repeat (LRR) transmembrane protein kinase (IRK; score 0.748) and *terpene synthase*/*cyclase* family protein (AT3G14490; score 0.716). The *TaPR1* gene also showed clear interaction with RR metabolite like, methyl jasmonic acid and other interacting partners, such as *PR5* (thaumatin-like protein), *MYC2*, β-1,3-glucanase, pectate lyase, terpene synthase. Incidentally, we also reported the metabolites belonging to pectates and terpenoids, such as RR amylopectin and four terpenes in *FgT* inoculated spikelets of Sumai3, but not in case of *Fgt* inoculated spikelets.

5.5 Discussion

Resistance in wheat against *F. graminearum* is complex. A metabolomics approach was used to identify resistance related metabolites, which in turn were mapped in a metabolic pathway to identify *R* genes. Gene expression and functional genomics studies have reported several genes associated with FHB resistance. However, the candidate genes responsible for spikelet resistance against *F. graminearum* initial infection and their molecular mechanisms have not been identified. This study reports the high fold change accumulation of RR metabolites and up-regulation of host *R* genes involved in FHB spikelets resistance in wheat.

5.5.1 Sumai3 spikelets resist FHB through RR metabolites

Spikelets of Sumai3 accumulated high amounts of flavonoids fatty acids and glycerolipids. This in turn reduced FHB severity, pathogen biomass and total DON accumulation. The JA phytohormone and glycerophosphate RR metabolites appear to activate the host resistance related genes by transducing the signals generated during pathogen infection (Saucedo-Garcia et al., 2015). A previous study also indicated glycerophospholipids accumulation only in spikelets rather than in the rachis in wheat, following *F. graminearum*, isolate 15–35, inoculation (Gunnaiah et al., 2012). Also, these long chain glycerophospholipids act as stress signal transducer during pathogen infection (Saucedo-Garcia et al., 2015).

Interestingly, the present study reports such key defense signalling JA metabolites ((-) 12-hydroxy-9, 10-dihydro-jasmonic acid, and dihydro JA-methyl ester), while these were less active in Roblin. The trichothecene produced by *Fg* induces oxidative burst damaging the host cells, which in turn release several elicitors (Ding et al., 2011). The necrotrophic nature of *F. graminearum* leads to the activation of JA signalling pathway (Ding et al., 2011). Transcriptomic profiling of winter wheat cultivars, Sumai3-Dream and Sumai3-wheat landrace Y1193-6, also induced JA signalling pathway only in Sumai3 (Gottwald et al., 2012). Further, JA signalling is also known for the induction of antifungal metabolites.

Several flavonoids were induced in the current study after *FgT* inoculation, such as naringenin 7-O-(2",6"-di-O-alpha-rhamnopyranosyl)-beta-glucopyranoside (FC >1.5) and 6-bezoylaminoflavanone (FC >2.8), which were also reported in a previous study and the latter are known antifungal compounds (Gunnaiah and Kushalappa, 2014). Naringenin 7-glucoside identified in this study strongly suppresses pathogen development (Bollina et al., 2010). On the contrary, no carbohydrate, fatty acid and flavonoids were detected among the RR metabolites identified in *Fgt* infected spikelets of Sumai3.

Several phenylpropanoid RR metabolites were also identified in *FgT* inoculated spikelets of Sumai3 genotype. The RRI metabolites detected in Sumai3 spikelets belong to hydroxycinnamic acid amides (HCAAs) such as trans-cinnamic acid, O-methoxyhydrocinnamic acid, and others such as arctigenin, syringin, furocoumarinic acid glucoside, and 2-methoxycinnamic acid. These were also known to be accumulated in both rachis and spikelets. Phenylpropanoids conjugate with amines to form HCAAs, which are involved in reinforcing the cell walls around the infection site to contain the pathogen to initial infection (Gunnaiah and Kushalappa, 2014; Gunnaiah et al., 2012). Several other studies also indicated that phenylpropanoids play a major role in imparting resistance in wheat and barley against FHB (Bollina et al., 2010; Bollina et al., 2011; Kumaraswamy et al., 2011b). Particularly, the metabolites of phenylpropanoid class like, monolignols, *trans*-cinnamate and glucosides of lignans like syringaresinol O-beta-D-glucoside were consistently found in the resistant genotype, Sumai3.

Apart from flavonoid and phenylpropanoids, we also identified several RR metabolites belonging to lipid, alkaloids and fatty acids like, docosahexaenoic acid, ankorine, alpha-

tocopherol nicotinate, dodecanedioic acid, stearidonic acid, butanoic acid, epoxyoctadeca-9,11-dienoic acid that are speculated to be accumulated during the initial phase of *Fg* infection. Though, it is difficult to differentiate the metabolites accumulated due to trichothecenes, the large number of RRI metabolites falling into signalling functions, implies host response in the early stage of *Fusarium spp.* infection. In conclusion, following the perception of *Fusarium spp.* pathogen the host plant accumulates stress signaling metabolites like, JA and glycerophospholipids, which probably triggers downstream regulatory genes that regulated *R* genes to biosynthesize several groups of RR metabolites, meaning Sumai3 has multiple resistance mechanisms.

5.5.2 FHB disease severity and fungal biomass in spikelets

The assessment of disease severity at three dpi of spikelets with *Fusarium spp*. indicated that the both *FgT* and *Fgt* can infect the spikelets, implicating trichothecenes are not necessary for spikelet initial infection. Similar results were witnessed in both barley and wheat spikes upon trichothecene mutant isolate inoculations (Jansen et al., 2005). The *FgT* fungal biomass was also significantly higher in susceptible Roblin (more than six fold) as compared to resistant Sumai3 at 72 hpi. The increased fungal biomass in the susceptible genotype is plausibly due to non-functional alleles of host resistance genes and low accumulation of antifungal RR metabolites. Also, the *Fg* isolate carrying the trichothecene producing gene is more aggressive and is responsible for killing host cells and letting the pathogen multiply by feeding on dead cells (Ding et al., 2011). The wild isolate, *FgT* might already be producing DON after 36 hpi and hence, there is a high accumulation of fungal biomass in Roblin spikelets. DON is generally produced in wheat spikelets at 48 and 36 hpi (Kang and Buchenauer, 1999; Mirocha et al., 1997). The significant increase in FgT biomass in Roblin is mainly due to its susceptibility to rachis infection, through which the pathogen can spread from the infected spikelets to other spikelets, whereas Sumai3 is well known for high rachis resistance, with no rachis colonization (Gunnaiah and Kushalappa, 2014; Hamzehzarghani et al., 2005). The colonization of *Fusarium* trichothecene mutant species is completely blocked at the rachis through heavy cell wall thickening in the wheat variety, Nandu (Jansen et al., 2005). However, the defined role of trichothecenes during FHB disease spread is unknown, even though trichothecenes DON and 15ADON are known as virulence factors for *Fg* pathogenesis. As expected, DON and 15ADON

were detected only in Sumai3 and Roblin spikelets inoculated with *FgT* isolate, confirming that *Fgt* lacks the ability to produce these trichothecenes. Brown spots were visible at 48 hpi of both *FgT* and *Fgt* isolates on both Sumai3 and Roblin spikelets. Several studies in the past indicated extracellular enzymes may also play a crucial role during initial colonization of *Fusarium spp.* (Balazs and Bagi, 1997; Miedaner et al., 1997).

5.5.3 RR metabolites were associated with highly expressed *R* genes during *F. graminearum* pathogenesis

The current study reveals, the upregulation of host genes expression in *FgT* inoculated Sumai3 and Roblin spikelets at 72 hpi based on quantitative and semi-quantitative analysis. A large number of glycerol and glycerol-phosphate metabolites accumulated in Sumai3, following inoculation with *FgT*, such as 1-dodecanoyl-2-(6Z,9Z,12Z-octadecatrienoyl)-glycero-3-phosphate (3-beta-D-galactosyl-sn-glycerol, glycerol; *FgT* inoculated spikelets, such as 3-beta-D-galactosyl-sn-glycerol also in mock inoculated spikelets, such as sn-glycero-3-phospho-1-inositol. Interestingly, the *TaAGPAT* gene showed very strong interaction with phosphatidate cytidylyltransferase and phospholipid/glycerol acyltransferase and glycerol-3-phosphate.

Similarly, both *TaTLP* and *TaPR1* gene also showed very strong interaction with pectate lyase family protein (AT3G53190; score 0.758), leucine-rich repeat (LRR) transmembrane protein kinase (IRK; score 0.748), β-1,3-glucanase and terpene synthase/cyclase family protein (AT3G14490; score 0.716). These thaumatin-like protein (*TaTLP*) and pathogenesis proteins (*PR1* along with *PR2*, *PR3*, *PR5*) and peroxidases were known to be induced during *Fg* initial infection in wheat (Pritsch et al., 2000; Steiner et al., 2009). These PR proteins induced against microbial and pest attack were classified from PR-1 to PR-17 groups (Christensen et al., 2002; Muthukrishnan et al., 2001; Van Loon et al., 2006). Particularly, *TaTLP* is known to express during both biotic and abiotic stresses in wheat (Deihimi et al., 2013). Accordingly, we also found RR metabolites like, methyl ester-dihydrojasmonic acid, amylopectin, several terpenes (deoxyloganin, secologanin, S-japonin, rehmaionoside-A, gnidicin, asebotoxin II and cuauhtemone).

The present study, however, confirmed accumulation of several of RR metabolites, following *F. graminearum* infection. Particularly, flavonoids (naringenin 7-O-(2",6"-di-O-alpha-

rhamnopyranosyl)-beta-glucopyranoside, naringenin 7-O-beta-D-glucoside, 6-bezoylaminoflavanone and cajanol), phenylpropanoids (trans-cinnamate, N-caffeoylputrescine, p-coumaroylagmatine, methoxycinnamic acids and syringin) and glycerophospholipids (sn-glycero-3-phospho-1-inositol, dodecanedioic acid, D-glucosyldihydrosphingosine, docosahexaenoic acid and butanoic acid) were reported in several studies. The *R* genes identified here can be used in breeding following their validation. However, we did not find the Arabidopsis orthologous genes for the *TaSTPK* and *TabHLH* genes to study their interaction with the RR metabolites. Further functional characterization of the reported host genes might help in understanding the actual contributions in the *Fg* spikelet resistance mechanism in wheat.

In conclusion, the current study revealed the mechanisms of spikelet resistance based on high fold change in abundances of RR metabolites and high expression of host *R* genes, following inoculation of *FgT* and *Fgt* isolates. Though, the role of trichothecene in pathogen spread in wheat is well documented, its function in wheat spikelet resistance is not well characterized in wheat compared to barley. Our results indicate that the fungal colonization varies among genotypes, and the *FgT* isolate can multiply faster than the *Fgt* within the spikelets. We also report induction of flavonoids, lipids and fatty acids by *FgT* infection. The JA and phospholipids are highly induced following pathogen invasion and the latter plausibly induced regulated by *TaAGPAT* gene. We postulated that the antifungal RR metabolites and RR proteins (*TaPR1* and *TaTLP*) may have a direct role in *Fg* fungal biomass suppression mechanism. In summary, we have reported novel RR metabolites and *R* genes associated with spikelet resistance in Sumai3. Further, functional characterization of the host *R* genes is essential to prove the effectiveness of each gene and its importance in FHB resistance. Following validation of host genes functions they can be used as biomarkers to replace the nonfunctional genes in elite cultivars to improve FHB resistance.

Table 5.1 The resistance related (RR) metabolites identified from spikelets of Sumai3, relative to Roblin, at 72 hpi with *Fusarium graminearum* trichothecene producing (*FgT*) or trichothecene non-producing (*Fgt*) isolates and mock (sterile water) inoculations.

m/z value	**Metabolites Class**	**RRI FC[a]**				**RRC[b]**
Mass (Da)	**Phenylpropanoids (monolignols, Hydroxycinnamic acid amides and their glucosides)**	***FgT***	***Fgt***	***FgTq***	***Fgtq***	
148.05	trans-cinnamic acid	1.3*	ND	ND	INF (1.1)	1.2*
250.13	N-caffeoylputrescine	ND	1.5**	INF (1.3)	INF (1.8)	ND
276.16	*p*-coumaroylagmatine	ND	1.5**	INF (1.7)	INF (1.1)	ND
366.09	Furocoumarinic acid glucoside	1.4*	ND	ND	ND	ND
180.08	O-methoxyhydrocinnamic acid	1.3*	ND	ND	ND	ND
372.15	Arctigenin	ND	2.2**	ND	ND	ND
578.20	Podorhizol beta-D-glucoside	ND	1.6*	ND	ND	ND
580.21	(+)-syringaresinol O-beta-D-glucoside	ND	ND	ND	ND	2.0*
372.14	Syringin	ND	ND	INF (1.3)	ND	ND
Mass (Da)	**Flavonoids**	***FgT***	***Fgt***	***FgTq***	***Fgtq***	**RRC**
316.09	Cajanol	ND	ND	INF (3.5)	INF (3.4)	ND
726.24	Naringenin 7-O-(2",6"-di-O-alpha-rhamnopyranosyl)-beta-glucopyranoside	1.5*	ND	ND	ND	ND
434.12	Naringenin 7-O-beta-D-glucoside	ND	ND	ND	INF (1.2)	ND
286.27	Salicyl alcohol hexoside	5.6**	ND	ND	ND	ND

343.11	6-Bezoylaminoflavanone	2.8*	ND	ND	ND	ND
656.23	Triphyllin A	1.2**	ND	ND	ND	ND
390.18	6,8-Di-DMA-chrysin	ND	ND	ND	ND	2.3*
Mass (Da)	**Lipids**	***FgT***	***Fgt***	***FgTq***	***Fgtq***	**RRC**
463.35	D-Glucosyldihydrosphingosine	1.9*	ND	ND	ND	ND
332.24	Endoperoxide prostaglandin H2	1.7*	ND	ND	ND	ND
436.26	25,26,27-trinorcholecalciferol	1.3*	ND	ND	ND	ND
386.26	6-deoxyerythronolide B	1.3*	ND	ND	ND	ND
186.12	10-oxodecanoate	ND	1.2*	ND	ND	ND
328.24	(4Z,7Z,10Z,13Z,16Z,19Z)-docosahexaenoic acid	ND	ND	ND	ND	2.3*
230.15	Dodecanedioic acid	ND	ND	ND	ND	2.0*
88.05	Butanoic acid	ND	ND	ND	ND	1.8*
294.22	(9Z)-(13S)-12,13-epoxyoctadeca-9,11-dienoic acid	ND	ND	ND	ND	1.7*
334.07	sn-glycero-3-phospho-1-inositol	ND	ND	ND	ND	1.4*
318.20	(-)-menthyl O-beta-D-glucoside	ND	ND	INF (1.6)	ND	ND
138.10	Nona-2,6-dienal	ND	ND	INF (1.2)	ND	ND
296.19	10-deoxymethynolide	ND	ND	ND	INF (1.3)	ND
Mass (Da)	**Fatty acids**	***FgT***	***Fgt***	***FgTq***	***Fgtq***	**RRC**
342.12	15-methanobenzo(a)naphto(2,3-f)cyclodecene	2.3*	ND	ND	ND	ND
440.09	9,10-dibromo-stearic acid	2.3*	ND	ND	ND	ND

162.04	1-tridecene-3,5,7,9,11-pentayne	1.9*	ND	ND	ND	ND
341.21	2-(2-butenoxy)-n-(2-diethylaminoethyl)-4-quinolinecarboxamide	1.6*	ND	ND	ND	ND
240.20	2,5-dimethyl-2E-tridecenoic acid	1.5**	ND	ND	ND	ND
332.25	9,10,18-trihydroxystearate	1.5**	ND	ND	ND	ND
194.05	2E,4E,6Z,8Z-decatetraenedioic acid	1.4*	ND	ND	ND	ND
104.01	Melonic Acid	1.3*	ND	ND	ND	ND
172.10	9-oxononanoic acid	1.3*	ND	ND	ND	ND
614.39	1-dodecanoyl-2-(6Z,9Z,12Z-octadecatrienoyl)-glycero-3-phosphate	1.3**	ND	ND	ND	ND
411.29	N-oleoyl glutamic acid	1.3**	ND	ND	ND	ND
656.44	3-O-(2-O-(2E-decenoyl)-alpha-L-rhamnopyranosyl)-3-hydroxydecanoic acid	1.3*	ND	ND	ND	ND
427.29	PGF2alpha-dihydroxypropanylamine	1.2*	ND	ND	ND	ND
134.03	6E-octene-2,4-diynoic acid	1.2**	ND	ND	ND	ND
276.20	Stearidonic acid	ND	ND	ND	ND	2.0*
Mass (Da)	**Terpenoids**	***FgT***	***Fgt***	***FgTq***	***Fgtq***	**RRC**
628.23	Gnidicin	1.7*	ND	ND	ND	ND
336.17	S-japonin	1.5*	ND	ND	ND	ND
390.22	Rehmaionoside A	1.3**	ND	ND	ND	ND
388.14	Secologanin	ND	1.3*	ND	ND	ND
Mass (Da)	**Unclassified metabolites**	***FgT***	***Fgt***	***FgTq***	***Fgtq***	**RRC**

150.05	Ribose	2.7**	ND	ND	ND	ND
342.11	Sucrose	2.4*	ND	ND	ND	ND
222.07	6-Acetyl-D-glucose	1.5*	ND	ND	ND	ND
330.13	3-(3,4-dihydroxyphenyl)-1-propanol 3'-glucoside	1.3*	ND	ND	ND	ND
828.27	Amylopectin	1.3*	ND	ND	ND	ND
268.09	Dimethyl,2-(3,4-dimethoxyphenyl)malonate	1.3**	ND	ND	ND	ND
454.10	1,2-dithiolane-3-pentanamide (CAY10506)	2.9*	ND	ND	ND	ND
313.18	Heliotrine	2.6**	ND	ND	ND	ND
241.16	Valeroidine	1.5**	ND	ND	ND	ND
372.21	Di(trimethylsilyl) 2-dodecenedioate	1.5*	ND	ND	ND	ND
300.12	Salidroside	ND	ND	ND	ND	2.1*
309.11	N-Acetylneuraminate	ND	ND	ND	ND	2.1**
149.05	L-Methionine	ND	ND	ND	ND	2.0**
135.05	Adenine	ND	ND	ND	ND	1.8*
126.04	Thymine	ND	ND	ND	ND	1.4**
244.07	Piceatannol	ND	ND	ND	ND	1.6*
226.16	Dihydrojasmonic acid, methyl ester	ND	ND	ND	ND	3.5*

[a]Resistance related induced (RRI) metabolites calculated based on (Sumai3 inoculated with *Fg* wild isolate producing DON (*FgT*) and non-producing isolate (*Fgt*) > Mock) > (Roblin inoculated with *Fg* isolate *FgT* and non-producing isolate *Fgt* > Mock).

[b]Resistance related constitutive (RRC) metabolites calculated based on Sumai3 with sterile water inoculated (mock) > Roblin Mock, INF = infinity, in this case metabolites were not detected in Mock inoculated samples of Sumai3 and Roblin, accordingly the fold change in parenthesis was calculated as Sumai3 *FgT*/Roblin *FgT* (also called qualitative metabolites, *FgTq*) and Sumai3 *Fgt*/Roblin *Fgt* (also called qualitative metabolites, *Fgtq*), where, T is trichothecene producing wild *Fg*; t is trichothecene nonproducing mutant *Fg* and ND is not detected.

** indicates the significance level at P<0.01, * indicates the significance level at P<0.05

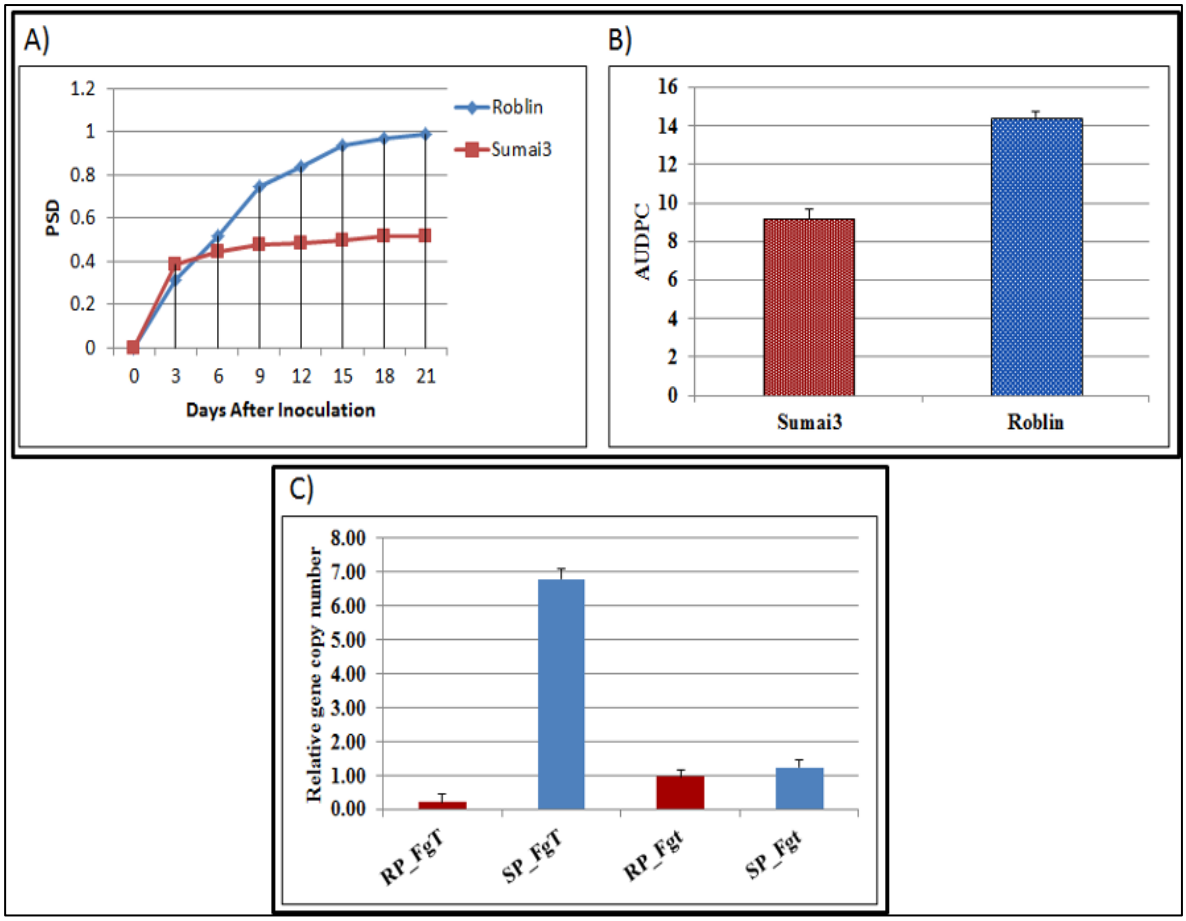

Figure 5.1 Disease severity in Sumai3 and Roblin genotypes, based on visual observations, following spray inoculation with *Fusarium graminearum,* trichothecene producing isolate (*FgT*) and fungal biomass quantification based on real-time qPCR in resistant (Sumai3) and susceptible (Roblin) spikelets, at 72 hpi; A) Proportion of spikelets diseased (PSD); B) Area under disease progress curve (AUDPC), calculated based on every 3 d observations until 21 dpi; C) *Fusarium graminearum* fungal biomass quantification based on *Tri6_10* gene copies. Where, RP_*FgT*= resistant genotype, Sumai3 point inoculated with trichothecene producing isolate of pathogen (*FgT*); SP_*FgT*= susceptible genotype, Roblin inoculated with pathogen, *FgT*); RP_*Fgt*= Sumai3 inoculated with trichothecene non-producing mutant isolate of pathogen (*Fgt*); SP_*Fgt*= susceptible Roblin inoculated with trichothecene non-producing mutant isolate of pathogen (*Fgt*).

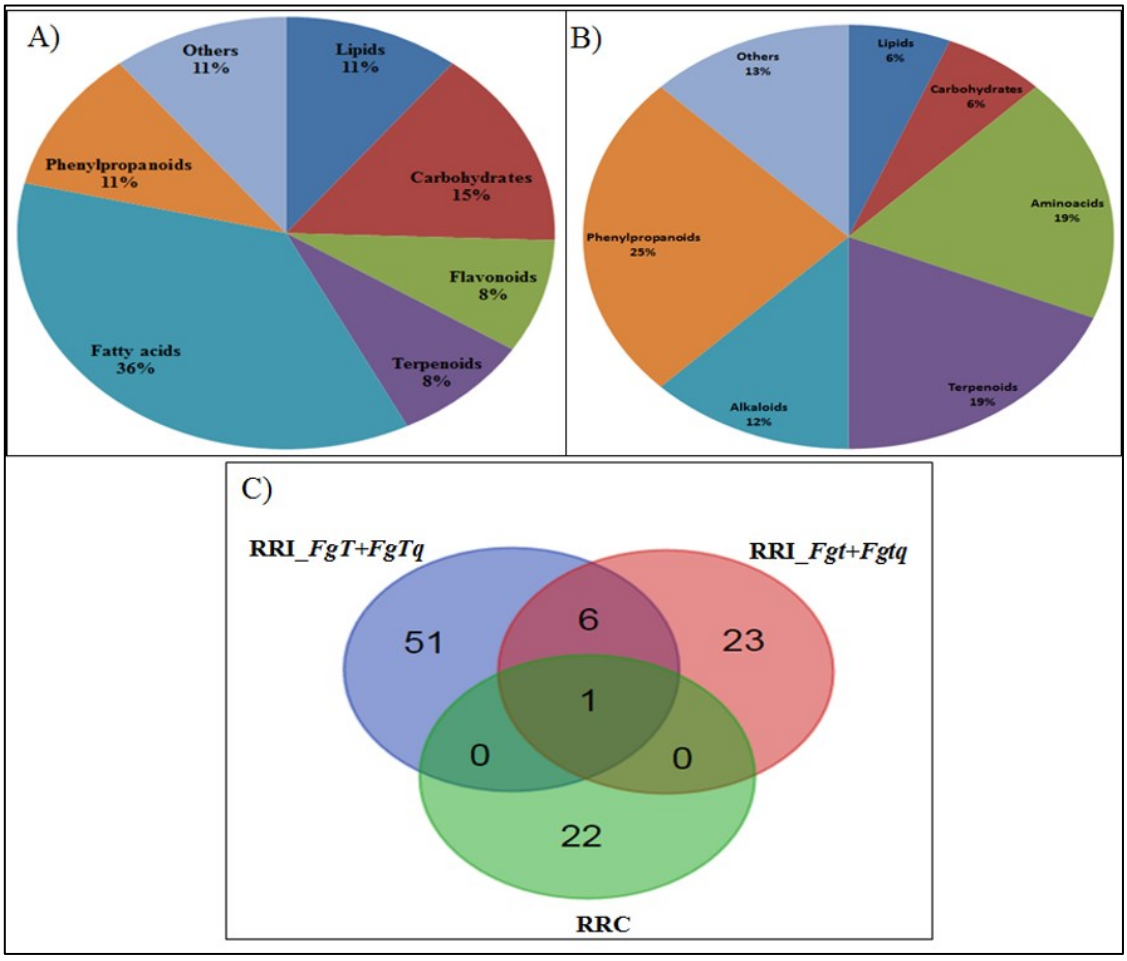

Figure 5.2 The chemical groups of resistant related induced (RRI) metabolites detected in resistant (Sumai3) and susceptible genotypes (Roblin). RRI metabolites accumulated only in Sumai3 upon inoculation of trichothecene producing isolate (*FgT*) and non-producing isolate (*Fgt*) of *F. graminearum* are called as RR_{FgTq} and RR_{Fgtq} respectively. A) RRI metabolites accumulated upon inoculation of trichothecene producing isolate of *F. graminearum* (*FgT*), (B) RRI metabolites accumulated upon inoculation of trichothecene non-producing isolate of *Fg* (*Fgt*), C) A ven diagram showing the classification of identified resistance related induced (RRI), qualitative (not detected in susceptible Roblin) (RR_{FgTq} and RR_{Fgtq}) and RR constitutive (RRC) metabolites following inoculation of *FgT* and *Fgt* isolate.

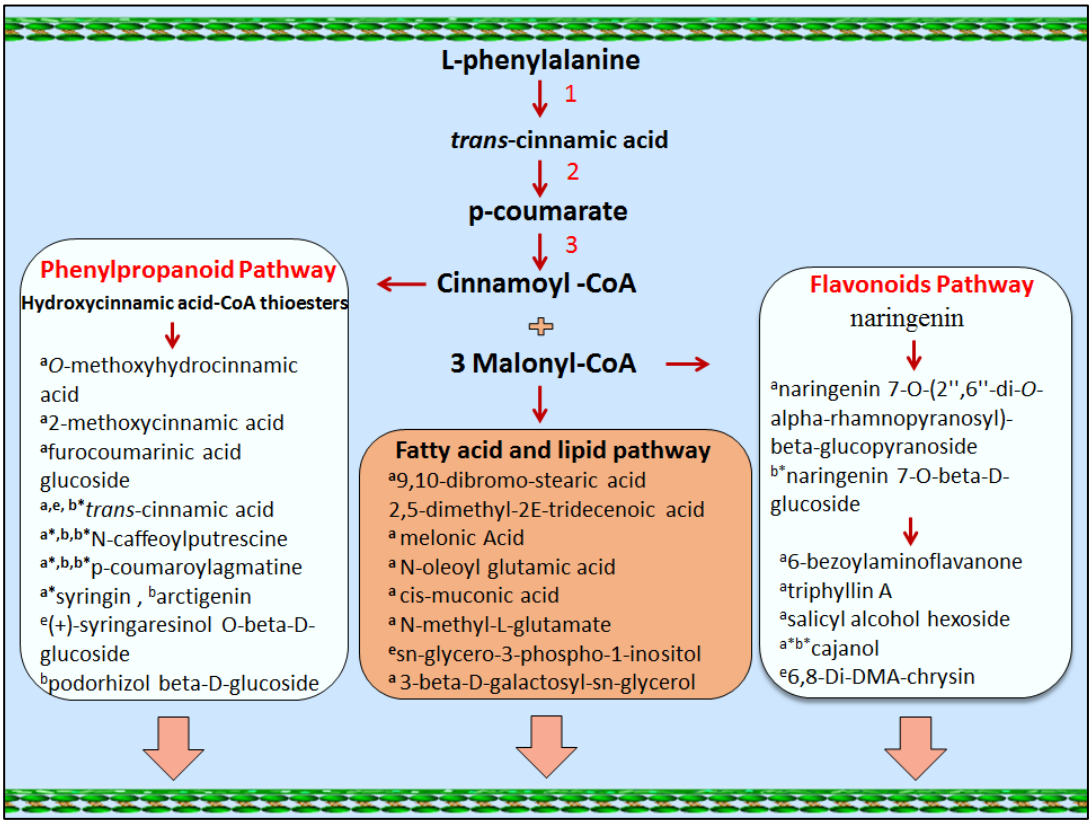

Figure 5.3. Resistant related metabolites mapped to phenylpropanoid, flavonoid, fatty acids and lipids schematic pathways. Where, 1=*phenylalanine ammonia lyase*, 2= *cinnamate 4-hydroxylase*, 3= *4-coumarate:CoA ligase*, a = resistant related induced metabolites upon isolate *FgT* inoculation, a*= resistant related induced metabolites only in *FgT* isolate inoculated spikelets but not in mock, b= resistant related induced metabolites upon isolate *Fgt* inoculation, b* = resistant related induced metabolites only in *Fgt* isolate inoculated spikelets but not in mock and e = resistant related constitutive metabolites.

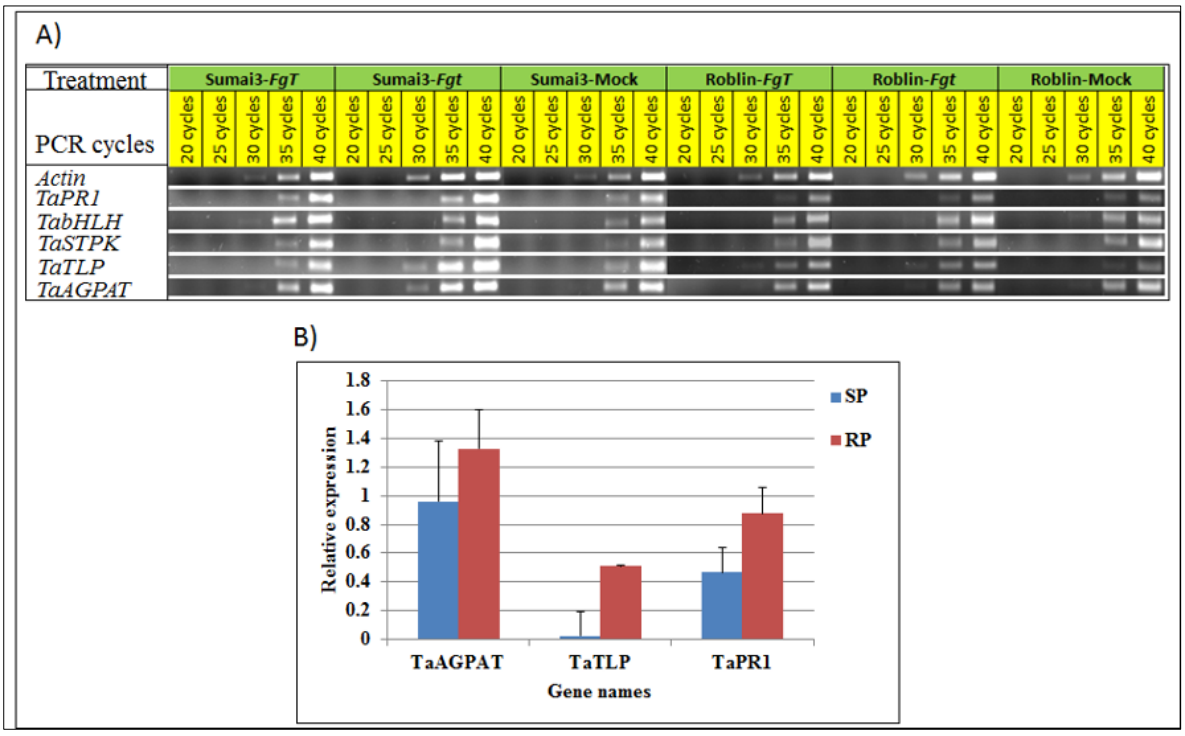

Figure 5.4. Differential expression of host resistance related genes based on semi-quantitative reverse-transcriptase polymerase chain reaction (RT-PCR) and quantitative real time PCR (RT-qPCR), in Sumai3 and Roblin spikelets following *F. graminearum FgT* and *Fgt* isolates, at 72 hpi. A) Quantification of host gene expression levels at different cycles of PCR based on band intensities; B) Relative quantification of host genes transcript accumulation based qRT-PCR. Samples inoculated with sterile water are considered as mock control. Wheat *Actin* gene used as control for amplicons optimization of the test genes like, *TaPR1* (*T. aestivum Pathogenesis related 1*), *TabHLH* (*T. aestivum* basic helix-loop-helix), *TaSTPK* (*T. aestivum* serine threonine protein kinase), *TaTLP* (*T. aestivum* thaumatin-like protein) and *TaAGPAT* (*T. aestivum* acyl-glycerol-3phosphate acyl transferase). Where, RP= resistant genotype (Sumai3) inoculated with *FgT*, SP= susceptible genotype (Roblin) inoculated with *FgT*.

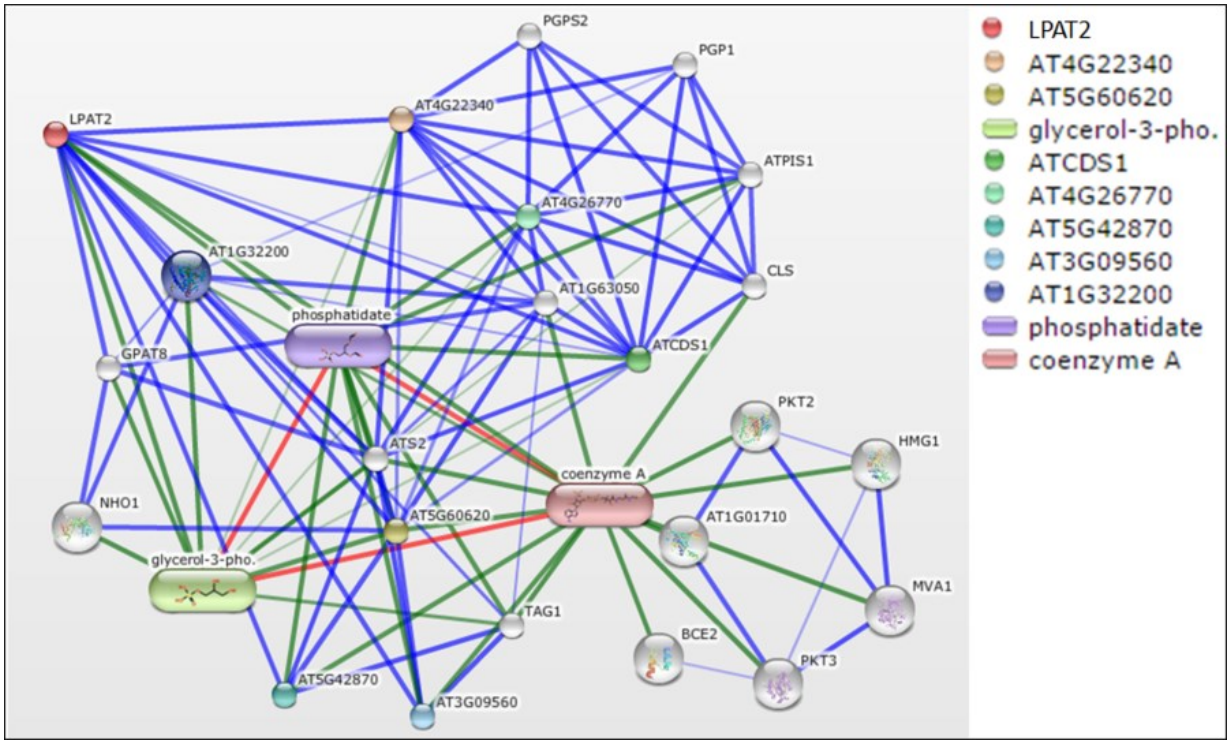

Figure 5.5. *T. aestivum acyl-glycerol-3phosphate acyl transferase* (*TaAGPAT*), orthologous gene (*LPAT2*) from *Arabidopsis thaliana* showing interaction with other host genes and metabolites like, *glycero-phospholipid transferases*, phosphatidate and glycero-phospholipid RR metabolites. The highest scoring interacting partner for *TaAGPAT* is alpha-glycero-phosphate and *phosphatidate cytidyltransferase*. Protein-protein interactions are shown in blue, chemical-protein interactions in green and interactions between chemicals in red.

CHAPTER VI

GENERAL DISCUSSION, SUMMARY AND SUGGESTIONS FOR FUTURE RESEARCH

6.1 General Discussion and Summary

Fusarium head blight (FHB) of wheat also known as wheat scab, is a common disease prevailing in warm humid conditions (Wagacha and Muthomi, 2007). The FHB disease is mainly caused by *Fusarium* species such as *Fusarium graminearum*, *F. culmorum*, *F. avenaceum*, and *F. poae* in small grain cereals like wheat, barley, oats, rye, corn, and triticale (Goswami and Kistler, 2004). FHB is a dreadful disease due drastic reduction in yield and harmful effects of mycotoxins contaminated food grains on human health. The major mycotoxin contaminants biosynthesized by *Fusarium spp*. are deoxynivalenol (DON)/ vomitoxin and NIV belonging to sesquiterpenoid secondary metabolites, known for pathogen aggressiveness (Miedaner et al., 2000). Regulations prevent high levels of mycotoxin contaminated grains to be used for human food products. The United States Department of Agriculture (USDA) and the Canadian Food Inspection Agency (CFIA) accept food grains contaminated with mycotoxins less than one parts per million (ppm). Therefore, controlling the *Fusarium spp*. infection and growing the healthy food grains without the mycotoxin contamination is essential. The best way to mitigate FHB disease is through genetic improvement of cultivars, which can be the major part of an integrated disease management practice in wheat (Bai and Shaner, 2004; Blandino et al., 2012). Among the FHB disease resistant cultivars, Sumai3, has high resistance to disease spread through the rachis compared to spikelet resistance. Several quantitative traits loci (QTL) associated with rachis resistance have been identified in Sumai3 (Bai and Shaner, 2004; Buerstmayr et al., 2009; Liu and Anderson, 2003). However, the genomic complexity of the wheat cultivars and quantitative inheritance of FHB disease are the big impediments to understanding molecular mechanisms involved in the resistance mechanism.

Plants have several mechanisms of resistance against a given pathogen. The mechanisms and the genes responsible for resistance can be better understood if a given genotype has only a few high resistance mechanisms. Accordingly, we chose here wheat near isogenic lines (NILs) with only the alleles varying at one QTL locus. The present study was envisaged to understand the differences in resistance mechanisms in wheat NILs based on metabolo-genomic approach.

A semi-comprehensive metabolic profiling revealed the resistance related (RR) metabolites accumulation following inoculation of Sumai3 and NILs derived from it carrying contrasting alleles for QTL-Fhb5, with *F. graminearum*. The QTL-Fhb5 was initially identified and consistently associated with resistance against spikelet infection in several studies, based on fine mapping of the region from 0.6 cM to 0.3 cM (Lin et al., 2006; Xue et al., 2011; Yang et al., 2005b). Therefore, the current study was oriented towards the dissection of fine mapped QTL-Fhb5 region to identify the possible FHB resistance genes involved and to reveal the RR metabolites biosynthesized by them, following pathogen inoculation. It was hypothesized that the wheat genotypes with the differences in the genomic constitution will also have a difference in metabolic profiles, both constitutive and induced following *F. graminearum* infection. Similarly, the NILs carrying the contrasting alleles for QTL-Fhb5 also have differences in gene nucleotide sequences, expression, and metabolic profiles, both constitutive and induced following spikelet infection by *F.graminearum*. To test this hypothesis, three studies were performed (Chapter III to V). These studies reported that the candidate genes identified from QTL-Fhb5 regulated several RR metabolic pathway enzymes encoding genes responsible for the high accumulation of RR metabolites against FHB in wheat.

The first study (Chapter III) was designed to dissect the QTL-Fhb5 in wheat near-isogenic lines (NILs) derived from Sumai3, along with metabolic profiling, to identify the specific genes and their biosynthetic RR metabolites associated with spikelet resistance. The NILs were inoculated with pathogen or mock and the spikelets collected at 72hpi were used in metabolic profiling. The metabolic profiling of the NILs spikelets showed accumulation of phenylpropanoids and flavonoids along with glycerophospholipids and terpenoids. Plant transcription factors are known to regulate the biosynthesis of plant secondary metabolites (Broun, 2004). The activation tagging of MYB transcription factor led to enhanced biosynthesis phenylpropanoids and flavonoids in Arabidopsis (Borevitz et al., 2000). Interestingly, the dissection of QTL-Fhb5 led to the identification of a novel R2R3 MYB transcription factor (TF) encoding gene known as *TaMYBFhb5* (GenBank: AHZ33834.1). Thus, the transient suppression of *TaMYBFhb5* gene expression was carried out to understand the role of R2R3 MYB TF in FHB resistance. The resistant NIL (R-NIL) and the susceptible NIL (SNIL) significantly varied not only in disease severity and fungal biomass accumulation, but there was also a significant decrease in RR metabolites accumulation after silencing the *TaMYBFhb5* gene and inoculation

of pathogen. Further, the key RR metabolic pathway enzymes encoding genes such as phenylalanine ammonia lyase (*PAL*), agmatine *p*-coumaroyl transferase (*ACT*) and chalcone synthase (*CHS*), which carry R2R3 MYB TF interacting domain in the promoters, were also highly upregulated, confirming the resistance effect of the *TaMYBFhb5* gene. The *TaMYBFhb5* TF is a master switch for regulating the expression of phenylpropanoid and flavonoid pathway key enzymes encoding genes, following *F. graminearum* infection. This study also indicated that plausibly the Sumai3 genotype is responding to pathogen infection by carrying the resistant allele of the *TaMYBFhb5* gene and this may be the most important gene in Sumai3 for both FHB spikelet and rachis resistance.

Consequently, the second study (Chapter IV) was conducted to further validate the resistance function of the novel TF resistance gene, *TaMYBFhb5*, identified from QTL-Fhb5 in Sumai3 genotype, through virus-induced gene silencing (VIGS). The Sumai3 spikelets inoculated with the wild *F. graminearum* macroconidia after silencing the *TaMYBFhb5* gene were profiled for metabolites. There was a decrease in the abundance of RR metabolites and an increase in the fungal biomass following silencing of this genee in Sumai3. Since Sumai3 is a genotype well known for its rachis resistance to spread of infection we also performed gene expression in rachis samples. The rachis sample analysis revealed the suppression of respective metabolic pathway genes such as *CHS* and *ACT* after the transient suppression of *TaMYBFhb5* gene. Further, we observed a drastic increase in DON accumulation after silencing the *TaMYBFhb5* in both spikelets and rachis, which was also associated with high fungal biomass and disease severity. Therefore, *TaMYBFhb5* TF gene was again proved as a master switch for several downstream metabolic pathways enzymes encoding genes. However, the influence of DON during spikelet resistance is largely unknown and hence, understanding the host response against mycotoxin producing (wild) and nonproducing (mutant) *Fusarium spp*. is essential.

Accordingly, the third study (Chapter V) was designed to explore the spikelet resistance mechanism in a highly resistant source genotype Sumai3, used in the Canadian breeding programs, and a moderately susceptible genotype Roblin were inoculated with a wild isolate of pathogen, a mutant isolate of pathogen or mock. The spikelet samples collected at 72hpi were used for metabolic profiling. Here a wild and a mutant pathogen, lacking trichothecene biosynthesis were used because several studies revealed that the mycotoxin, DON acts as a

virulence factor. Thus, we hypothesized these also would vary in their metabolic and genomic profiles, not only in resistant but also in susceptible genotypes. The pathogen-induced RR metabolites were mapped onto the metabolic pathway to trace the major metabolic pathways that biosynthesized RR metabolites, that were responsible for FHB resistance. Interestingly, the phenylpropanoid and flavonoid pathways related metabolites were accumulated in high abundance as reported in earlier studies (Gunnaiah and Kushalappa, 2014; Hamzehzarghani et al., 2005). In addition to these, glycerophospholipids and fatty acids were found only following inoculation of spikelets with the wild isolate of *F. graminearum*. Therefore, the RR metabolites identified in the current study can be used as biomarkers for the FHB resistance. The host genes, such as *T. aestivum* acyl glycerol-3 phosphate acyltransferase (*TaAGPAT*), pathogenesis-related protein1 (*TaPR1*= β-1,3 glucanase) and thaumatin-like protein (*TaTLP*) were significantly expressed. The *TaAGPAT* may be associated with co-regulation host genes and RR metabolites accumulation following *F. graminearum* inoculation, to resist the pathogen. Hence, these genes can be considered as candidates for improving FHB upon functional validation. In conclusion, the Sumai3 genotype showed more resistance to FHB disease through RR metabolites accumulation and suppression of fungal biomass accumulation as compared to Roblin genotype. In conclusion, the *TaMYBFhb5* gene and *R* genes identified in the current study can be used in marker assisted selection (MAS) breeding for FHB resistance in wheat and barley and also, replacing the non-functional alleles of *TaMYBFhb5* gene in susceptible cultivars through genome editing in commercial varieties (Kage et al., 2016; Kushalappa et al., 2016b).

6.2 Suggestions for the Future Research

- Resistance is controlled by hierarchies of genes. We have silenced only the TF and the upstream genes that trigger them and the downstream genes they regulate to eventually biosynthesize RR metabolites that suppress pathogen have to be proved based on individually silencing each candidate gene.
- The effect of candidate RR metabolites on the suppression of *F. graminearum* should be proved. If the resistance is due to cell wall reinforcement then the cell wall thickening and the metabolites that are deposited must be proved.

- The *TaMYBFhb5* gene tagged simple sequence repeats (SSR) markers identified in the current study can be employed for marker assisted breeding for FHB resistance in small grain crops.
- The FHB susceptible commercial wheat cultivars carrying susceptible alleles for *TaMYBFhb5* can be identified and replaced based on advanced genome editing tools.

REFERENCES

Agarwal, M., Shrivastava, N., and Padh, H. (2008). Advances in molecular marker techniques and their applications in plant sciences. *Plant Cell Reports, 27*(4), 617-631.

Al-Taweel, K., Fernando, W. D., and Brule-Babel, A. L. (2014). Transcriptome profiling of wheat differentially expressed genes exposed to different chemotypes of *Fusarium graminearum*. *Theoretical and Applied Genetics, 127*(8), 1703-1718.

Allwood, J. W., Ellis, D. I., Heald, J. K., Goodacre, R., and Mur, L. A. (2006). Metabolomic approaches reveal that phosphatidic and phosphatidyl glycerol phospholipids are major discriminatory non-polar metabolites in responses by Brachypodium distachyon to challenge by Magnaporthe grisea. *The Plant Journal, 46*(3), 351-368.

Alves, M. S., Dadalto, S. P., Goncalves, A. B., De Souza, G. B., Barros, V. A., and Fietto, L. G. (2013). Plant bZIP transcription factors responsive to pathogens: a review. *International Journal of Molecular Sciences, 14*(4), 7815-7828.

Amarasinghe, C., Tittlemier, S., and Fernando, W. (2015). Nivalenol-producing *Fusarium cerealis* associated with Fusarium head blight in winter wheat in Manitoba, Canada. *Plant Pathology, 64*(4), 988-995.

Amarasinghe, C. C., Simsek, S., Brule-Babel, A., and Fernando, W. D. (2016). Analysis of deoxynivalenol and deoxynivalenol-3-glucosides content in Canadian spring wheat cultivars inoculated with *Fusarium graminearum*. *Food Additives & Contaminants: Part A*(just-accepted).

Ambawat, S., Sharma, P., Yadav, N. R., and Yadav, R. C. (2013). MYB transcription factor genes as regulators for plant responses: an overview. *Physiology and Molecular Biology of Plants, 19*(3), 307-321.

Andersen, A. (1948). The development of Gibberella-zeae head blight of wheat. *Phytopathology, 38*(8), 595-611.

Anderson, J. A. (2007). Marker-assisted selection for Fusarium head blight resistance in wheat. *International journal of food microbiology, 119*(1), 51-53.

Anderson, J. A., Stack, R., Liu, S., Waldron, B., Fjeld, A., Coyne, C., . . . Frohberg, R. (2001). DNA markers for Fusarium head blight resistance QTLs in two wheat populations. *TAG Theoretical and Applied Genetics, 102*(8), 1164-1168.

Aoyagi, L. N., Lopes Caitar, V. S., de Carvalho, M. C., Darben, L. M., Polizel-Podanosqui, A., Kuwahara, M. K., . . . Marcelino-Guimarães, F. C. (2014). Genomic and transcriptomic characterization of the transcription factor family R2R3-MYB in soybean and its involvement in the resistance responses to Phakopsora pachyrhizi. *Plant Science, 229*, 32-42.

Atanasova-Penichon, V., Barreau, C., and Richard Forget, F. (2016). Antioxidant Secondary Metabolites in Cereals: Potential Involvement in Resistance to Fusarium and Mycotoxin Accumulation. *Frontiers in Microbiology, 7*.

Aukerman, M. J., and Sakai, H. (2003). Regulation of flowering time and floral organ identity by a microRNA and its APETALA2-like target genes. *The Plant Cell, 15*(11), 2730-2741.

Bae, H. K., and Pestka, J. J. (2008). Deoxynivalenol induces p38 interaction with the ribosome in monocytes and macrophages. *Toxicological Sciences, 105*(1), 59-66.

Bai, G.-H., Desjardins, A., and Plattner, R. (2002). Deoxynivalenol-nonproducing *Fusarium graminearum* causes initial infection, but does not cause DiseaseSpread in wheat spikes. *Mycopathologia, 153*(2), 91-98.

Bai, G., LiFeng, C., Shaner, G., Leonard, K., and Bushnell, W. (2003). Breeding for resistance to Fusarium head blight of wheat in China. *Fusarium head blight of wheat and barley*, 296-317.

Bai, G., and Shaner, G. (1994). Scab of wheat: prospects for control. *Plant Disease, 78*(8), 760-766.

Bai, G., and Shaner, G. (2004). Management and resistance in wheat and barley to Fusarium head blight. [Review]. *Annu Rev Phytopathol, 42*, 135-161.

Balazs, F., and Bagi, F. (1997). Polygalacturonase and cellulase activity of different strains of *Fusarium graminearum*. *Cereal Research Communications*, 725-726.

Barone, A., Chiusano, M. L., Ercolano, M. R., Giuliano, G., Grandillo, S., and Frusciante, L. (2008). Structural and functional genomics of tomato. *International Journal of Plant Genomics, 2008*. 2008:820274. doi: 10.1155/2008/820274.

Bartos, P., Sip, V., Chrpova, J., Vacke, J., Stuchlikova, E., Blazkova, V., . . . Hanzalova, A. (2002). Achievements and prospects of wheat breeding for disease resistance. *Czech Journal of Genetics and Plant Breeding, 38*, 16-28.

Bernardo, A., Bai, G., Guo, P., Xiao, K., Guenzi, A. C., and Ayoubi, P. (2007). *Fusarium graminearum* induced changes in gene expression between Fusarium head blight-resistant and susceptible wheat cultivars. *Functional and Integrative Genomics, 7*(1), 69-77.

Blandino, M., Haidukowski, M., Pascale, M., Plizzari, L., Scudellari, D., and Reyneri, A. (2012). Integrated strategies for the control of Fusarium head blight and deoxynivalenol contamination in winter wheat. *Field Crops Research, 133*, 139-149.

Boddu, J., Cho, S., Kruger, W. M., and Muehlbauer, G. J. (2006). Transcriptome analysis of the barley *Fusarium graminearum* interaction. *Molecular Plant-Microbe Interactions, 19*(4), 407-417.

Bollina, V., Kumaraswamy, G. K., Kushalappa, A. C., Choo, T. M., Dion, Y., Rioux, S., . . . Hamzehzarghani, H. (2010). Mass spectrometry-based metabolomics application to identify quantitative resistance-related metabolites in barley against Fusarium head blight. [Research Support, Non-U.S. Gov't]. *Mol Plant Pathol, 11*(6), 769-782.

Bollina, V., Kushalappa, A. C., Choo, T. M., Dion, Y., and Rioux, S. (2011). Identification of metabolites related to mechanisms of resistance in barley against *Fusarium graminearum*, based on mass spectrometry. *Plant Molecular Biology*, 77(4-5):355-70.

Borevitz, J. O., Xia, Y., Blount, J., Dixon, R. A., and Lamb, C. (2000). Activation tagging identifies a conserved MYB regulator of phenylpropanoid biosynthesis. *The Plant Cell, 12*(12), 2383-2393.

Borrill, P., Connorton, J. M., Balk, J., Miller, A. J., Sanders, D., and Uauy, C. (2014). Biofortification of wheat grain with iron and zinc: integrating novel genomic resources and knowledge from model crops. *From soil to seed: micronutrient movement into and within the plant*, 21;5:53.

Braun, E. L., Dias, A. P., Matulnik, T. J., and Grotewold, E. (2001). Transcription factors and metabolic engineering: novel applications for ancient tools. *Recent Advances in Phytochemistry, 35*, 79-110.

Braun, E. L., and Grotewold, E. (1999). Newly discovered plant c-myb-like genes rewrite the evolution of the plant myb gene family. *Plant Physiology, 121*(1), 21-24.

Bray, E. A. (1997). Plant responses to water deficit. *Trends Plant Sci, 2*(2), 48-54.

Broun, P. (2004). Transcription factors as tools for metabolic engineering in plants. *Current opinion in plant biology, 7*(2), 202-209.

Broun, P., Liu, Y., Queen, E., Schwarz, Y., Abenes, M. L., and Leibman, M. (2006). Importance of transcription factors in the regulation of plant secondary metabolism and their relevance to the control of terpenoid accumulation. *Phytochemistry Reviews, 5*(1), 27-38.

Brown, N. A., Antoniw, J., and Hammond-Kosack, K. E. (2012). The predicted secretome of the plant pathogenic fungus *Fusarium graminearum*: a refined comparative analysis. *PLoS One, 7*(4), e33731.

Buerstmayr, H., Ban, T., and Anderson, J. (2009). QTL mapping and marker-assisted selection for Fusarium head blight resistance in wheat: a review. *Plant breeding, 128*(1), 1-26.

Buerstmayr, H., Steiner, B., Hartl, L., Griesser, M., Angerer, N., Lengauer, D., . . . Lemmens, M. (2003). Molecular mapping of QTLs for Fusarium head blight resistance in spring wheat. II. Resistance to fungal penetration and spread. *TAG Theoretical and Applied Genetics, 107*(3), 503-508.

Buerstmayr, M., and Buerstmayr, H. (2015). Comparative mapping of quantitative trait loci for Fusarium head blight resistance and anther retention in the winter wheat population Capo× Arina. *Theoretical and Applied Genetics, 128*(8), 1519-1530.

Buhrow, L. M., Clark, S. M., and Loewen, M. C. (2016). Identification of an attenuated barley stripe mosaic virus for the virus-induced gene silencing of pathogenesis-related wheat genes. *Plant methods, 12*(1), 1.

Burch-Smith, T. M., Anderson, J. C., Martin, G. B., and Dinesh-Kumar, S. P. (2004). Applications and advantages of virus-induced gene silencing for gene function studies in plants. *The Plant Journal, 39*(5), 734-746.

Burt, C., Steed, A., Gosman, N., Lemmens, M., Bird, N., Ramirez-Gonzalez, R., . . . Nicholson, P. (2015). Mapping a Type 1 FHB resistance on chromosome 4AS of Triticum macha and deployment in combination with two Type 2 resistances. *Theoretical and Applied Genetics, 128*(9), 1725-1738.

Buschges, R., Hollricher, K., Panstruga, R., Simons, G., Wolter, M., Frijters, A., . . . Groenendijk, J. (1997). The barley Mlo gene: a novel control element of plant pathogen resistance. *Cell, 88*(5), 695-705.

Bushnell, W., Perkins-Veazie, P., Russo, V., Collins, J., and Seeland, T. (2010). Effects of deoxynivalenol on content of chloroplast pigments in barley leaf tissues. *Phytopathology, 100*(1), 33-41.

Cai, J. (2016). Meta-analysis of QTL for Fusarium head blight resistance in chinese wheat landraces using genotyping by sequencing. Kansas State University.

Campbell, J., and Huang, L. (2010). Silencing of multiple genes in wheat using Barley stripe mosaic virus. *J Biotech Res, 2*, 12-20.

Campos-Bermudez, V. A., Fauguel, C. M., Tronconi, M. A., Casati, P., Presello, D. A., and Andreo, C. S. (2013). Transcriptional and metabolic changes associated to the infection by *Fusarium verticillioides* in maize inbreds with contrasting ear rot resistance. *PLoS One, 8*(4), e61580.

Cerqueira, N., Ribeiro, J., Fernandes, P., andRamos, M. (2011). vsLab An implementation for virtual high-throughput screening using AutoDock and VMD. *International Journal of Quantum Chemistry, 111*(6), 1208-1212.

Chakrabarti, B., Singh, S., Nagarajan, S., andAggarwal, P. (2011). Impact of temperature on phenology and pollen sterility of wheat varieties. *Australian Journal of Crop Science, 5*(8), 1039.

Chen, J., Griffey, C., Saghai Maroof, M., Stromberg, E., Biyashev, R., Zhao, W., . . . Zeng, Z. (2006). Validation of two major quantitative trait loci for Fusarium head blight resistance in Chinese wheat line W14. *Plant breeding, 125*(1), 99-101.

Chen, P., Liu, W., Yuan, J., Wang, X., Zhou, B., Wang, S., . . . Liu, G. (2005). Development and characterization of wheat-Leymus racemosus translocation lines with resistance to Fusarium head blight. *Theoretical and Applied Genetics, 111*(5), 941-948.

Choura, M., Hanin, M., Rebai, A., and Masmoudi, K. (2016). From FHB Resistance QTLs to Candidate Genes Identification in *Triticum aestivum* L. *Interdisciplinary Sciences: Computational Life Sciences*, 1-5.

Christensen, A. B., Cho, B. H., Næsby, M., Gregersen, P. L., Brandt, J., Madriz-Ordeñana, K., . . . Thordal Christensen, H. (2002). The molecular characterization of two barley proteins establishes the novel PR-17 family of pathogenesis-related proteins. *Mol Plant Pathol, 3*(3), 135-144.

Chu, C., Niu, Z., Zhong, S., Chao, S., Friesen, T. L., Halley, S., . . . Xu, S. S. (2011). Identification and molecular mapping of two QTLs with major effects for resistance to Fusarium head blight in wheat. *Theoretical and Applied Genetics, 123*(7), 1107-1119.

Clasquin, M. F., Melamud, E., and Rabinowitz, J. D. (2012). LC-MS data processing with MAVEN: a metabolomic analysis and visualization engine. *Current Protocols in Bioinformatics*, 14.11. 11-14.11. 23.

Collard, B., Jahufer, M., Brouwer, J., and Pang, E. (2005). An introduction to markers, quantitative trait loci (QTL) mapping and marker-assisted selection for crop improvement: the basic concepts. *Euphytica, 142*(1-2), 169-196.

Collard, B. C., and Mackill, D. J. (2008). Marker-assisted selection: an approach for precision plant breeding in the twenty-first century. *Philosophical Transactions of the Royal Society B: Biological Sciences, 363*(1491), 557-572.

Conrath, U., Pieterse, C. M., and Mauch-Mani, B. (2002). Priming in plant–pathogen interactions. *Trends Plant Sci, 7*(5), 210-216.

Cuperlovic-Culf, M., Wang, L., Forseille, L., Boyle, K., Merkley, N., Burton, I., and Fobert, P. R. (2016). Metabolic Biomarker Panels of Response to Fusarium head blight Infection in Different Wheat Varieties. *PLoS One, 11*(4), e0153642.

Cuthbert, P. A., Somers, D. J., Thomas, J., Cloutier, S., and Brule-Babel, A. (2006). Fine mapping Fhb1, a major gene controlling Fusarium head blight resistance in bread wheat (*Triticum aestivum* L.). *Theoretical and Applied Genetics, 112*(8), 1465-1472.

De Geyter, N., Gholami, A., Goormachtig, S., and Goossens, A. (2012). Transcriptional machineries in jasmonate-elicited plant secondary metabolism. *Trends Plant Sci, 17*(6), 349-359.

De Vos, R. C., Moco, S., Lommen, A., Keurentjes, J. J., Bino, R. J., and Hall, R. D. (2007). Untargeted large-scale plant metabolomics using liquid chromatography coupled to mass spectrometry. *Nature protocols, 2*(4), 778-791.

De Wolf, E., Madden, L., and Lipps, P. (2003). Risk assessment models for wheat Fusarium head blight epidemics based on within-season weather data. *Phytopathology, 93*(4), 428-435.

Deihimi, T., Niazi, A., and Ebrahimie, E. (2013). Identification and expression analysis of TLPs as candidate genes promoting the responses to both biotic and abiotic stresses in wheat.

Deluc, L., Barrieu, F., Marchive, C., Lauvergeat, V., Decendit, A., Richard, T., . . . Hamdi, S. (2006). Characterization of a grapevine R2R3-MYB transcription factor that regulates the phenylpropanoid pathway. *Plant Physiology, 140*(2), 499-511.

Desjardins, A., and Proctor, R. (2007). Molecular biology of Fusarium mycotoxins. *International Journal of Food Microbiology, 119*(1), 47-50.

Desjardins, A. E., and Hohn, T. M. (1997). Mycotoxins in plant pathogenesis. *Molecular Plant-Microbe Interactions, 10*(2), 147-152.

Dhokane, D., Karre, S., Kushalappa, A. C., and McCartney, C. (2016). Integrated Metabolo-Transcriptomics Reveals Fusarium head blight Candidate Resistance Genes in Wheat QTL-Fhb2. *PLoS One, 11*(5), e0155851.

Ding, L., Xu, H., Yi, H., Yang, L., Kong, Z., Zhang, L., . . . Ma, Z. (2011). Resistance to hemi-biotrophic F. graminearum infection is associated with coordinated and ordered expression of diverse defense signaling pathways. [Research Support, Non-U.S. Gov't]. *PLoS One, 6*(4), e19008. doi: 10.1371/journal.pone.0019008

Dixon, J., Braun, H.-J., Kosina, P., and Crouch, J. H. (2009). *Wheat facts and futures 2009*: CIMMYT.

Dixon, R. A., Achnine, L., Kota, P., Liu, C. J., Reddy, M., and Wang, L. (2002). The phenylpropanoid pathway and plant defence-a genomics perspective. *Molecular Plant Pathology, 3*(5), 371-390.

Dixon, R. A., and Harrison, M. J. (1990). Activation, structure, and organization of genes involved in microbial defense in plants. *Advances in Genetics, 28*, 165-234.

Dong, F., Qiu, J., Xu, J., Yu, M., Wang, S., Sun, Y., . . . Shi, J. (2016). Effect of environmental factors on Fusarium population and associated trichothecenes in wheat grain grown in Jiangsu province, China. *International Journal of Food Microbiology, 230*, 58-63.

Doohan, F., Brennan, J., and Cooke, B. (2003). Influence of climatic factors on *Fusarium* species pathogenic to cereals. *European Jouranal of Plant Pathology,* vol 109, Issue 7, pp 755-768.

Draeger, R., Gosman, N., Steed, A., Chandler, E., Thomsett, M., Schondelmaier, J., . . . Mesterhazy, A. (2007). Identification of QTLs for resistance to Fusarium head blight, DON accumulation and associated traits in the winter wheat variety Arina. *Theoretical and Applied Genetics, 115*(5), 617-625.

Dubcovsky, J., and Dvorak, J. (2007). Genome plasticity a key factor in the success of polyploid wheat under domestication. *Science, 316*(5833), 1862-1866.

Dubos, C., Stracke, R., Grotewold, E., Weisshaar, B., Martin, C., and Lepiniec, L. (2010). MYB transcription factors in Arabidopsis. *Trends Plant Sci, 15*(10), 573-581.

Ebrahim, S., Usha, K., and Singh, B. (2011). Pathogenesis related (PR) proteins in plant defense mechanism. *Sci Against Microb Pathog, 2*, 1043-1054.

Edreva, A., Velikova, V., Tsonev, T., Dagnon, S., Gurel, A., Aktaş, L., and Gesheva, E. (2008). Stress-protective role of secondary metabolites: diversity of functions and mechanisms. *Gen Appl Plant Physiol, 34*(1-2), 67-78.

Eulgem, T., Rushton, P. J., Robatzek, S., and Somssich, I. E. (2000). The WRKY superfamily of plant transcription factors. *Trends Plant Sci, 5*(5), 199-206.

Fantini, E., Falcone, G., Frusciante, S., Giliberto, L., and Giuliano, G. (2013). Dissection of tomato lycopene biosynthesis through virus-induced gene silencing. *Plant Physiology, 163*(2), 986-998.

Fattorusso, E., Lanzotti, V., and Taglialatela-Scafati, O. (1999). Antifungal N-feruloyl amides from roots of two Allium species. *Plant Biosystem, 133*(2), 199-203.

Fernie, A. R., and Schauer, N. (2009). Metabolomics assisted breeding: a viable option for crop improvement? *Trends in Genetics, 25*(1), 39-48.

Ferreira, R. B., Monteiro, S., Freitas, R., Santos, C. N., Chen, Z., Batista, L. M., . . . Teixeira, A. R. (2007). The role of plant defence proteins in fungal pathogenesis. *Molecular Plant Pathology, 8*(5), 677-700.

Feuillet, C., Travella, S., Stein, N., Albar, L., Nublat, A., and Keller, B. (2003). Map-based isolation of the leaf rust disease resistance gene Lr10 from the hexaploid wheat (*Triticum aestivum* L.) genome. *Proceedings of the National Academy of Sciences, 100*(25), 15253-15258.

Fiehn, O. (2002). Metabolomics–the link between genotypes and phenotypes. *Plant Molecular Biology, 48*(1-2), 155-171.

Fiehn, O., Kopka, J., Trethewey, R. N., and Willmitzer, L. (2000). Identification of uncommon plant metabolites based on calculation of elemental compositions using gas chromatography and quadrupole mass spectrometry. *Analytical chemistry, 72*(15), 3573-3580.

Foroud, N., Ouellet, T., Laroche, A., Oosterveen, B., Jordan, M., Ellis, B., and Eudes, F. (2012). Differential transcriptome analyses of three wheat genotypes reveal different host response pathways associated with Fusarium head blight and trichothecene resistance. *Plant Pathology, 61*(2), 296-314.

Foroud, N. A., and Eudes, F. (2009). Trichothecenes in cereal grains. *International Journal of Molecular Sciences, 10*(1), 147-173.

Frampton, J., Gibson, T., Ness, S., Doderlein, G., and Graf, T. (1991). Proposed structure for the DNA-binding domain of the Myb oncoprotein based on model building and mutational analysis. *Protein Engineering, 4*(8), 891-901.

Fujita, M., Fujita, Y., Noutoshi, Y., Takahashi, F., Narusaka, Y., Yamaguchi-Shinozaki, K., and Shinozaki, K. (2006). Crosstalk between abiotic and biotic stress responses: a current view from the points of convergence in the stress signaling networks. *Current Opinion in Plant Biology, 9*(4), 436-442.

Gauthier, L., Atanasova-Penichon, V., Chereau, S., and Richard-Forget, F. (2015). Metabolomics to decipher the chemical defense of cereals against *Fusarium graminearum* and deoxynivalenol accumulation. *International Journal of Molecular Sciences, 16*(10), 24839-24872.

Geddes, J., Eudes, F., Laroche, A., and Selinger, L. B. (2008). Differential expression of proteins in response to the interaction between the pathogen *Fusarium graminearum* and its host, Hordeum vulgare. *Proteomics, 8*(3), 545-554.

Gilbert, J., and Tekauz, A. (2000). Review: recent developments in research on Fusarium head blight of wheat in Canada. *Canadian Journal of Plant Pathology, 22*(1), 1-8.

Gill, B. S., Appels, R., Botha-Oberholster, A.-M., Buell, C. R., Bennetzen, J. L., Chalhoub, B., . . . Keller, B. (2004). A workshop report on wheat genome sequencing. *Genetics, 168*(2), 1087-1096.

Gill, K. S., Gill, B. S., Endo, T. R., and Boyko, E. V. (1996). Identification and high-density mapping of gene-rich regions in chromosome group 5 of wheat. *Genetics, 143*(2), 1001-1012.

Gill, K. S., Gill, B. S., Endo, T. R., and Taylor, T. (1996). Identification and high-density mapping of gene-rich regions in chromosome group 1 of wheat. *Genetics, 144*(4), 1883-1891.

Glazier, A. M., Nadeau, J. H., and Aitman, T. J. (2002). Finding genes that underlie complex traits. *Science, 298*(5602), 2345-2349.

Golkari, S., Gilbert, J., Prashar, S., and Procunier, J. D. (2007). Microarray analysis of *Fusarium graminearum* induced wheat genes: identification of organ-specific and differentially expressed genes. *Plant Biotechnology Journal, 5*(1), 38-49.

Goswami, R. S., and Kistler, H. C. (2004). Heading for disaster: *Fusarium graminearum* on cereal crops. *Molecular Plant Pathology, 5*(6), 515-525.

Gottwald, S., Samans, B., Luck, S., and Friedt, W. (2012). Jasmonate and ethylene dependent defence gene expression and suppression of fungal virulence factors: two essential mechanisms of Fusarium head blight resistance in wheat? *BMC Genomics, 13*(1), 369.

Griffey, C. A., Brown-Guedira, G., Liu, S., Murphy, J. P., and Sneller, C. (2012). Characterization and development of FHB resistant soft winter wheat cultivars in the eastern US. Paper presented at the 2008 National Fusarium head blight Forum.

Griffin, H. G., and Griffin, A. M. (1993). DNA sequencing. Applied biochemistry and biotechnology, 38(1-2), 147-159.

Grotewold, E., Drummond, B. J., Bowen, B., and Peterson, T. (1994). The myb-homologous P gene controls phlobaphene pigmentation in maize floral organs by directly activating a flavonoid biosynthetic gene subset. *Cell, 76*(3), 543-553.

Gunnaiah, R., and Kushalappa, A. C. (2014). Metabolomics deciphers the host resistance mechanisms in wheat cultivar Sumai-3, against trichothecene producing and non-producing isolates of *Fusarium graminearum*. *Plant Physiology and Biochemistry, 83*, 40-50.

Gunnaiah, R., Kushalappa, A. C., Duggavathi, R., Fox, S., and Somers, D. J. (2012). Integrated metabolo-proteomic approach to decipher the mechanisms by which wheat QTL (Fhb1) contributes to resistance against *Fusarium graminearum*. *PLoS One, 7*(7), e40695.

Gupta, P., Varshney, R. K., Sharma, P., and Ramesh, B. (1999). Molecular markers and their applications in wheat breeding. *Plant breeding, 118*(5), 369-390.

Hammond-Kosack, K. E., and Jones, J. (1996). Resistance gene-dependent plant defense responses. *The Plant Cell, 8*(10), 1773.

Hamzehzarghani, H., Kushalappa, A., Dion, Y., Rioux, S., Comeau, A., Yaylayan, V., . . . Mather, D. (2005). Metabolic profiling and factor analysis to discriminate quantitative

resistance in wheat cultivars against Fusarium head blight. *Physiological and Molecular Plant Pathology, 66*(4), 119-133. doi: 10.1016/j.pmpp.2005.05.005

Hamzehzarghani, H., Paranidharan, V., Abu-Nada, Y., Kushalappa, A., Mamer, O., and Somers, D. (2008). Metabolic profiling to discriminate wheat near isogenic lines, with quantitative trait loci at chromosome 2DL, varying in resistance to Fusarium head blight. *Canadian Journal of Plant Science, 88*(4), 789-797.

Handa, H., Namiki, N., Xu, D., and Ban, T. (2008). Dissecting of the FHB resistance QTL on the short arm of wheat chromosome 2D using a comparative genomic approach: from QTL to candidate gene. *Molecular Breeding, 22*(1), 71-84. doi: 10.1007/s11032-008-9157-7

Harris, L. J., Balcerzak, M., Johnston, A., Schneiderman, D., and Ouellet, T. (2016). Host-preferential *Fusarium graminearum* gene expression during infection of wheat, barley, and maize. *Fungal Biology, 120*(1), 111-123.

Hawkesford, M. J., Araus, J. L., Park, R., Calderini, D., Miralles, D., Shen, T., . . . Parry, M. A. (2013). Prospects of doubling global wheat yields. *Food and Energy Security, 2*(1), 34-48.

Heim, M. A., Jakoby, M., Werber, M., Martin, C., Weisshaar, B., and Bailey, P. C. (2003). The basic helix–loop–helix transcription factor family in plants: a genome-wide study of protein structure and functional diversity. *Molecular Biology and Evolution, 20*(5), 735-747.

Hieter, P., and Boguski, M. (1997). Functional genomics: it's all how you read it. *Science, 278*(5338), 601-602.

Higo, K., Ugawa, Y., Iwamoto, M., and Higo, H. (1998). PLACE: a database of plant cis-acting regulatory DNA elements. *Nucleic Acids Research, 26*(1), 358-359.

Hirai, M. Y., Klein, M., Fujikawa, Y., Yano, M., Goodenowe, D. B., Yamazaki, Y., . . . Suzuki, H. (2005). Elucidation of gene-to-gene and metabolite-to-gene networks in Arabidopsis by integration of metabolomics and transcriptomics. *Journal of Biological Chemistry, 280*(27), 25590-25595.

Hirai, M. Y., Sugiyama, K., Sawada, Y., Tohge, T., Obayashi, T., Suzuki, A., . . . Aoki, K. (2007). Omics-based identification of Arabidopsis Myb transcription factors regulating aliphatic glucosinolate biosynthesis. *Proceedings of the National Academy of Sciences, 104*(15), 6478-6483.

Holl, J., Vannozzi, A., Czemmel, S., D'Onofrio, C., Walker, A. R., Rausch, T., . . . Bogs, J. (2013). The R2R3-MYB transcription factors MYB14 and MYB15 regulate stilbene biosynthesis in Vitis vinifera. *The Plant Cell, 25*(10), 4135-4149.

Holzberg, S., Brosio, P., Gross, C., and Pogue, G. P. (2002). Barley stripe mosaic virus-induced gene silencing in a monocot plant. *The Plant Journal, 30*(3), 315-327.

Huang, W., Khaldun, A., Lv, H., Du, L., Zhang, C., and Wang, Y. (2016). Isolation and functional characterization of a R2R3-MYB regulator of the anthocyanin biosynthetic pathway from Epimedium sagittatum. *Plant Cell Reports, 35*(4), 883-894.

Humphrey, W., Dalke, A., and Schulten, K. (1996). VMD: visual molecular dynamics. *Journal of Molecular Graphics, 14*(1), 33-38.

Jansen, C., Von Wettstein, D., Schafer, W., Kogel, K.-H., Felk, A., and Maier, F. J. (2005). Infection patterns in barley and wheat spikes inoculated with wild-type and trichodiene synthase gene disrupted *Fusarium graminearum*. *Proceedings of the National Academy of Sciences of the United States of America, 102*(46), 16892-16897.

Jaradat, A. A. (2011). Ecogeography, genetic diversity, and breeding value of wild emmer wheat (*Triticum dicoccoides* Korn ex Asch. & Graebn.) Thell. *Australian Journal of Crop Science, 5*(9), 1072.

Jia, G., Chen, P., Qin, G., Bai, G., Wang, X., Wang, S., . . . Liu, D. (2005). QTLs for Fusarium head blight response in a wheat DH population of Wangshuibai/Alondra‘s’. *Euphytica, 146*(3), 183-191.

Jia, H., Cho, S., and Muehlbauer, G. J. (2009). Transcriptome analysis of a wheat near-isogenic line pair carrying Fusarium head blight-resistant and-susceptible alleles. *Molecular Plant-Microbe Interactions, 22*(11), 1366-1378.

Kage, U., Karre, S., Kushalappa, A. C., and McCartney, C. (2016). Identification and characterization of a Fusarium head blight resistance gene *TaACT* in wheat QTL-2DL. *Plant Biotechnology Journal*. doi: 10.1111/pbi.12641.

Kang, Z., and Buchenauer, H. (1999). Immunocytochemical localization of Fusarium toxins in infected wheat spikes by *Fusarium culmorum*. *Physiological and Molecular Plant Pathology, 55*(5), 275-288.

Kant, R., Sharma, S., and Dasgupta, I. (2015). Virus-Induced Gene Silencing (VIGS) for Functional Genomics in Rice Using Rice tungro bacilliform virus (RTBV) as a Vector. *Plant Gene Silencing: Methods and Protocols*, 201-217.

Keen, N. T. (1999). Plant disease resistance: progress in basic understanding and practical application. *Advances in Botanical Research, 30*, 291-328.

Keller, B., Feuillet, C., and Yahiaoui, N. (2005). Map-based isolation of disease resistance genes from bread wheat: cloning in a supersize genome. *Genetical Research, 85*(02), 93-100.

Kelley, L. A., Mezulis, S., Yates, C. M., Wass, M. N., and Sternberg, M. J. (2015). The Phyre2 web portal for protein modeling, prediction and analysis. *Nature Protocols, 10*(6), 845-858.

Kirigia, D., Runo, S., and Alakonya, A. (2014). A virus-induced gene silencing (VIGS) system for functional genomics in the parasitic plant Striga hermonthica. *Plant methods, 10*(1), 1.

Kitayama, T., and Hatada, K. (2013). *NMR spectroscopy of polymers*: Springer Science & Business Media.

Kondou, Y., Higuchi, M., and Matsui, M. (2010). High-throughput characterization of plant gene functions by using gain-of-function technology. *Annual Review of Plant Biology, 61*, 373-393.

Kosaka, A., Ban, T., and Manickavelu, A. (2015). Genome-wide transcriptional profiling of wheat infected with *Fusarium graminearum*. *Genomics data, 5*, 260-262.

Kosina, P., Reynolds, M., Dixon, J., and Joshi, A. (2007). Stakeholder perception of wheat production constraints, capacity building needs, and research partnerships in developing countries. *Euphytica, 157*(3), 475-483.

Kranz, H. D., Denekamp, M., Greco, R., Jin, H., Leyva, A., Meissner, R. C., . . . Martin, C. (1998). Towards functional characterisation of the members of the R2R3-MYB gene family fromArabidopsis thaliana. *The Plant Journal, 16*(2), 263-276.

Kruger, W. M., Pritsch, C., Chao, S., and Muehlbauer, G. J. (2002). Functional and comparative bioinformatic analysis of expressed genes from wheat spikes infected with *Fusarium graminearum*. *Molecular Plant-Microbe Interactions, 15*(5), 445-455.

Kumar, A., Karre, S., Dhokane, D., Kage, U., Hukkeri, S., and Kushalappa, A. C. (2015). Real-time quantitative PCR based method for the quantification of fungal biomass to

discriminate quantitative resistance in barley and wheat genotypes to Fusarium head blight. *Journal of Cereal Science, 64*, 16-22.

Kumar, A., Yogendra, K. N., Karre, S., Kushalappa, A. C., Dion, Y., and Choo, T. M. (2016). WAX INDUCER1 (HvWIN1) transcription factor regulates free fatty acid biosynthetic genes to reinforce cuticle to resist Fusarium head blight in barley spikelets. *Journal of Experimental Botany*, 67(14):4127-39.

Kumaraswamy, G., Kushalappa, A., Choo, T., Dion, Y., and Rioux, S. (2012). Differential metabolic response of barley genotypes, varying in resistance, to trichothecene-producing and nonproducing (*tri5*$^-$) isolates of *Fusarium graminearum*. *Plant Pathology, 61*(3), 509-521.

Kumaraswamy, G. K., Bollina, V., Kushalappa, A. C., Choo, T. M., Dion, Y., Rioux, S., . . . Faubert, D. (2011a). Metabolomics technology to phenotype resistance in barley against Gibberella zeae. *European Journal of Plant Pathology*, 1-15.

Kumaraswamy, K. G., Kushalappa, A. C., Choo, T. M., Dion, Y., and Rioux, S. (2011b). Mass Spectrometry Based Metabolomics to Identify Potential Biomarkers for Resistance in Barley against Fusarium head blight (*Fusarium graminearum*). *Journal of chemical ecology*, 1-11.

Kushalappa, A. C., and Gunnaiah, R. (2013). Metabolo-proteomics to discover plant biotic stress resistance genes. *Trends Plant Sci, 18*(9), 522-531.

Kushalappa, A. C., Yogendra, K. N., and Karre, S. (2016a). Plant innate immune response: Qualitative and Quantitative resistance. *Critical Reviews in Plant Sciences, 35*(1), 38-55.

Kushalappa, A. C., Yogendra, K. N., Sarkar, K., Kage, U., and Karre, S. (2016b). Gene discovery and genome editing to develop cisgenic crops with improved resistance against pathogen infection. *Canadian Journal of Plant Pathology* (just-accepted).

La Rota, M., and Sorrells, M. E. (2004). Comparative DNA sequence analysis of mapped wheat ESTs reveals the complexity of genome relationships between rice and wheat. *Functional and Integrative Genomics, 4*(1), 34-46.

Lantican, M. A., Braun, H. J., Payne, T. S., Singh, R., Sonder, K., Baum, M., . . . Erenstein, O. (2016). Impacts of international wheat improvement research, 1994-2014.

Lemmens, M., Scholz, U., Berthiller, F., Dall'Asta, C., Koutnik, A., Schuhmacher, R., . . . Krska, R. (2005). The ability to detoxify the mycotoxin deoxynivalenol colocalizes with a major

quantitative trait locus for Fusarium head blight resistance in wheat. *Molecular Plant-Microbe Interactions, 18*(12), 1318-1324.

Li, C., Zhu, H., Zhang, C., Lin, F., Xue, S., Cao, Y., . . . Ma, Z. (2008a). Mapping QTLs associated with Fusarium damaged kernels in the Nanda 2419× Wangshuibai population. *Euphytica, 163*(2), 185-191.

Li, G., and Yen, Y. (2008b). Jasmonate and ethylene signaling pathway may mediate Fusarium head blight resistance in wheat. *Crop Science, 48*(5), 1888-1896.

Lin, F., Xue, S., Zhang, Z., Zhang, C., Kong, Z., Yao, G., . . . Cao, Y. (2006). Mapping QTL associated with resistance to Fusarium head blight in the Nanda2419× Wangshuibai population. II: Type I resistance. *Theoretical and Applied Genetics, 112*(3), 528-535.

Linthorst, H. J., and Van Loon, L. (1991). Pathogenesis-related proteins of plants. *Critical Reviews in Plant Sciences, 10*(2), 123-150.

Lipsick, J. S. (1996). One billion years of Myb. *Oncogene, 13*(2), 223-235.

Lipsick, J. S., and Wang, D.-M. (1999). Transformation by v-Myb. *Oncogene, 18*(19), 3047-3055.

Lisec, J., Schauer, N., Kopka, J., Willmitzer, L., and Fernie, A. R. (2006). Gas chromatography mass spectrometry–based metabolite profiling in plants. *Nature protocols, 1*(1), 387-396.

Liu, S., and Anderson, J. (2003). Marker assisted evaluation of Fusarium head blight resistant wheat germplasm. *Crop Science, 43*(3), 760-766.

Liu, S., Hall, M. D., Griffey, C. A., and McKendry, A. L. (2009). Meta-Analysis of QTL Associated with Fusarium head blight Resistance in Wheat. *Crop Science, 49*(6), 1955. doi: 10.2135/cropsci2009.03.0115

Liu, S., Pumphrey, M., Gill, B., Trick, H., Zhang, J., Dolezel, J., . . . Anderson, J. (2008). Toward positional cloning of Fhb1, a major QTL for Fusarium head blight resistance in wheat. *Cereal Research Communications, 36*(Supplement 6), 195-201.

Liu, S., Zhang, X., Pumphrey, M. O., Stack, R. W., Gill, B. S., and Anderson, J. A. (2006). Complex microcolinearity among wheat, rice, and barley revealed by fine mapping of the genomic region harboring a major QTL for resistance to Fusarium head blight in wheat. *Functional and Integrative Genomics, 6*(2), 83-89.

Liu, Y., Schiff, M., Marathe, R., and Dinesh-Kumar, S. (2002). Tobacco Rar1, EDS1 and NPR1/NIM1 like genes are required for N-mediated resistance to tobacco mosaic virus. *The Plant Journal, 30*(4), 415-429.

Livak, K. J., and Schmittgen, T. D. (2001). Analysis of relative gene expression data using real-time quantitative PCR and the $2^{-\Delta\Delta CT}$ method. M*ethods, 25*(4), 402-408.

Luo, J., Butelli, E., Hill, L., Parr, A., Niggeweg, R., Bailey, P., . . . Martin, C. (2008). *AtMYB12* regulates caffeoyl quinic acid and flavonol synthesis in tomato: expression in fruit results in very high levels of both types of polyphenol. *The Plant Journal, 56*(2), 316-326.

Luongo, D., Severino, L., Bergamo, P., D'Arienzo, R., and Rossi, M. (2010). Trichothecenes NIV and DON modulate the maturation of murine dendritic cells. *Toxicon, 55*(1), 73-80.

Mackintosh, C. A., Lewis, J., Radmer, L. E., Shin, S., Heinen, S. J., Smith, L. A., . . . Kravchenko, S. (2007). Overexpression of defense response genes in transgenic wheat enhances resistance to Fusarium head blight. *Plant Cell Reports, 26*(4), 479-488.

Manmathan, H., Shaner, D., Snelling, J., Tisserat, N., and Lapitan, N. (2013). Virus-induced gene silencing of Arabidopsis thaliana gene homologues in wheat identifies genes conferring improved drought tolerance. *Journal of Experimental Botany, 64*(5), 1381-1392.

Mardi, M., Pazouki, L., Delavar, H., Kazemi, M., Ghareyazie, B., Steiner, B., . . . Buerstmayr, H. (2006). QTL analysis of resistance to Fusarium head blight in wheat using a 'Frontana'-derived population. *Plant Breeding, 125*(4), 313-317.

Marza, F., Bai, G.-H., Carver, B., and Zhou, W.-C. (2006). Quantitative trait loci for yield and related traits in the wheat population Ning7840× Clark. *Theoretical and Applied Genetics, 112*(4), 688-698.

Matny, O. N. (2015). Fusarium head blight and crown rot on wheat & barley: losses and health risks. *Adv Plants Agric Res, 2*(1), 00039.

McCartney, C. A., Brule-Babel, A. L., Fedak, G., Martin, R. A., McCallum, B. D., Gilbert, J., . . . Pozniak, C. J. (2016). Fusarium head blight resistance QTL in the spring wheat cross Kenyon/86ISMN 2137. *Frontiers in Microbiology, 7*, 1542.

McCough, S. R., and Doerge, R. W. (1995). QTL mapping in rice. *Trends in Genetics, 11*(12), 482-487.

McMullen, M., Jones, R., and Gallenberg, D. (1997). Scab of wheat and barley: a re-emerging disease of devastating impact. *Plant disease, 81*(12), 1340-1348.

McMullen, M., Leonard, K., and Bushnell, W. (2003). Impacts of Fusarium head blight on the North American agricultural community: the power of one disease to catapult change. *Fusarium head blight of wheat and barley*, 484-503.

Mellway, R. D., Tran, L. T., Prouse, M. B., Campbell, M. M., and Constabel, C. P. (2009). The wound-, pathogen-, and ultraviolet B-responsive MYB134 gene encodes an R2R3 MYB transcription factor that regulates proanthocyanidin synthesis in poplar. *Plant Physiology, 150*(2), 924-941.

Mengiste, T., Chen, X., Salmeron, J., and Dietrich, R. (2003). The BOTRYTIS SUSCEPTIBLE1 gene encodes an R2R3MYB transcription factor protein that is required for biotic and abiotic stress responses in Arabidopsis. *The Plant Cell, 15*(11), 2551-2565.

Mesterhazy, A. (1989). Progress in breeding of wheat and corn genotypes not susceptible to infection by fusaria. *Topics in Secondary Metabolism (Netherlands)*.

Mesterhazy, A. (1995). Types and components of resistance to Fusarium head blight of wheat. *Plant Breeding, 114*(5), 377-386.

Mesterhazy, A. (1997). Methodology of resistance testing and breeding against Fusarium head blight in wheat and results of the selection. *Cereal Research Communications*, 631-637.

Mesterhazy, A., Bartók, T., Kászonyi, G., Varga, M., Tóth, B., and Varga, J. (2005). Common resistance to different *Fusarium* spp. causing Fusarium head blight in wheat. *European Journal of Plant Pathology, 112*(3), 267-281.

Miedaner, T. (1997). Breeding wheat and rye for resistance to Fusarium diseases. *Plant breeding, 116*(3), 201-220.

Miedaner, T., Gang, G., Schilling, A., and Geiger, H. (1997). Aggressiveness and mycotoxin production of populations of *Fusarium culmorum* and *Fusarium graminearum* in winter rye. *Cereal Research Communications*, 471-475.

Miedaner, T., Reinbrecht, C., and Schilling, A. G. (2000). Association among aggressiveness, fungal colonization, and mycotoxin production of 26 isolates of *Fusarium graminearum* in winter rye head blight/Beziehung zwischen Aggressivität, Myzelwachstum und Mykotoxinproduktion von 26 *Fusarium graminearum* Isolaten bei der hrenfusariose des

Winterroggens. *Zeitschrift für Pflanzenkrankheiten und Pflanzenschutz/Journal of Plant Diseases and Protection*, 124-134.

Miedaner, T., Wilde, F., Steiner, B., Buerstmayr, H., Korzun, V., and Ebmeyer, E. (2006). Stacking quantitative trait loci (QTL) for Fusarium head blight resistance from non-adapted sources in an European elite spring wheat background and assessing their effects on deoxynivalenol (DON) content and disease severity. *Theoretical and Applied Genetics, 112*(3), 562-569.

Miller, Young, and Sampson. (1985). Deoxynivalenol and Fusarium head blight resistance in spring cereals. *Journal of phytopathology, 113*(4), 359-367.

Mirocha, C., Yu, H., Evans, C., Kolaczkowski, E., and Dillmacky, R. (1997). Chemistry and physiology of deoxynivalenol in pathogenesis. *Cereal Research Communications*, 309-313.

Moco, S., Bino, R. J., Vorst, O., Verhoeven, H. A., de Groot, J., van Beek, T. A., . . . De Vos, C. R. (2006). A liquid chromatography-mass spectrometry-based metabolome database for tomato. *Plant Physiology, 141*(4), 1205-1218.

Munteanu, M. G., Vlahovicek, K., Parthasarathy, S., Simon, I., and Pongor, S. (1998). Rod models of DNA: sequence-dependent anisotropic elastic modelling of local bending phenomena. *Trends in Biochemical Sciences, 23*(9), 341-347.

Murray, M., and Thompson, W. F. (1980). Rapid isolation of high molecular weight plant DNA. *Nucleic acids research, 8*(19), 4321-4326.

Muthomi, J., Oerke, E. C., Dehne, H. W., and Mutitu, E. (2002). Susceptibility of Kenyan wheat varieties to head blight, fungal invasion and deoxynivalenol accumulation inoculated with *Fusarium graminearum*. *Journal of Phytopathology, 150*(1), 30-36.

Muthukrishnan, S., Liang, G. H., Trick, H. N., and Gill, B. S. (2001). Pathogenesis-related proteins and their genes in cereals. *Plant Cell, Tissue and Organ Culture, 64*(2-3), 93-114.

Nakazawa, M., Ichikawa, T., Ishikawa, A., Kobayashi, H., Tsuhara, Y., Kawashima, M., . . . Matsui, M. (2003). Activation tagging, a novel tool to dissect the functions of a gene family. *The Plant Journal, 34*(5), 741-750.

Naz, A. A., Kunert, A., Flath, K., Pillen, K., and Léon, J. (2012). Advanced backcross quantitative trait locus analysis in winter wheat: dissection of stripe rust seedling

resistance and identification of favorable exotic alleles originated from a primary hexaploid wheat (Triticum turgidum ssp. dicoccoides× Aegilops tauschii). *Molecular Breeding, 30*(2), 1219-1229.

Nicolli, C. P., Spolti, P., Tibola, C. S., Fernandes, J. M. C., and Del Ponte, E. M. (2015). Fusarium head blight and trichothecene production in wheat by *Fusarium graminearum* and F. meridionale applied alone or in mixture at post-flowering. *Tropical Plant Pathology, 40*(2), 134-140.

Nie, L., Vázquez, A. E., and Yamoah, E. N. (2009). Identification of Transcription Factor–DNA Interactions Using Chromatin Immunoprecipitation Assays. *Auditory and Vestibular Research: Methods and Protocols*, 311-322.

Nishiuchi, T., Masuda, D., Nakashita, H., Ichimura, K., Shinozaki, K., Yoshida, S., . . . Yamaguchi, K. (2006). Fusarium phytotoxin trichothecenes have an elicitor-like activity in Arabidopsis thaliana, but the activity differed significantly among their molecular species. *Molecular Plant-Microbe Interactions, 19*(5), 512-520.

Niwa, S., Kubo, K., Lewis, J., Kikuchi, R., Alagu, M., and Ban, T. (2014). Variations for Fusarium head blight resistance associated with genomic diversity in different sources of the resistant wheat cultivar 'Sumai 3'. *Breeding Science, 64*(1), 90.

Oliveira, M., Varanda, C., and Félix, M. (2016). Induced resistance during the interaction pathogen x plant and the use of resistance inducers. *Phytochemistry Letters, 15*, 152-158.

Onkokesung, N., Gaquerel, E., Kotkar, H., Kaur, H., Baldwin, I. T., and Galis, I. (2012). MYB8 controls inducible phenolamide levels by activating three novel hydroxycinnamoyl-coenzyme A: polyamine transferases in Nicotiana attenuata. *Plant Physiology, 158*(1), 389-407.

Osborne, L. E., and Stein, J. M. (2007). Epidemiology of Fusarium head blight on small-grain cereals. *International journal of food microbiology, 119*(1), 103-108.

Ostergaard, L., and Yanofsky, M. F. (2004). Establishing gene function by mutagenesis in Arabidopsis thaliana. *The Plant Journal, 39*(5), 682-696.

Paranidharan, V., Abu-Nada, Y., Hamzehzarghani, H., Kushalappa, A., Mamer, O., Dion, Y., . . . Choiniere, L. (2008). Resistance-related metabolites in wheat against *Fusarium graminearum* and the virulence factor deoxynivalenol (DON). *Botany, 86*(10), 1168-1179.

Parry, D., Jenkinson, P., and McLeod, L. (1995). Fusarium ear blight (scab) in small grain cereals-a review. *Plant Pathology, 44*(2), 207-238.

Peng, X., Liu, H., Wang, D., and Shen, S. (2016). Genome-wide identification of the Jatropha curcas MYB family and functional analysis of the abiotic stress responsive gene *JcMYB2*. *BMC Genomics, 17*(1), 1.

Pestka, J. J., and Smolinski, A. T. (2005). Deoxynivalenol: toxicology and potential effects on humans. *Journal of Toxicology and Environmental Health, Part B, 8*(1), 39-69.

Petersen, G., Seberg, O., Yde, M., and Berthelsen, K. (2006). Phylogenetic relationships of Triticum and Aegilops and evidence for the origin of the A, B, and D genomes of common wheat (*Triticum aestivum*). *Molecular phylogenetics and evolution, 39*(1), 70-82.

Piques, M., Schulze, W. X., Höhne, M., Usadel, B., Gibon, Y., Rohwer, J., and Stitt, M. (2009). Ribosome and transcript copy numbers, polysome occupancy and enzyme dynamics in Arabidopsis. *Molecular Systems Biology, 5*(1), 314.

Pireyre, M., and Burow, M. (2015). Regulation of MYB and bHLH transcription factors: a glance at the protein level. *Molecular Plant, 8*(3), 378-388.

Pluskal, T., Castillo, S., Villar-Briones, A., and Oresic, M. (2010). MZmine 2: modular framework for processing, visualizing, and analyzing mass spectrometry-based molecular profile data. *BMC Bioinformatics, 11*(1), 395.

Poppenberger, B., Berthiller, F., Lucyshyn, D., Sieberer, T., Schuhmacher, R., Krska, R., . . . Adam, G. (2003). Detoxification of the Fusarium mycotoxin deoxynivalenol by a *UDP-glucosyltransferase* from Arabidopsis thaliana. *Journal of Biological Chemistry, 278*(48), 47905-47914.

Pritsch, C., Muehlbauer, G. J., Bushnell, W. R., Somers, D. A., and Vance, C. P. (2000). Fungal development and induction of defense response genes during early infection of wheat spikes by *Fusarium graminearum*. *Molecular Plant-Microbe Interactions, 13*(2), 159-169.

Proctor, R. H., Hohn, T. M., and McCormick, S. P. (1995). Reduced virulence of Gibberella zeae caused by disruption of a trichthecine toxin biosynthetic gene. *MPMI-Molecular Plant Microbe Interactions, 8*(4), 593-601.

Qi, P.-F., Balcerzak, M., Rocheleau, H., Leung, W., Wei, Y.-M., Zheng, Y.-L., and Ouellet, T. (2016). Jasmonic acid and abscisic acid play important roles in host–pathogen interaction between *Fusarium graminearum* and wheat during the early stages of Fusarium head blight. *Physiological and Molecular Plant Pathology, 93*, 39-48.

Quarrie, S., Quarrie, S. P., Radosevic, R., Rancic, D., Kaminska, A., Barnes, J., . . . Dodig, D. (2006). Dissecting a wheat QTL for yield present in a range of environments: from the QTL to candidate genes. *Journal of Experimental Botany, 57*(11), 2627-2637.

Ramegowda, V., Senthil-Kumar, M., Udayakumar, M., and Mysore, K. S. (2013). A high-throughput virus-induced gene silencing protocol identifies genes involved in multi-stress tolerance. *BMC Plant Biology, 13*(1), 1.

Rawat, N., Pumphrey, M., Liu, S., Zhang, X., Tiwari, V., Ando, K.,….Gill, B (2016). Wheat Fhb1 encodes a chimeric lectin with agglutinin domains and a pore-forming toxin-like domain conferring resistance to Fusarium head blight. Nature Genetics, doi:10.1038/ng.3706.

Razdan, V., and Sabitha, M. (2009). Integrated disease management: Concepts and practices *Integrated Pest Management: Innovation-Development Process* (pp. 369-389): Springer.

Riechmann, J. L., Heard, J., Martin, G., Reuber, L., Jiang, C. Z., Keddie, J., . . . Samaha, R. (2000). Arabidopsis transcription factors: genome wide comparative analysis among eukaryotes. *Science, 290*(5499), 2105-2110.

Rischer, H., and Oksman-Caldentey, K. M. (2006). Unintended effects in genetically modified crops: revealed by metabolomics? *Trends in biotechnology, 24*(3), 102-104.

Rocha, O., Ansari, K., and Doohan, F. (2005). Effects of trichothecene mycotoxins on eukaryotic cells: a review. *Food Additives and Contaminants, 22*(4), 369-378.

Rosinski, J. A., and Atchley, W. R. (1998). Molecular evolution of the Myb family of transcription factors: evidence for polyphyletic origin. *Journal of Molecular Evolution, 46*(1), 74-83.

Rossi, V., Ravanetti, A., Pattori, E., and Giosue, S. (2001). Influence of temperature and humidity on the infection of wheat spikes by some fungi causing Fusarium head blight. *Journal of Plant Pathology*, 189-198.

Sadeghi, M., Zolfaghari, B., Senatore, M., and Lanzotti, V. (2013). Antifungal cinnamic acid derivatives from Persian leek (*Allium ampeloprasum* Subsp. Persicum). *Phytochemistry Letters*.

Sarma, R., Fish, L., Gill, B., and Snape, J. (2000). Physical characterization of the homoeologous Group 5 chromosomes of wheat in terms of rice linkage blocks, and physical mapping of some important genes. *Genome, 43*(1), 191-198.

Saucedo-Garcia, M., Gavilanes Ruiz, M., and Arce-Cervantes, O. (2015). Long-chain bases, phosphatidic acid, MAPKs, and reactive oxygen species as nodal signal transducers in stress responses in Arabidopsis. *Frontiers in Plant Science, 6*.

Schmale, D., and Bergstrom, G. (2003). Fusarium head blight in wheat. *The Plant Health Instructor*, 612.

Schmidt, M., Horstmann, S., De Colli, L., Danaher, M., Speer, K., Zannini, E., and Arendt, E. K. (2016). Impact of fungal contamination of wheat on grain quality criteria. *Journal of Cereal Science, 69*, 95-103.

Schrodinger, L. (2015). The PyMOL molecular graphics system, version 1.3 r1. 2010. *There is no corresponding record for this reference*.

Schroeder H.W., Christensen J. (1963) Factors affecting resistance of wheat to scab caused by *Gibberella zeae* (Schw.) Petch. Phytopathology. 53:831-838.

Schweiger, W., Steiner, B., Ametz, C., Siegwart, G., Wiesenberger, G., Berthiller, F., . . . Muehlbauer, G. J. (2013). Transcriptomic characterization of two major Fusarium resistance quantitative trait loci (QTLs), Fhb1 and *Qfhs.ifa-5A*, identifies novel candidate genes. *Molecular Plant Pathology, 14*(8), 772-785.

Schweiger, W., Steiner, B., Vautrin, S., Nussbaumer, T., Siegwart, G., Zamini, M., . . . Mayer, K. (2016). Suppressed recombination and unique candidate genes in the divergent haplotype encoding Fhb1, a major Fusarium head blight resistance locus in wheat. *Theoretical and Applied Genetics*, 1-17.

Scofield, S. R., and Brandt, A. S. (2012). Virus-induced gene silencing in hexaploid wheat using barley stripe mosaic virus vectors. *Antiviral Resistance in Plants: Methods and Protocols*, 93-112.

Scofield, S. R., Huang, L., Brandt, A. S., and Gill, B. S. (2005). Development of a virus-induced gene-silencing system for hexaploid wheat and its use in functional analysis of the Lr21-mediated leaf rust resistance pathway. *Plant Physiology, 138*(4), 2165-2173.

Senthil-Kumar, M., and Mysore, K. S. (2011). New dimensions for VIGS in plant functional genomics. *Trends Plant Sci, 16*(12), 656-665.

Shan, T., Rong, W., Xu, H., Du, L., Liu, X., and Zhang, Z. (2016). The wheat R2R3-MYB transcription factor TaRIM1 participates in resistance response against the pathogen Rhizoctonia cerealis infection through regulating defense genes. *Scientific Reports, 6*.

Shaner, G., and Buechley, G. (2003). *Control of Fusarium head blight with fungicide in Indiana.* Paper presented at the Natl. Fusarium head blight Forum Proc. Bloomington, MN.

Sharma, A., and Chauhan, R. S. (2012). In silico identification and comparative genomics of candidate genes involved in biosynthesis and accumulation of seed oil in plants. *Comparative and Functional Genomics, 2012*.

Shih, C.-H., Chu, I. K., Yip, W. K., and Lo, C. (2006). Differential expression of two flavonoid 3′-hydroxylase cDNAs involved in biosynthesis of anthocyanin pigments and 3-deoxyanthocyanidin phytoalexins in sorghum. *Plant and Cell Physiology, 47*(10), 1412-1419.

Singh, K. B., Foley, R. C., and Onate-Sánchez, L. (2002). Transcription factors in plant defense and stress responses. *Current Opinion in Plant Biology, 5*(5), 430-436.

Siranidou, E., Kang, Z., and Buchenauer, H. (2002). Studies on symptom development, phenolic compounds and morphological defence responses in wheat cultivars differing in resistance to Fusarium head blight. *Journal of Phytopathology, 150*(4-5), 200-208.

Sobrova, P., Adam, V., Vasatkova, A., Beklova, M., Zeman, L., and Kizek, R. (2010). Deoxynivalenol and its toxicity. *Interdisciplinary Toxicology, 3*(3), 94.

Somers, D. J., Fedak, G., and Savard, M. (2003). Molecular mapping of novel genes controlling Fusarium head blight resistance and deoxynivalenol accumulation in spring wheat. *Genome, 46*(4), 555-564. doi: 10.1139/g03-033

Somers, D. J., Thomas, J., DePauw, R., Fox, S., Humphreys, G., and Fedak, G. (2005). Assembling complex genotypes to resist Fusarium in wheat (*Triticum aestivum* L.). *TAG Theoretical and Applied Genetics, 111*(8), 1623-1631.

Somssich, I. E., and Hahlbrock, K. (1998). Pathogen defence in plants—a paradigm of biological complexity. *Trends Plant Sci, 3*(3), 86-90.

Sourdille, P., Singh, S., Cadalen, T., Brown-Guedira, G. L., Gay, G., Qi, L., . . . Bernard, M. (2004). Microsatellite-based deletion bin system for the establishment of genetic-physical map relationships in wheat (*Triticum aestivum* L.). *Functional and Integrative Genomics, 4*(1), 12-25.

Stack, R. (2000). Return of an Old Problem: Fusarium head blight of Small Grains. *Plant Health Progress*.

Stadhouders, R., Den Heuvel, V., Van, A., Kolovos, P., Jorna, R., Leslie, K., . . . Soler, E. (2012). Transcription regulation by distal enhancers. *Transcription (2154-1264), 3*(4).

Steiner, B., Kurz, H., Lemmens, M., and Buerstmayr, H. (2009). Differential gene expression of related wheat lines with contrasting levels of head blight resistance after *Fusarium graminearum* inoculation. *Theoretical and Applied Genetics, 118*(4), 753-764.

Steiner, B., Lemmens, M., Griesser, M., Scholz, U., Schondelmaier, J., and Buerstmayr, H. (2004). Molecular mapping of resistance to Fusarium head blight in the spring wheat cultivar Frontana. *Theoretical and Applied Genetics, 109*(1), 215-224.

Stoskopf, N. C. 1985. Cereal grain crops. Reston Publishing Co., Inc. Prentice-Hall, Reston, VA. 516p

Stracke, R., Werber, M., and Weisshaar, B. (2001). The R2R3-MYB gene family in Arabidopsis thaliana. *Current opinion in plant biology, 4*(5), 447-456.

Sun, J., Ohm, H. W., Poland, J. A., and Williams, C. E. (2016). Mapping Four Quantitative Trait Loci Associated with Type I Fusarium head blight Resistance in Winter Wheat 'INW0412'. *Crop Science, 56*(3), 1163-1172.

Sutton, J. (1982). Epidemiology of wheat head blight and maize ear rot caused by *Fusarium graminearum*. *Canadian Journal of Plant Pathology, 4*(2), 195-209.

Suzuki, T., Sato, M., and Takeuchi, T. (2012). Evaluation of the effects of five QTL regions on Fusarium head blight resistance and agronomic traits in spring wheat (*Triticum aestivum* L.). *Breeding Science, 62*(1), 11.

Sverdlov, E., and Azhikina, T. (2005). Primer Walking. *eLS*. doi: 10.1038/npg.els.0005382

Tamburic-Ilincic, L., Wragg, A., and Schaafsma, A. (2015). Mycotoxin accumulation and *Fusarium graminearum* chemotype diversity in winter wheat grown in southwestern Ontario. *Canadian Journal of Plant Science, 95*(5), 931-938.

Tautenhahn, R., Böttcher, C., and Neumann, S. (2007). Annotation of LC/ESI-MS mass signals *Bioinformatics Research and Development* (pp. 371-380): Springer.

Tekauz, A., McCallum, B., Ames, N., and Fetch, J. M. (2004). Fusarium head blight of oat—current status in western Canada. *Canadian Journal of Plant Pathology, 26*(4), 473-479.

Tohge, T., and Fernie, A. R. (2010). Combining genetic diversity, informatics and metabolomics to facilitate annotation of plant gene function. *Nature Protocols, 5*(6), 1210-1227.

Tohge, T., Nishiyama, Y., Hirai, M. Y., Yano, M., Nakajima, J. i., Awazuhara, M., . . . Kitayama, M. (2005). Functional genomics by integrated analysis of metabolome and transcriptome of Arabidopsis plants over-expressing an MYB transcription factor. *The Plant Journal, 42*(2), 218-235.

Tolstikov, V. V., Lommen, A., Nakanishi, K., Tanaka, N., and Fiehn, O. (2003). Monolithic silica-based capillary reversed-phase liquid chromatography/electrospray mass spectrometry for plant metabolomics. *Analytical Chemistry, 75*(23), 6737-6740.

Touati-Hattab, S., Barreau, C., Verdal-Bonnin, M. N., Chereau, S., Richard-Forget, F., Hadjout, S., . . . Bouznad, Z. (2016). Pathogenicity and trichothecenes production of *Fusarium culmorum* strains causing head blight on wheat and evaluation of resistance of the varieties cultivated in Algeria. *European Journal of Plant Pathology*, 1-18.

Tuszynska, I., Magnus, M., Jonak, K., Dawson, W., and Bujnicki, J. M. (2015). NPDock: a web server for protein–nucleic acid docking. *Nucleic Acids Research*, gkv493.

Van Eck, L., Schultz, T., Leach, J. E., Scofield, S. R., Peairs, F. B., Botha, A. M., and Lapitan, N. L. (2010). Virus-induced gene silencing of WRKY53 and an inducible phenylalanine ammonia-lyase in wheat reduces aphid resistance. *Plant Biotechnology Journal, 8*(9), 1023-1032.

Van Loon, L. C., Rep, M., and Pieterse, C. (2006). Significance of inducible defense-related proteins in infected plants. *Annu. Rev. Phytopathol., 44*, 135-162.

Varallyay, E., Giczey, G., and Burgyan, J. (2012). Virus-induced gene silencing of Mlo genes induces powdery mildew resistance in *Triticum aestivum*. *Archives of Virology, 157*(7), 1345-1350.

Varshney, G. K., and Burgess, S. M. (2016). DNA-guided genome editing using structure-guided endonucleases. *Genome Biology, 17*(1), 187.

Velu, G., Ortiz-Monasterio, I., Cakmak, I., Hao, Y., and Singh, R. (2014). Biofortification strategies to increase grain zinc and iron concentrations in wheat. *Journal of Cereal Science, 59*(3), 365-372.

Velu, G., Singh, R., Huerta-Espino, J., Pena, R., Arun, B., Mahendru-Singh, A., . . . Crossa, J. (2012). Performance of biofortified spring wheat genotypes in target environments for grain zinc and iron concentrations. *Field Crops Research, 137*, 261-267.

Vitulo, N., Albiero, A., Forcato, C., Campagna, D., Dal Pero, F., Bagnaresi, P., . . . Šimková, H. (2011). First survey of the wheat chromosome 5A composition through a next generation sequencing approach. *PLoS One, 6*(10), e26421.

Vom Endt, D., Kijne, J. W., and Memelink, J. (2002). Transcription factors controlling plant secondary metabolism: what regulates the regulators? *Phytochemistry, 61*(2), 107-114.

Von Ropenack, E., Parr, A., and Schulze-Lefert, P. (1998). Structural analyses and dynamics of soluble and cell wall-bound phenolics in a broad spectrum resistance to the powdery mildew fungus in barley. *Journal of Biological Chemistry, 273*(15), 9013-9022.

Voss, H., Wiemann, S., Grothues, D., Sensen, C., Zimmermann, J., Schwager, C., . . . Ansorge, W. (1993). Automated low-redundancy large-scale DNA sequencing by primer walking. *Biotechniques, 15*(4), 714-721.

Wagacha, J., and Muthomi, J. (2007). *Fusarium culmorum*: Infection process, mechanisms of mycotoxin production and their role in pathogenesis in wheat. *Crop Protection, 26*(7), 877-885.

Walters, D., Meurer-Grimes, B., and Rovira, I. (2001). Antifungal activity of three spermidine conjugates. *FEMS Microbiology Letters, 201*(2), 255-258.

Wang, H., Wang, H., Shao, H., and Tang, X. (2016). Recent Advances in Utilizing Transcription Factors to Improve Plant Abiotic Stress Tolerance by Transgenic Technology. *Frontiers in Plant Science, 7*.

Wang, H., Wijeratne, A., Wijeratne, S., Lee, S., Taylor, C. G., St Martin, S. K., . . . Dorrance, A. E. (2012). Dissection of two soybean QTL conferring partial resistance to Phytophthora sojae through sequence and gene expression analysis. *BMC Genomics, 13*(1), 1.

Wang, L., Wan, Z. Y., Bai, B., Huang, S. Q., Chua, E., Lee, M., . . . Liu, F. (2015). Construction of a high-density linkage map and fine mapping of QTL for growth in Asian seabass. *Scientific Reports, 5*.

Wang, Y., Yang, L., Xu, H., Li, Q., Ma, Z., and Chu, C. (2005). Differential proteomic analysis of proteins in wheat spikes induced by *Fusarium graminearum*. *Proteomics, 5*(17), 4496-4503.

Waterhouse, P. M., and Helliwell, C. A. (2003). Exploring plant genomes by RNA-induced gene silencing. *Nature Reviews Genetics, 4*(1), 29-38.

Woldemariam, M. G., Baldwin, I. T., and Galis, I. (2011). Transcriptional regulation of plant inducible defenses against herbivores: a mini-review. *Journal of Plant Interactions, 6*(2-3), 113-119.

Xie, R., Zheng, L., Deng, L., He, S., Yi, S., Lv, Q., and Zheng, Y. (2014). The role of R2R3MYB transcription factors in plant stress tolerance. *JAPS, Journal of Animal and Plant Sciences, 24*(6), 1821-1833.

Xue, S., Li, G., Jia, H., Lin, F., Cao, Y., Xu, F., . . . Zhang, Z. (2010). Marker-assisted development and evaluation of near-isogenic lines for scab resistance QTLs of wheat. *Molecular Breeding, 25*(3), 397-405.

Xue, S., Xu, F., Tang, M., Zhou, Y., Li, G., An, X., . . . Zhang, L. (2011). Precise mapping Fhb5, a major QTL conditioning resistance to Fusarium infection in bread wheat (*Triticum aestivum* L.). *Theoretical and Applied Genetics, 123*(6), 1055-1063.

Yan, L., Loukoianov, A., Tranquilli, G., Helguera, M., Fahima, T., and Dubcovsky, J. (2003). Positional cloning of the wheat vernalization gene VRN1. *Proceedings of the National Academy of Sciences, 100*(10), 6263-6268.

Yang, J., Bai, G., and Shaner, G. E. (2005a). Novel quantitative trait loci (QTL) for Fusarium head blight resistance in wheat cultivar Chokwang. [Comparative Study Research Support, Non-U.S. Gov't]. *Theoretical and Applied Genetics, 111*(8), 1571-1579.

Yang, K., Qi, L., and Zhang, Z. (2014). Isolation and characterization of a novel wall-associated kinase gene TaWAK5 in wheat (*Triticum aestivum*). *The Crop Journal, 2*(5), 255-266.

Yang, Z., Gilbert, J., Fedak, G., and Somers, D. J. (2005b). Genetic characterization of QTL associated with resistance to Fusarium head blight in a doubled-haploid spring wheat population. *Genome, 48*(2), 187-196.

Yogendra, K. N., Kumar, A., Sarkar, K., Li, Y., Pushpa, D., Mosa, K. A., . . . Kushalappa, A. C. (2015). Transcription factor StWRKY1 regulates phenylpropanoid metabolites conferring late blight resistance in potato. *Journal of Experimental Botany, 66*(22), 7377-7389.

Yogendra, K. N., Pushpa, D., Mosa, K. A., Kushalappa, A. C., Murphy, A., and Mosquera, T. (2014). Quantitative resistance in potato leaves to late blight associated with induced hydroxycinnamic acid amides. *Functional and Integrative Genomics, 14*(2), 285-298.

Yoshida, M., Kawada, N., and Tohnooka, T. (2005). Effect of row type, flowering type and several other spike characters on resistance to Fusarium head blight in barley. *Euphytica, 141*(3), 217-227. doi: 10.1007/s10681-005-7008-8

Yoshio, U., Nakajima, M., Sakai, K., Ishii, K., and Shimada, N. (1973). Comparative toxicology of trichothec mycotoxins: inhibition of protein synthesis in animal cells. *Journal of Biochemistry, 74*(2), 285-296.

Younis, A., Siddique, M. I., Kim, C.-K., and Lim, K.-B. (2014). RNA interference (RNAi) induced gene silencing: a promising approach of hi-tech plant breeding. *International Journal of Biological Sciences, 10*(10), 1150-1158.

Zadoks, J. C., Chang, T. T., and Konzak, C. F. (1974). A decimal code for the growth stages of cereals. *Weed Research, 14*(6), 415-421.

Zhang, Z., Liu, X., Wang, X., Zhou, M., Zhou, X., Ye, X., and Wei, X. (2012). An R2R3 MYB transcription factor in wheat, *TaPIMP1*, mediates host resistance to *Bipolaris sorokiniana* and drought stresses through regulation of defense-and stress-related genes. *New Phytologist, 196*(4), 1155-1170.

Zhou, W., Kolb, F. L., and Riechers, D. E. (2005). Identification of proteins induced or upregulated by Fusarium head blight infection in the spikes of hexaploid wheat (*Triticum aestivum*). *Genome, 48*(5), 770-780.

Zhu, X., Zhong, S., and Cai, X. (2016). Effects of D-Genome Chromosomes and Their A/B-Genome Homoeologs on Fusarium head blight Resistance in Durum Wheat. *Crop Science, 56*(3), 1049-1058.

APPENDICES

Appendix Table A3.1. Fusarium head blight resistance related metabolites identified from the spikelets of wheat NILs carrying QTL-Fhb5 resistant and susceptible alleles following *F. graminearum* or mock inoculations.

m/z Value	Metabolites class	Observed Fragmentation	Database fragmentation	FC®	Database ID©
Mass (Da)	**Phenylpropanoids**				
148.0524	trans-Cinnamate	89.16,99.21,101.1,103.14,116.95,127.15,129.1,130.02		1.37** (PRr)	PlantCyc:DIHYDROCOUMARIN;KEGG:C00423
164.0473	m-coumaric acid	89.09,91.05,**97.12,**145.03	74.0,93.0,**97.0**,149.0	4.17** (PRr)	**METLIN :305**
178.0630	Coniferaldehyde	**177.03, 162.00**, 145.04, 117.99	**177.0, 162.0,** 134.0	2.79*** (PRr)	PlantCyc:CONIFERYL-ALDEHYDE;KEGG:C02666, **McGill MD C00002728**
234.1368	4-Coumaroylputrescine	**119.01,** 191.13,218.25, **233.11**	**119.04**, 190.08, 218.11, **233.12**	38.81** (PRr)	HMDB:HMDB33461;Metlin:2371; LIPIDMAPS:LMFA01090008;pUBcHEM:4983;**In silico, (Muroi et al., 2009)**
250.1317	N-Caffeoylputrescine	**207.19**;219.44;230.95;234.35;**250.37**;231.37;248.81;**221.16**	**207.00,250.00,221.00**	11.92***(PRr)	KEGG:C03002;**METLIN:3380**
276.1586	4-coumaroyl agmatine	**119.07, 233.33, 258.30**	**119.04, 233.129, 258.14**	126.05***(PRr) 1.21**(RRI)	PlantCyc :N-4-GUANIDINOBUTYL-4-HYDROXYCINNAMAMID; ChEBI:58644;KEGG:C04498;PubChem:25245514; **METLIN :43471;In silico(Gunnaiah et al. 2012)**
292.1535	4-coumaroyl-3-hydroxyagmatine	93.24,112.34,119.03,154.2,171.14,232.2,249.18,274.21		27.46*** (PRr)	PlantCyc:CPD-12237; KEGG:C11633;METLIN:64338
326.1002	4-O-beta-D-Glucosyl-4-hydroxycinnamate	96.08,113.05,119.22,132.91,145.13,163.1,187.17,265.29		1.23*** (PRr)	KEGG:C04415
344.1471	Dihydroconiferyl	109.15,209.27,3		1.67***	PlantCyc:CPD-

	alcohol glucoside	07.15,325.32,328.09		(PRr)	82;METLIN:41168;KEGG:C11652;GUN:2012
372.1420	Syringin	**353.27,** 310.6, 249.26, **209.23,** 149.13	**353, 311, 209**	8.65*(PRr) 1.00*(RRI)	PlantCyc:CPD-63;KEGG:C01533;**METLIN:64181**
Mass (Da)	**Lipids and Fatty Acids**				
130.0630	6-oxohexanoate	59.2,70.92,83.11,84.98,101.03,111.06,129.09		1.30** (PRr)	PlantCyc:6-OXO-HEXANOATE;KEGG:C06102;HMDB:HMDB12882
182.0790	L-iditol	58.90,73.13,**89.06,101.06,181.07**	59.0149,71.015,73.0309,**89.0242,101.0249,181.0712**	1.96*(PRr) 1.42*(RRC)	PlantCyc:CPD-369;KEGG:C01507;HMDB:HMDB11632;**MASSBANK:PR100483**
278.2246	Crepenynate	83.03,97.11,179.32,233.29,257.24,259.25,277.37		1.57* (PRr)	PlantCyc:CREPENYNATE;KEGG:C07289
310.2297	14'-apo-beta-Carotenal	95.08,114.91,171.22,187.16,193.18,207.25,209.13,247.28,291.38		1.22* (RRC)	KEGG:C06734:LIPIDMAPS:LMPR01070297
328.2250	2,3-Dinor-8-iso prostaglandin F1alpha	109.1,121.13,165.38,209.19,282.31,291.27,309.28,313.21		1.68* (PRr)	KEGG:C14795
328.2613	Avocadene Acetate	115.43,125.16,198.30,245.01,251.35,295.31309.2		1.28* (RRI)	METLIN:43512;HMDB:31043
375.2773	N-Arachidonoyl-L-Alanine	135.97,190.35,237.28,293.02,301.44,314.47,330.47,344.25,358.23		1.45* (RRC)	METLIN:64920;LIPIDMAPS:LMFA08020153
392.2021	(6RS)-22-oxo-23,24,25,26,27-pentanorvitamin D3 6,19-sulfur dioxide adduct	113.08,142.97,160.95,178.83,271.25,291.58,309.22,331.09,373.75		1.26* (RRC)	LIPIDMAPS:LMST03020008
416.3142	2-(Trimethylsilyl)Oxy-Hexadecanoic Acid Trimethylsilyl Ester	132.92,281.38,303.19,315.23,333.08,354.93,379.02,400.6841430		1.49* (RRC)	MASSBANK:JP000609
537.1060	Phenanthridine-2-carboxylic acid	199.94,241.17,251.17,329.19,455.64,490.96		2.06*** (PRr)	KEGG:C11471
572.2962	Phosphatidylinositol lyso	209.16,301.84,**496.34**,**539.44**	255.04,314.85,**496.95,539.16**	1.66*** (PRr) 1.47*(R	**MASSBANK:UT001490**

				RC)	
698.3514	Corchorusoside A	223.89,233.43,327.85,343.343.27,482.48,636.58,650.87,674.41,688.73		1.22* (RRC)	METLIN:88745:HMDB:HMDB32823
Mass (Da)	**Aromatic compounds and Flavonoids**				
300.1209	Salidroside	**87.18,89.12,101.12,119.11,217.11**	**85.0291,89.0248,101.0278,119.0505**,137.0653	1.39* (RRC)	PlantCyc:CPD-13354;KEGG:C06046;**METLIN : 44847**
316.0794	2,5-dihydroxybenzoate 2-O-β-D-glucoside	93.18,108.26,123.13,151.08,152.02,153.10,165.11,181.20,225.14,297.11		1.37** (RRC)	PlantCyc:CPD-12663
326.1453	Acepromazine	101.05,126.97,145.19,154.14,195.13,224.00,265.06,277.17,307.15		2.56* (RRC)	METLIN:85533
330.0951	1-O-Vanilloyl-beta-D-glucose	97.03,113.14,123.13,152.27,167.08,181.17,		1.42* (RRC)	KEGG:C20470
340.1311	8-prenylnaringenin	122.95,146.09,179.25,188.19,203.22,309.18,324.19,325.01		1.35*** (PRr)	PlantCyc:CPD-9440
400.1376	Zuclopenthixol	119.26,133.37,157.04,160.21,173.06,175.91,196.99,219.08,297.74,311.11		1.51** (RRC)	METLIN:3109
504.2032	Chlorhexidine	**150.94,153.05,191.69,471.46**	**150.91,153.07,191.12,471.4588**	1.25* (RRC)	KEGG:C06902;**METLIN:1720**
514.3308	2-((4-Dodecylphenyl)azo)-4-(2,4-xylylazo)resorcinol	159.08,161.10,212.47,235.15,253.22,277.31,284.26,439.52		14.02* (RRC)	PubChem:110018
542.1210	3,3"-binaringenin	161.20,171.16,215.06,316.27,325.34,343.20,350.34,394.22,412.18,523.16		1.42* (RRC)	KEGG:C09758;METLIN:47514;LIPIDMAPS:LMPK12040001
566.1424	Poriolide	161.20,192.30,353.11,384.16,444.15,474.10,504.15,546.16		1.63* (RRC)	LIPIDMAPS:LMPK12140226;METLIN:52714
586.1320	Prunin 6"-O-gallate	222.98,242.18,285.13,353.52,375.10,464.97,495.05,524.99		1.34* (RRC)	LIPIDMAPS:LMPK12140244

594.1585	Isoorientin 2"-O-rhamnoside	179.03,227.16,255.09,284.16,323.14,371.09,429.07,443.12,575.18		1.47** (RRC)	KEGG:C04024;PlantCyc:VITEXIN-2-O-BETA-D-GLUCOSIDE
595.1452	Cyanidin 3-(p-coumaroyl)-glucoside	177.23,313.27,353.82,414.15,474.24,504.26,533.85,575.88		2.44*** (PRr) 1.98*(RRC)	PlantCyc:CPD-7866;KEGG:C12095;
595.1660	Pelargonidin-3,5-diglucoside	178.98,**268.31,430.23**,431.35,479.40	147.009,**268.0381,430.0922**,431.1004	1.38*** (PRr)	PlantCyc:CPD-7137;KEGG:C08725; **MASSBANK:PR100645**
760.2579	Epimedoside	229.36,261.42,279.32,329.23,497.37,699.58		1.62** (RRC)	LIPIDMAPS:LMPK12112021
770.2058	Pelargonidin 3-(6"-ferulylglucoside)-5-glucoside	224.28,283.78,507.27,525.09,547.15,559.01,686.99,708.29		1.35*** (PRr)	METLIN:46811;LIPIDMAPS: LMPK12010044
782.2068	Pelargonidin 3-(6"-p-coumarylglucoside)-5-(6"'-acetylglucoside)	471.30,582.74,661.67,683.12,707.95,723.17,736.37		2.67* (RRC)	METLIN:46814;LIPIDMAPS:LMPK12010047
Mass (Da)	**Unclassified Metabolites**				
152.0685	Xylitol	89.21,108.97,118.70,123.08,131.3,136.08		1.74** (PRr)	KEGG:C00379
165.0790	L-phenylalanine	**72.10**,79.13,**103.10,**135.99,147.07	**72.0093**,80.3995,**103.0543**,116.0503	1.21*** (PRr)	PlantCyc:PHE;KEGG:C00079;**METLIN:28**
204.0899	L-tryptophan	**74.24,116.10,142.21,159.07,203.01**	**74.02,116.05,142.06,159.09,203.0821**	1.85*** (PRr)	KEGG:C00078;**MASSBANK:PR100498**
214.1200	Methyl 2-diazoacetamidohexonate	83.05,97.6,111.1,151.1,167.25,183.18,195.17,213.1		1.91*** (PRr)	KEGG:C01223
224.1412	(-)-jasmonic acid methyl ester	**149.24,151.22,162.91,207.02,223.11**	134.9907,**149.0448,151.026,162.9327,207.0458,223.0833**	1.36* (RRC)	PlantCyc:CPD1F-2;KEGG:C11512;LIPIDMAPS:LMFA02020010;**MASSBANK:PR100748**
226.1569	Dihydrojasmonic acid, methyl ester	83.1,97.22,109.08,123.11,137.05,181.17,197.17,207.18,209.11,225.27		1.36* (RRI)	METLIN:43916
230.0192	D-ribulose-5-phosphate	85.05,**96.95,229.16**	78.959,**96.967,229.011**	1.23*** (PRr)	KEGG:C00199;**METLIN :159**

234.1620	Zealexin A1	93.28,119.05,162.17,191.14,21.08,233.29		1.27* (RRC)	PlantCyc:CPD-13573
260.0202	D-Galactose 6-sulfate	78.89,87.04,96.93,139.03,168.99,179.13,199.10,223.09,240.99,250.70		2.75*** (RRC)	KEGG:C01067
282.2433	Tropane	82.99,97.09,111.04,137.19,167.38,249.18,261.10,263.35281.17		3.44*** (RRC)	PubCHem:4157
290.1226	N-(L-Arginino)succinate	**112.06,109.27,125.20**	**109.013,112.0501,125.066**	1.09** (RRI)	KEGG:C03406;**METLIN:389**
313.1889	Heliotrine	95.11,112.12,125.19,142.16,134.15,171.29,185.16,266.52,276.21,277.27,294.20		1.69*** (PRr)	KEGG:C10324
334.1125	Asp Ser Asn	101.1,113.14,127.11,143.12,153.13,161.08,171.19,255.24		1.27** (RRI)	METLIN:16742
343.0903	DIBOA-β-D-glucoside	101.89,117.98,124.21,134.12,152.15,162.16,180.1		1.25** (PRr)	PlantCyc:CPD-13811;KEGG:C15772
346.1264	Aucubin	110.98,123.32,155.41,171.22,201.26,229.34,271.27,309.34,327.30		1.62* (RRC)	KEGG:C09771;LIPIDMAPS:LMPR0102070006;METLIN:41151
360.1420	7-deoxyloganate	112.93,153.04,197.1,211.21,239.17,269.09,299.23,327.15		1.93*** (PRr) 1.42*(RRC)	PlantCyc:CPD-9981;KEGG:C11636
390.1526	Loganin	164.34,192.12,207.04,209.12,243.18,328.97,345.48,357.17,371.28		1.44** (RRC)	PlantCyc:LOGANIN;KEGG:C01433;MASSBANK:C01433
406.2396	Calcium undecylenate	123.23,133.87,180.24,183.24,223.21,267.02,328.30,3441.91		8.61* (RRC)	PubChem:14865
436.2590	1-oleyl-2-lyso-phosphatidate	**150.99,152.12,153.16**	**150.98,152.9972,153.1043**,171.00	2.09** (RRC)	PlantCyc:L-1-LYSOPHOSPHATIDATE;**METLIN:5432**;HMDB:HMDB07855
458.1424	2'-(E)-Feruloyl-3-(arabinosylxylose)	134.00,144.98,175.13,193.21,253.09,263.27,267.09,281.11,381.29,425.17		1.47* (RRC)	METLIN:86818;HMDB:HMDB30230

532.3764	Pentanoic acid ester	173.13,193.21,269.06,281.09,449.41	32.28*** (PRr)	PubChem: 157226 ChemSpider: 138374
544.2632	Perindopril glucuronide	170.94,207.09,307.32,410.34,445.22,461.13,483.28,498.86	1.44* (RRC)	METLIN:1796

* *t* test significance at $P<0.05$, ** *t* test significance at $P<.01$, *** *t* test significance at $P<.001$

® FC (Fold change) calculation: were based on relative intensity of metabolites, RRC(Resistance related constitutive) = RM/SM, PRr(Pathogen related in resistant NIL) = RP/RM, RRI(Resistance related induced) = (RP/RM)/(SP/SM); RP: resistant NIL with pathogen inoculation, RM: resistant NIL with mock inoculation, SP: susceptible NIL with pathogen inoculation, SM: susceptible NIL with mock inoculation.

©Database ID in bold is the fragmentation match.

Appendix Table A3.2. The *in-silico* annotated gene list of QTL-Fhb5 sequences retrieved using flanking markers Xgwm415 (Xgwm415_Ta5A_QTL) and Xgwm304 (Xgwm304_Ta5A_QTL).

*AUGUSTUS prediction	Putative names	Gene size (bp)	#Hits	e-Value	**GOs
FM_304_415:g13.t2	Phosphoglycerate kinase	594	20	2.24E-65	Response to stress, kinase activity
FM_304_415:g33.t1	Pathogenesis-related protein class I (PR1)	456	20	4.61E-88	Extracellular region; cytoplasm
FM_304_415:g88.t1	Serine threonine-protein kinase (STPK)	543	20	8.48E-81	Kinase activity; Cellular protein modification process
FM_304_415:g96.t1	Homeobox-leucine zipper protein hox33-like	1068	20	1.42E-42	Sequence-specific DNA binding transcription factor activity; flower development
FM_304_415:g101.t1	R2R3-myb transcription factor	684	20	5.36E-114	DNA binding; Chromatin binding
FM_304_415:g8.t1	Receptor-like protein kinase	465	20	2.54E-96	Hydrolase activity
FM_304_415:g63.t1	Probable carboxylesterase 17-like	603	20	5.95E-85	Metabolic process
FM_304_415:g69.t1	Wall-associated receptor kinase 2-like	912	20	2.68E-94	Cellular protein modification process; kinase activity
FM_304_415:g39.t1	Retrotransposon ty3-gypsy subclass	846	20	8.03E-45	RNA-dependent DNA replication; Ribonuclease H activity
FM_304_415:g3.t1	Transcription factor bhlh25	645	20	1.05E-46	Protein binding
FM_304_415:g17.t1	Zinc knuckle family expressed	441	19	1.27E-50	Plastid; Mitochondrion

* AUGUSTUS predicted numbers for predicted genes from QTL-Fhb5 sequence between Xgwm304_Ta5A_QTL and Xgwm415_Ta5A_QTL flankning markers (FM)

**BLAST2GO analysis for gene ontology (GO) analysis for the predicted genes from AUGUSTUS

Appendix Table A5.1. The primer combinations used for semi-quantitative reverse transcriptase polymerase chain reaction (qRT-PCR) and fungal biomass quantification of *F. graminearum* strains.

Gene name	NCBI ID	Orientation	Sequence (5' to 3')
TaPR1	KR351308	F	CACCACAGTACGGGGAGAAC
TaPR1	KR351308	R	GGCGTAGTTGTAGTTGGCCT
TabHLH	KR351307	F	CGTGCTCGTCAGCAAGAAGA
TabHLH	KR351307	R	TCTGAGAGATGGCGAGTCGT
TaSTPK	KR351309	F	ACACATGCAGAACAACGTGC
TaSTPK	KR351309	R	TGGACCATGGCTCATCCCTA
TaAGPAT	XP_003575968.1	F	TGGTGGTCCTGTCTTGGTCA
TaAGPAT	XP_003575968.1	R	GCAGTCACCATTGCCAATCC
TaTLP	BM135805.1	F	AACTAGAGCTTGCAGCAATGG
TaTLP	BM135805.1	R	TCTTGATGTTGAAGGTGGCCG
Fg_Gao	M86819	F	ACCTCTGTTGTTCTTCCAGACGG
Fg_Gao	M86819	R	CTGGTCAGTATTAACCGTGTGTG

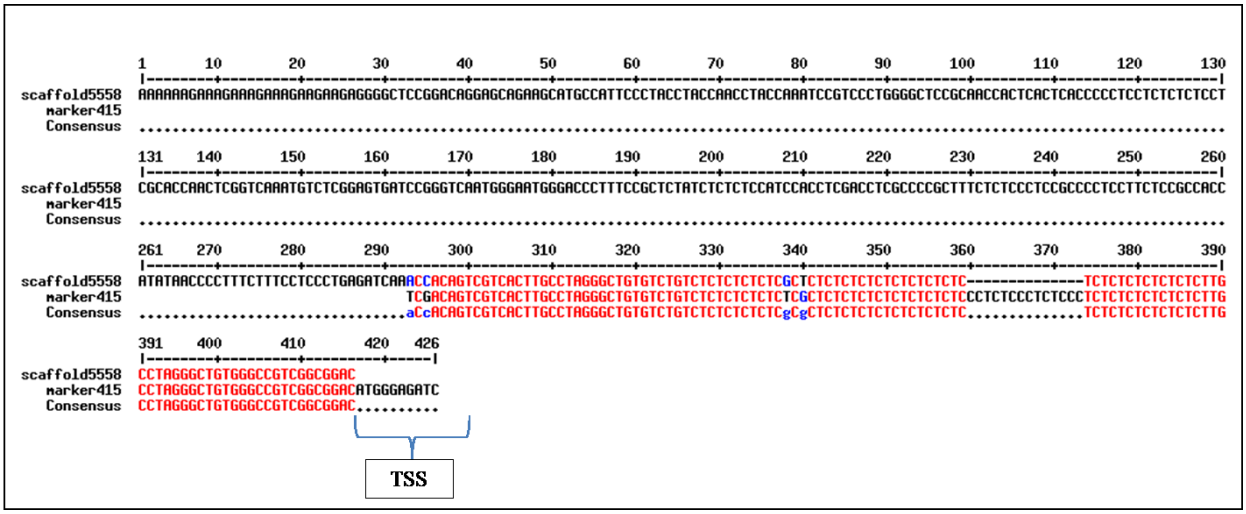

Appendix Figure A3.1: The QTL-Fhb5 flanking marker (marker415= Xgwm415_Ta5A_QTL) tagged to *TaMYBFhb5* gene. Where, TSS is transcription start site of *TaMYBFhb5* gene and scaffold5558 was used as reference genome of *T. urartu* (Ling et al., 2013).

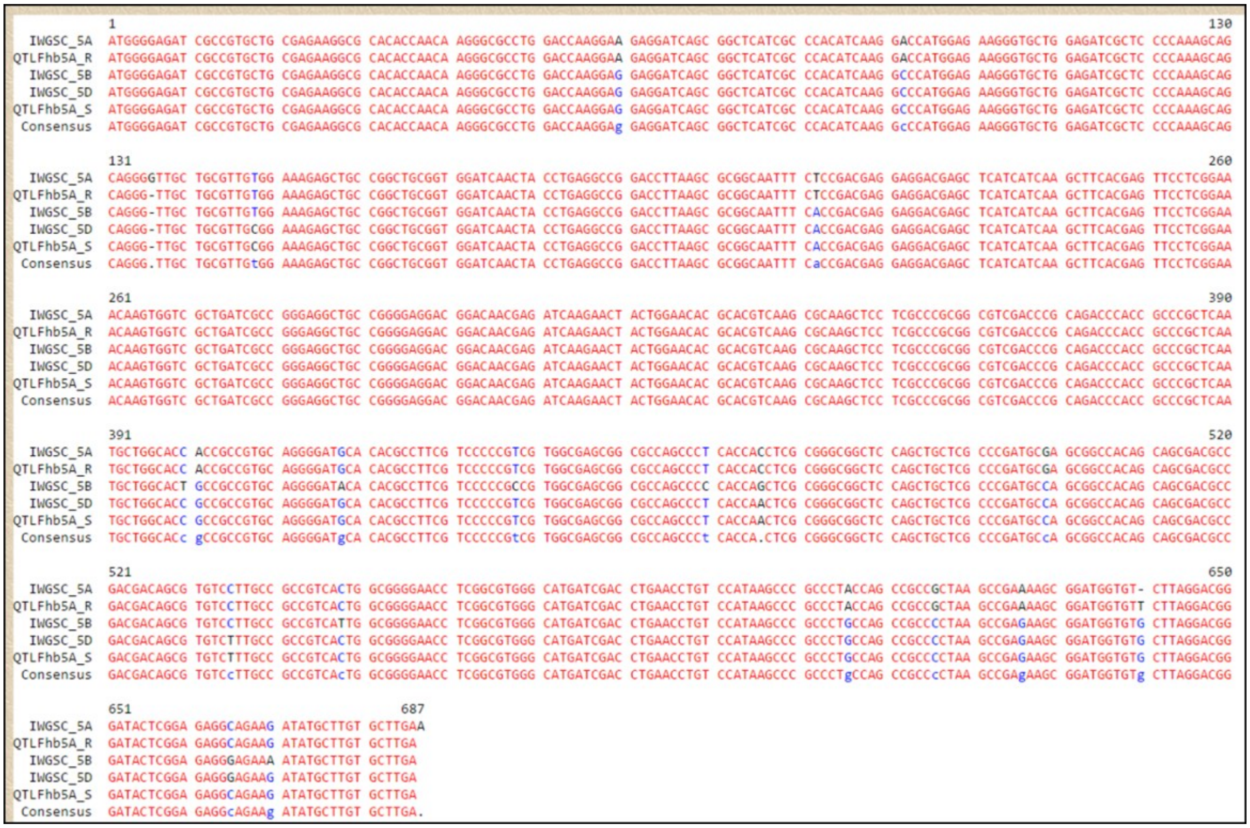

Appendix Figure A3.2: The allelic variation of *TaMYBFhb5* gene. Where, QTLFhb5_R= RNIL *TaMYBFhb5* allele, QTLFhb5_S= SNIL *TaMYBFhb5* allele and ABD alleles from International wheat genome sequencing consortium (IWGSC).

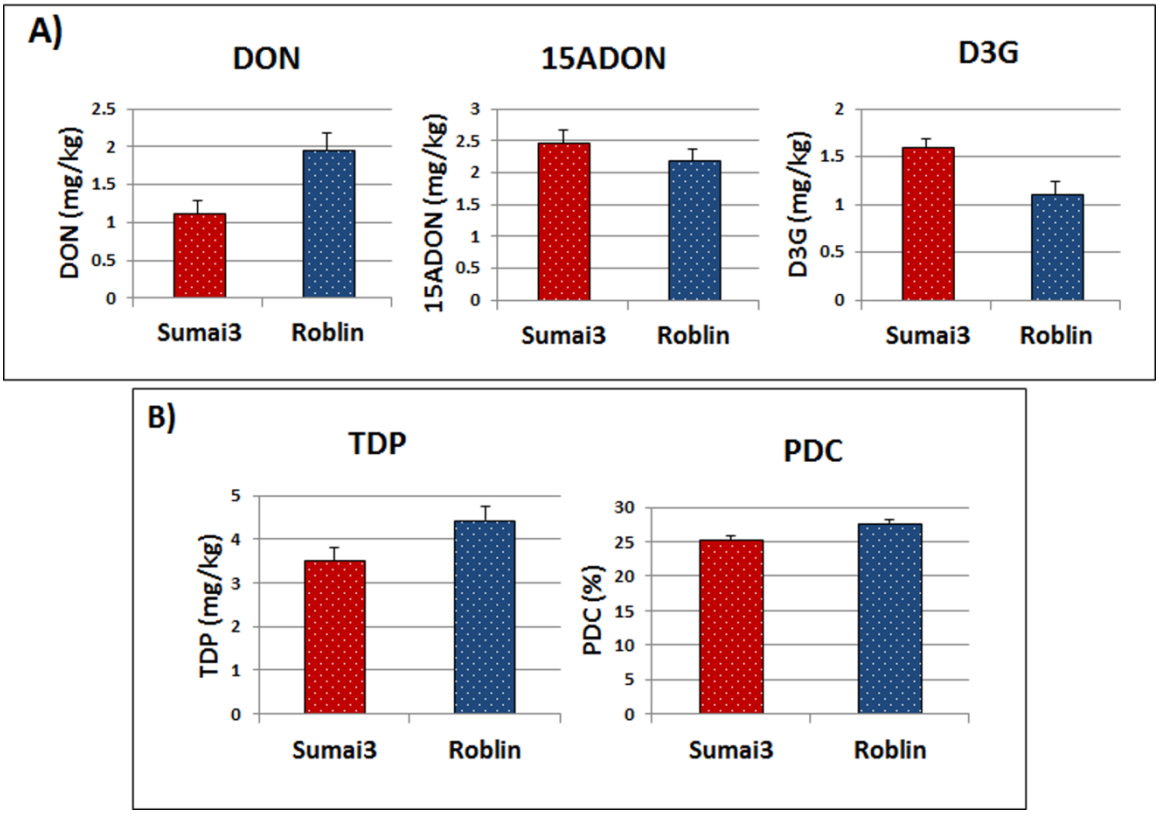

Appendix Figure A5.1. The mycotoxins (DON and 15-ADON) accumulation and conversion (D3G) within the plant system of Sumai3 and Roblin after 3 dpi of *F. graminearum FgT* strain; A) the differential accumulation of DON, 15ADON and D3G in (mg/kg). B) Total DON produced (TDP= DON+ 15ADON+ D3G) accumulated and proportion of DON converted as D3G (%). Where, DON = 4-deoxynivalenol, 15ADON = 15-*O*-acetyl DON, D3G = DON-3-*O*-glucoside, PDC = proportion of DON (DON+15ADON) converted to D3G.

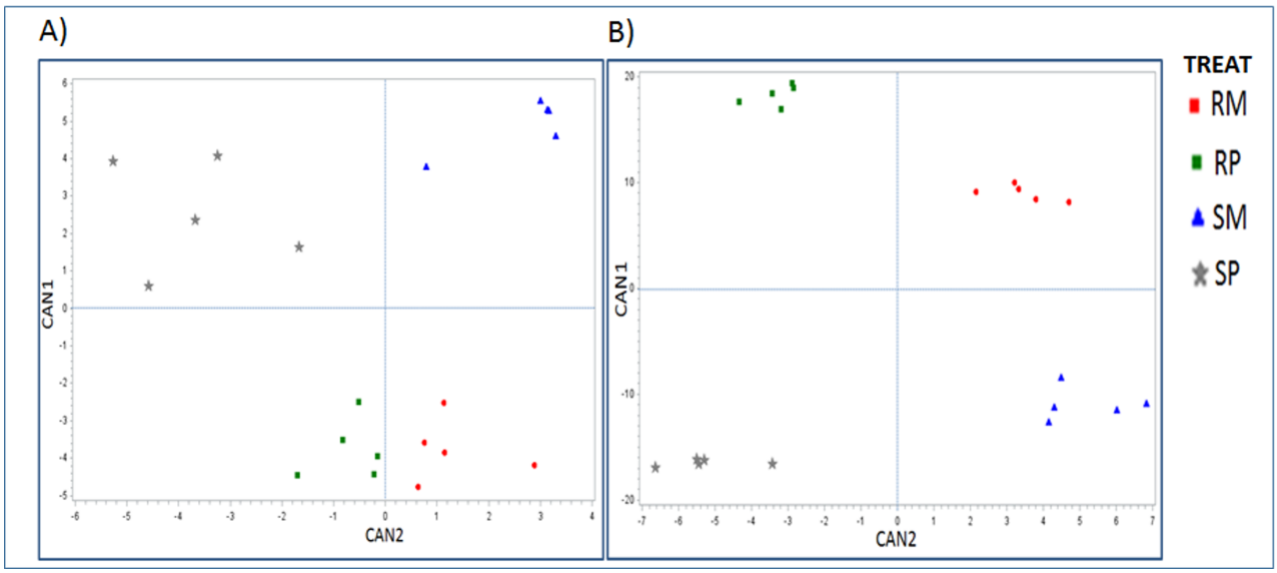

Appendix Figure A5.2. Scatter plot of canonical discriminant analysis of significant metabolites ($P < 0.05$) found between Sumai3 and Roblin genotypes. A) Total 393 significant metabolites found upon *F.graminearum* trichothecene producing pathogen inoculation (*FgT*). B) Total 506 significant metabolites found upon *F.graminearum* trichothecene non-producing pathogen inoculation (*Fgt*). CAN1 separated the genotypes with distinct subgroups of mock and pathogen treatments, whereas, CAN2 separated inoculations, with subgroups of two genotypes. Where, RM; resistant genotype (Sumai3) inoculated with mock (sterile water), RP; resistant genotype (Sumai3) inoculated with trichothecene producing pathogen (*FgT*), SM; susceptible genotype (Roblin) inoculated with mock (sterile water), SP; susceptible genotype (Roblin) inoculated with trichothecene non-producing pathogen (*Fgt*).